Energy Access in Resource-Constrained Environments

by

Maitreyee Sanjiv Marathe

A dissertation submitted in partial fulfillment
of the requirements for the degree of
Doctor of Philosophy
(Electrical and Computer Engineering)

at the
University of Wisconsin-Madison
2024

Date of Final Oral Exam: 11/25/2024
The dissertation is approved by the following members of the final oral committee:
Line Roald, Associate Professor, Electrical and Computer Engineering
Giri Venkataramanan, Professor, Electrical and Computer Engineering
Gregory Nemet, Professor, La Follette School of Public Affairs
Johanna Mathieu, Associate Professor, Electrical and Computer Engineering,
University of Michigan Ann Arbor

Energy Access in Resource-Constrained Environments

Maitreyee Sanjiv Marathe

Abstract

Reliable access to electricity is critical to advancing human development. It is estimated that about 3.5 billion people globally have unreliable or no access to electricity. This issue stems from a lack of access to modern energy services, or limiting one's energy use due to socioeconomic constraints. It affects households in both emerging and developed economies, and is expected to worsen because of climate change and rising electricity prices. Designing equitable energy access frameworks for such environments is challenging because of diverse constraints and requirements such as resilience to intermittent remote communication, compatibility with locally available heterogeneous hardware, affordability, and agreement with sociocultural elements of the community. This necessitates inter-disciplinary research beyond the scope of traditional power engineering tools. This thesis focuses on developing technology-driven solutions for residential energy access in such resource-constrained environments.

The thesis proposes a holistic approach that involves (1) identifying complex problems through community-engagement, (2) distilling technical questions, (3) developing solutions using power engineering research tools such as analytical modeling, mathematical optimization, numerical simulations, and hardware prototyping, (4) deploying the solutions through pilots, and (5) disseminating findings through energy education platforms. First, it presents findings from field experiences that illustrate this workflow in diverse environments including energy access in off-grid rural communities, energy resilience for individuals dependent on in-home medical devices, and energy access for people experiencing homelessness. Next, the thesis proposes *optimized threshold-based energy management* as a candidate framework for energy access in such resource-constrained environments. Specifically, the proposed framework is developed in the context of energy management for low-income prepaid electricity customers. The framework shows comparable or improved performance when compared to benchmarks as validated through numerical simulations using real-world energy usage data. Additionally, it does not need frequent remote communication, detailed demand forecasts, or expensive custom hardware as validated by implementing it on a basic low-cost microcontroller. Furthermore, the thesis proposes *Picogrid*, a low-cost hardware platform for energy research and education, and presents its use cases in real-world settings. The platform lowers the barrier to entry into hardware validation for energy researchers and can be used to develop an energy literacy toolkit for energy awareness and education. Finally, directions for future work are identified. This thesis aspires to be a roadmap for developing equitable energy access solutions through holistic approaches.

Acknowledgments

I am grateful for the opportunity to pursue graduate studies at the University of Wisconsin-Madison. The support I have received through this journey has been humbling.

I would like to thank my advisors Prof. Line Roald and Prof. Giri Venkataramanan for their support and guidance. Thank you, Prof. Giri for being a mentor during my undergraduate summer internship, for inspiring me to engage in fieldwork before graduate school, for recruiting me as a PhD student, and for encouraging me to think about unstructured grassroots problems. Thank you, Prof. Line for agreeing to be my advisor, inspiring me to use optimization for energy access problems, encouraging me to aim higher, and for your contagious enthusiasm and curiosity. I am deeply grateful to both of you for your support, within and beyond the walls of the lab.

I would like to express my sincere gratitude to my committee members, Prof. Johanna Mathieu and Prof. Greg Nemet, for their time and feedback, and for their support in my pursuit of post-doctoral opportunities.

A significant part of my early graduate work was in collaboration with Ashray Manur. He has been a mentor and a friend, always generous with his time. I am grateful for the opportunity to participate in outreach events and projects alongside him, particularly the NSF I-Corps program to study energy resilience and home healthcare.

Thank you to the Morgridge Center for Public Service for introducing me to community-engaged scholarship and for your support through the Morgridge Fellows program.

I am grateful to everyone on the Electric Little Free Library project team. Thank you, to Chris Litzau and the veterans at the Great Lakes Community Conservation Corps. Thank you, Dr. Lennon Rodgers and Maggie Muldowney at the UW Design and Innovation Lab, for giving us a space to tinker, build, and break things. Thank you, Megan Levy for your incessant enthusiastic support. Thank you, Rebecca Taylor for being a great team mate and friend. Thank you to all undergraduate and graduate students, community partners, and supporters of this project.

I am grateful to the Energy Analysis and Policy program cohort, faculty, and administration, especially Scott Williams and Prof. Tracey Holloway. Thank you for supporting me through fellowships and for your support to my Electric Little Free Library capstone project. Thank you to my capstone team Brittany Bondi, Stephanie Ortland, and William Keenan. The project greatly benefited from your expertise and contributions.

Thank you, Dr. Greg Ledva, Director Emerging Technologies at Virtual Peaker Inc, for your mentorship during my summer internship.

I am grateful to all the undergraduate students I have had the pleasure to mentor and work with: Grace Jensen, Tricia Nazareth, Gabriela Setyawan, Savannah Ahnen, Mridhul Baskaran, Varun Balan, Shreya Mukherjee, Aayushi Singh, James Wang.

I am grateful to all the graduate students I have had the pleasure to work with. Thank you for being great collaborators, David Sehloff, Raul Martins, Sofia Taylor, Jennifer Bui. Thank you to my peers for their support and engaging discussions: Aditya Ghule, Nikhil Deshpande, Marisa Liben, Shalini Manna, David Skrovanek, Noah Rhodes, Aditya Rangarajan, Kshitij Girigoudar, Sogol Babaeinejadsarookolaee, Yasmine Abdennadher, and many more in the WEMPEC and WISPO family.

Thank you to the WEMPEC administrative and research team, especially Kathy Young, Kelly Camp, Kyle Hanson, Pia Strampp, for keeping the show going.

I am grateful to the J N Tata Endowment and the Tata Education and Development Trust for providing support towards my graduate studies.

I am grateful to all my friends in Madison for making my stay here memorable and to my friends outside Madison for keeping me motivated! Thank you, Sangeetha, Allison, Tanmayee, Karan, Akshay, Sindhu, Nischita, Anjana, Neha, Vinay.

I am deeply grateful to my family for encouraging me to pursue my dreams. I thank my parents, Deepti and Sanjiv Marathe, for teaching me the importance of resilience and grit. Thank you to my fiancé, Saketh Sridhara, for being my constant support.

Contents

1 Introduction **2**
1.1 Motivation . . . 2
1.2 Methodology . . . 4
1.3 Document Organization . . . 7
1.4 Background Papers and Reports . . . 9

I Field Experiences **12**

2 Energy Access and Off-Grid Rural Communities **15**
2.1 Introduction . . . 15
2.2 Rural Household as an Energy Hub . . . 17
2.3 Optimization Problem Formulation . . . 19
2.4 Case Study . . . 22
2.5 Conclusion and Future Work . . . 26

3 Energy Resilience and Home Healthcare **27**
3.1 Insights from the NSF I-Corps Program . . . 29
3.2 Table-Top Exercise . . . 34
3.3 Load Scheduler for the EAK . . . 38
3.4 Conclusion and Future Work . . . 45

4 Energy Access and Homelessness **47**
4.1 Problem Identification and Scoping . . . 48
4.2 Prototype Development and Deployment . . . 49
4.3 Results, Discussion, and Continuing Work . . . 52

II Threshold-Based Energy Management **57**

5 Stability Study **58**
5.1 Introduction . . . 59
5.2 Model . . . 63
5.3 Stability Study . . . 64
5.4 Case Studies . . . 69
5.5 Rules for Operating Entities . . . 73

5.6 Conclusion . . . 74

6 Application to Community-Scale Microgrids 76
6.1 Introduction . . . 77
6.2 Distributed Optimal Scheduling . . . 79
6.3 Optimal Scheduler Design . . . 81
6.4 Three-Entity Microgrid Network - Simulation Study . . . 86
6.5 Three-Entity Microgrid Network - Experimental Study . . . 93
6.6 Conclusion . . . 96

III Optimized Threshold-Based Energy Management 98

7 Energy Management for Prepaid Customers 99
7.1 Introduction . . . 100
7.2 Model . . . 104
7.3 Case Study . . . 112
7.4 Conclusion . . . 117

8 Addressing Imperfect Forecasts and Implementation Constraints 119
8.1 Introduction . . . 120
8.2 Model Formulations . . . 122
8.3 Qualitative Comparison - Computation, Communication, and Information Requirements . . . 129
8.4 Quantitative Comparison - Case Study . . . 132
8.5 Conclusion . . . 138

IV Picogrid 139

9 Picogrid: An Experimental Platform for Prosumer Microgrids 140
9.1 Introduction . . . 141
9.2 Platform . . . 144
9.3 Experimental Results . . . 149
9.4 Conclusion . . . 157

10 Custom Cloud-Based Solution for Remote Access to the Picogrid 159
10.1 Introduction . . . 160
10.2 Platform . . . 162
10.3 Experimental Results . . . 167
10.4 Demonstration of Demand Response at a Community Workshop . . . 175
10.5 Conclusion . . . 177

11 Conclusions, Contributions, and Future Work 178
11.1 Conclusions and Contributions . . . 179
11.2 Future Work . . . 181

List of Figures

1.1 A holistic approach to power engineering research 5
1.2 Simple local nodes interacting with the remote node 7

2.1 Rural house modeled as an energy hub 18
2.2 Microgrid in the village of Shisawli 22
2.3 Microgrid network diagram 23
2.4 Recommended number of lights with variation in weather: When sufficient insolation is available, no kerosene lights recommended. This agrees with the popular findings that electric lights are more economical than kerosene and do not degrade indoor air quality. 24
2.5 Bus voltage with variation in weather: When solar insolation is sufficient, all illumination load is served by electricity leading to more voltage drop across the radial distribution line. 25
2.6 Recommended cooking fuel use with variation in firewood cost 25

3.1 Medical load scheduler block diagram 39
3.2 Switching state of medical devices during the outage 44

4.1 Racine field visit and the summer solar makeathon 49
4.2 Electric Little Free Library prototype 50
4.3 Electric Little Free Library: power circuit 51
4.4 Electric Little Free Library: control circuit 51
4.5 Electric Little Free Library deployments 52

5.1 Illustration of an entity in a self-organizing local electrical energy network . 62
5.2 Phase-plane plot for System 1: system converges to $x = x_d$ 65
5.3 System 2: phase plane and Lyapunov function plots 66
5.4 System 2: x against time for two different initial conditions; system converges to $x_d = 0.5$ in both cases 67
5.5 System 1: x against time for two different initial conditions; system converges to $x_d = 0.3$ in both cases 69
5.6 System 1: Low demand case 70
5.7 System 1: High demand case 71
5.8 x against time for System 1 switching from low demand to high demand; system converges to the high demand case equilibrium of $x = 0.1$ 72
5.9 System 1: Instability when a source becomes a load 72

6.1 Sketch of a community scale microgrid with three electrical entities (EE) illustrating various layers of hierarchical control 78
6.2 Classes of entities and loads in the community microgrid 81
6.3 Energy price vs aggregate network energy as determined by the revenue/energy aggregator 83
6.4 Three-entity dc microgrid network 86
6.5 Entity-wise state of charge (SOC, top) and traces of load profile (bottom) without schedulers (left) and with schedulers (right); Critical load profile request in blue outline, solid when served, and non-critical load profile request in orange outline, solid when served. *Needs of the critical loads are fully met in all entities with DOS.* 88
6.6 Critical service factor, non-critical service factor, and revenue with and without optimal schedulers. *Critical service factor for all entities are improved, revenue seeker gets better revenue and service seeker gets better service with DOS* 88
6.7 Critical service factor (CSF), non-critical service factor(NCSF), and revenue for different β_r and β_s: *CSF for all entities remains at almost 100% irrespective of variation in β_r and β_s.* 90
6.8 Using β_r and β_s as user-defined control handles to vary service factors and revenue on a day to day basis 92
6.9 Weather parameter, critical service factor, non-critical service factor, and revenue with and without optimal schedulers and with variation in solar irradiance; *CSF improved for all entities at the expense of NSCF/revenue* . 94
6.10 Experimental Setup 95
6.11 Simulation and Hardware-in-the-loop results: From top to bottom - battery voltage, export current, revenue 96

7.1 Top: Wallet balance (blue) and load threshold (red) in $. Bottom: Enable signal for the load. A value of 1 indicates that the load can be turned on, while a value of 0 indicates that the load should remain off. 106
7.2 Load power demand for 30 days (W). 112
7.3 Service factor for the 4 loads and overall priority service factor (PSF) at a recharge frequency of 5 per month and recharge amount of 70%. Load priority: Load D > Load A > Load C > Load B 115
7.4 Top: PSF against recharge amount at a recharge frequency of 5 per month. Bottom: PSF against monthly recharge frequency at a recharge amount of 70%. 116

8.1 Illustration of virtual wallet recharge 123
8.2 Perfect forecast: Percentage point (%pt.) improvement in priority service factor (PSF) over baseline for the proposed AFG model (blue) and the benchmark models DFM (red) and OBM (green) 134
8.3 Imperfect forecast: Priority service factor (PSF) and customer disconnections (indicated by 'x' mark) for the proposed model AFG (blue), the benchmark models DFM (red), OBM (green), and the baseline BSL model (purple) 137

9.1 A sketch of microgrid architectures 141
9.2 A sketch of layers of the Picogrid platform 144
9.3 Pico board block diagram. The inputs to and outputs from the energy manager are: $\mathbf{v} = [v_{PV}\ v_{AS}\ v_{IM}\ v_{CE}\ v_{BO}]$, $\mathbf{i} = [i_{PV}\ i_{AS}\ i_{IM}\ i_{CE}\ i_{L1}\ i_{L2}\ i_{L3}\ i_{EX}]$, $\mathbf{u} = [u_{PV}\ u_{AS}\ u_{IM}\ u_{L1}\ u_{L2}\ u_{L3}\ u_{EX}]$. (Labels: PB = Pico board, PV = PV Source channel, AS = Auxiliary Source channel, IM = Import channel, CE = cell, CH = charger, BO = boost converter, EM = energy manager, L1 = Load 1 channel, L2 = Load 2 channel, L3 = Load 3 channel, EX = Export channel) 145
9.4 Photograph of a Pico board that represents a prosumer entity with sources, loads, storage, import/export channels, and an energy manager. 145
9.5 Photograph of multiple Pico boards that fit easily on a lab bench. 148
9.6 Screenshot of the cloud dashboard showing a Pico board data channel . . . 149
9.7 Variation in unit price of a Pico board with number of units 150
9.8 Power variation across PV, Load 1, Load 2 obtained experimentally matches closely with that from the dataset 150
9.9 Energy supplied by PV and consumed by Loads 1 and 2. Values indicated on top of simulation and experiment bars represent percentage error with respect to the dataset 152
9.10 Top: State of charge (*soc*) variation and load thresholds. Bottom: Load current. Loads are switched off when the *soc* is less than their respective thresholds. 154
9.11 Experimental setup showing three radially connected Pico boards 155
9.12 Simulation and experimental results (clockwise from top left in each subfigure: Load 1 current, state of charge, Import current, Export current) for a network of three prosumers. Plots show that the simulation model can effectively represent the behavior of the hardware. 156

10.1 Photograph of a Pico board, highlighting important components 163
10.2 Sketch of data pipeline between Pico boards and cloud dashboard 163
10.3 Screenshot of Data Retrieval Page: Waveform of selected quantity (PV Voltage) during the selected interval (14:00-14:55 May 14, 2024) from the selected board (Co). 164
10.4 Screenshot of Setpoint Input Page for selecting threshold levels for Photo-Voltatic (PV) and Utility Source (US) channels, import (IM) and export (EX) channels, and load channels (Load 1 to 3) 165
10.5 Demonstration of a smart solar home system, where 20 minutes are mapped to a full day. Remote users managed sources (top: solar or from charger input) and loads (bottom) according to solar PV availability. 169
10.6 Sketch of VPP experimental setup illustrating hardware and simulated Pico boards, aggregator, cloud dashboard 170
10.7 VPP operation: Power consumption of a combination of hardware and simulated Pico boards was coordinated to track a target signal 171
10.8 Sketch of DR experimental setup illustrating hardware and simulated Pico boards, third-party users, utility, cloud dashboard 173

10.9 Top: User of Pico board on price-based DR reduced consumption during on-peak period between 16:00 and 21:00. Bottom: User of Pico board on incentive-based DR participated in direct load control during DR event from 16:00 to 20:00 175
10.10Photograph of a workshop facilitator showing a Pico board to participants . 176
10.11Photograph of the educational toolkit consisting of a Picoboard, 3D printed models of three appliances, and a device mat. Participants used the green area of the mat to indicate turning a device ON and the red area to indicate turning it OFF. 177

List of Tables

1.1 Research questions and methodology mapping 8

2.1 Case study parameter values 23

3.1 Specifications of loads served by the load scheduler 43

5.1 System 1: source specifications 64
5.2 System 1: load specifications 64

6.1 Effects of various discrete switching state functions 84
6.2 Power and energy specifications for 1hr case-study 87
6.3 Optimization Parameters for 1hr case-study 87
6.4 Power and energy specifications for the 24-hour and 5-day case studies . . . 90

7.1 Nomenclature 107
7.2 Load data 112
7.3 Energy Usage per Load 115

8.1 Nomenclature 122
8.2 Qualitative comparison of models 131
8.3 Perfect forecast: Percentage point improvement in priority service factor (PSF) over baseline for the proposed AFG model and the benchmarks DFM and OBM 135
8.4 Imperfect forecast: PSF in percent and improvement in PSF over baseline BSL in percentage points in parentheses for the proposed model AFG, the benchmarks DFM and OBM, and PSF and disconnection duration (# days) for the BSL model 136

9.1 Comparison of microgrid education and experimental platforms 143
9.2 Power scaling parameters 152
9.3 Δ_k values for each interval and load 154
9.4 Error in change in state of charge for each entity in the experiment as compared to that in the simulation is found to be under 6 % 157

Chapter 1

Introduction

1.1 Motivation

Access to a reliable electricity supply has been shown to play a vital role in supporting and advancing human development across emerging and developed economies [1–3]. The seventh sustainable development goal (SDG) proposed by the United Nations as a part of its 17 SDGs under the 2030 Agenda for Sustainable Development [4] is "Ensure access to affordable, reliable, sustainable and modern energy for all". In 2022, there were about 685 million people in the world without access to electricity [5]. The definition of "access to electricity" used by international statistics is "having an electricity source that can provide very basic lighting, and charge a phone or power a radio for 4 hours per day" [6]. Access to electricity does not necessarily ensure reliability of supply. Using the definition of a "reasonably reliable" supply as "a maximum threshold of 12 outages in a typical year and 12 hours of power outage per year", a 2020 study [7] estimated that there are almost 3.5 billion people globally without reasonably reliable access to electricity.

The electric utility industry metrics for measuring reliability are System Average Interruption Duration Index or SAIDI ("minutes of non-momentary electric interruptions, per year, the average customer experienced") and System Average Interruption Frequency Index or SAIFI ("number of non-momentary electric interruptions, per year, the average customer experienced") [8]. However, these metrics do not account for factors like the

causes of outages or the equity of their distribution across different communities [9]. It is important to consider such factors that account for the nuanced contexts of the end-users in order to design energy solutions that are sustainable, reliable, and affordable. A household may lack reliable access to electricity for various factors, including infrastructure issues, such as insufficient generation or equipment damage from extreme weather, or socioeconomic factors, such as unaffordability of services. In this study, the term *energy poverty* is used to refer to a lack of energy services due to absent or damaged infrastructure, while *energy insecurity* is used to denote the inability to meet energy needs due to socioeconomic constraints.

Various forms of energy poverty are experienced by households in emerging as well as developed economies. Emerging economies are working to extend electricity infrastructure to remote areas through grid expansion or off-grid solutions like microgrids and solar home systems, though these solutions often encounter reliability challenges [10, 11]. Developed economies have achieved complete electrification but are experiencing increasing disruptions due to increasing extreme weather events caused by climate change. In the United States, power outages caused by extreme weather events have doubled in the past decade and their duration and frequency are at their highest [12]. Similarly, energy insecurity is prevalent across different parts of the world. Along with outages due to insufficient solar irradiance and equipment failures, off-grid households served by pay-as-you-go solar microgrids can face outages when customers run out of energy credits [9]. Grid-connected customers are disconnected by the utility if they fail to pay bills in time. A million U.S. households were disconnected across 17 states between March 2020 to April 2021 despite the moratorium on disconnections due to the COVID-19 pandemic [13]. The U.S. Residential Household Energy Consumption Survey data for 2020 reported that 27% U.S. households experience some form of energy insecurity [14].

Energy poverty and insecurity are known to disproportionately affect historically underserved and vulnerable communities [15]. It follows that in addition to limitations on the energy that is available for such households, there are limitations on various factors that

potential energy access solutions need to account for. Households may not have sufficient disposable funds to spend on purchasing residential energy management hardware, such as smart home energy management systems (HEMS), and to pay for their maintenance. Rural areas in emerging economies often lack skilled technicians to service equipment. In remote areas, cellular communication infrastructure is often unreliable. Additionally, low-income households with overdue energy bills may also have outstanding internet bills. Consequently, energy access solutions should minimize reliance on frequent remote communication with cloud-based resources for computation. Residential demand is inherently volatile making it challenging to generate accurate granular forecasts. Ideally, end-users want a consistent and affordable electricity supply, greater control over their bills, and more awareness of their consumption. The goal of this thesis is to develop energy access frameworks, that meet these objectives for end-users, in environments with constraints on resources such as local computation and maintenance, remote communication, and demand forecasts.

1.2 Methodology

The first energy transition was driven by the Industrial Revolution and the shift to using electricity, a more efficient source of energy than wood. Consequently, energy access has traditionally been approached as a power engineering problem. However, this transition, heavily reliant on coal and other fossil fuels, led to significant environmental burdens, with vulnerable communities disproportionately affected by both environmental harms and unreliable energy access. With the current energy transition from fossil fuel-based generation to renewable energy sources, distributed energy resources, and digitization, it is essential that the transition is rooted in equitable access to clean energy. Therefore, in addition to power engineering tools, it is necessary to adopt a holistic approach to designing sustainable energy access frameworks.

The works presented in this thesis are based on steps outlined in this holistic approach, which is adopted from community-based participatory research frameworks [16]. The steps

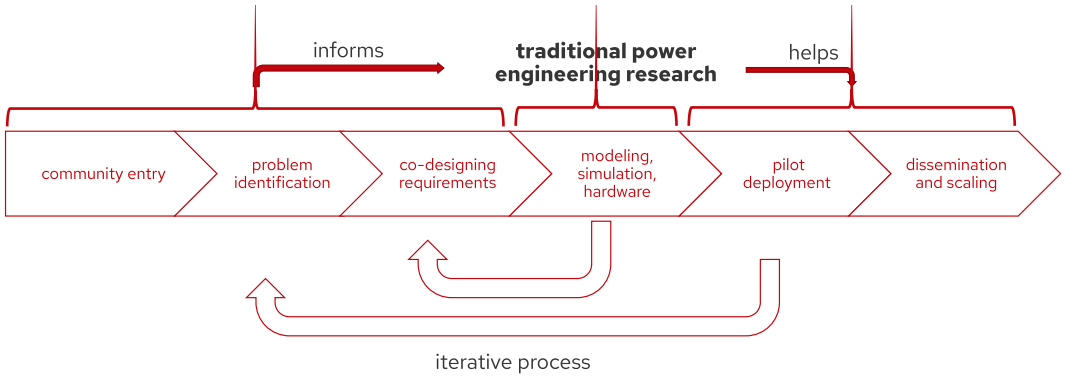

Figure 1.1: A holistic approach to power engineering research

in this framework are outlined in Figure 1.1. The first step is to establish a relationship and a sense of trust with the community of interest. Once the community consents to participation, the problem identification phase can include field visits and interviews to understand the context of the community and identify key problems. Next, researchers collaborate with the community and other stakeholders to identify requirements for potential solutions. The next step consists of analytical modeling, simulations, and/or hardware prototyping. Traditional power engineering research has expertise to execute this step but has often restricted its scope to this step. It is important to recognize the contributions of the first three steps in informing the problem that is solved by traditional power engineering research tools. In order to translate this research to real-world impact, the solution developed through these tools is then deployed through a pilot to gather feedback from the community. This is an iterative process, i.e., there can be multiple iterations between different steps before developing a solution that can be scaled. This approach enables development of solutions that solve community-identified problems, cater to the nuanced requirements of the end-users, and are therefore more sustainable. Thus, this approach facilitates translational power engineering research.

The ideas of community-engaged research are reflected in the field experiences presented in this thesis. Field experiences in the following three contexts significantly contributed to the motivation for the work in this thesis: energy access in rural Indian communities, energy resilience for home healthcare in the United States, and energy access

for people experiencing homelessness in Wisconsin; these are presented in Part I. These contexts are chosen since they reflect experiences across diverse environments in emerging and developed economies. Each context presented a set of unique as well as overlapping challenges, requirements, and open questions for energy access frameworks. The challenges that generalize across the three contexts are listed as follows:

- Hardware heterogeneity: The framework has to work with heterogeneous hardware components including microcontrollers, meters, inverters, chargers, storage devices, with minimal requirements for additional custom hardware.
- Topology independence: The framework has to work with minimal or no information about the topology of the electrical network and support ad hoc operation.
- Intermittent remote communication: The framework has to work with intermittent and slow remote communication infrastructure.
- Multi-objective driven management of limited energy: The framework should support multiple objectives of each household such as energy expenditure and serving critical loads.
- Uncertainty mitigation: The framework should reduce the uncertainty of outages and energy availability for critical needs.
- Hardware experimental platforms: The need for hardware-based experimental verification was identified, highlighting that the framework should be demonstrated on hardware platforms to facilitate translation to real-life deployments.
- Energy education platforms: The need for energy education platforms and energy literacy was identified to facilitate adoption of such frameworks.

The generic framework proposed in this thesis for energy access in resource-constrained environments, that addresses the aforementioned requirements and challenges, is depicted in Figure 1.2. The local nodes represent end-users such as households in grid-connected or off-grid communities. Each local node has basic computation, communication, and control capabilities and is responsible for the *necessary* requirement of stable operation of the entity. The remote node represents a load serving entity with advanced computation

capabilities, such as a remote server of an electric utility or microgrid operator. It is responsible for the *desirable* requirement of optimal operation of all entities.

For reliable operation of a local node irrespective of the state of communication infrastructure, local nodes need to be primarily responsible for their own operational stability, i.e., decision-making at the local level should not have the remote node in the critical path, but the remote node can inform local decision-making through set points communicated on a slower timescale. Therefore, simple computation, control, and communication hardware at the local nodes is necessary. The local hardware is limited by the aforementioned constraints such as purchasing power of the end-users and access to skilled technicians for maintenance.

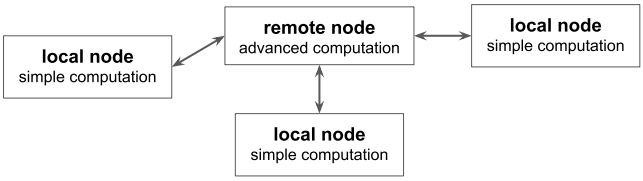

Figure 1.2: Simple local nodes interacting with the remote node

1.3 Document Organization

Part I of this thesis presents field experiences utilizing the workflow summarized in Figure 1.1. Parts II, III, and IV focus on traditional modeling, simulation, and hardware prototyping steps of the workflow, proposing frameworks that adhere to the overarching architecture and theme of the generic framework shown in Figure 1.2. A literature review focused on the specific environment targeted by each part is included within the respective chapters. Although Parts II, III, and IV design frameworks for environments that may differ from those in Part I, some requirements overlap across these environments while also presenting unique challenges. Table 1.1 shows the mapping between the questions identified in Part I that generalize across environments and are addressed by investigations presented in Parts II, III, and IV of this thesis.

Part I presents field experiences in three contexts, and they are organized into the

Table 1.1: Research questions and methodology mapping

Research questions	Part II	Part III	Part IV
hardware heterogeneity	×	×	
topology independence	×		
intermittent remote communication	×	×	
multi-objective driven limited energy management		×	
uncertainty mitigation		×	
hardware experimental platforms			×
energy education platforms			×

following chapters.

- *Chapter 2* – energy access in off-grid rural communities in India
- *Chapter 3* – energy resilience and home healthcare in the United States
- *Chapter 4* – energy access and homelessness in Wisconsin

In each context, the problem is identified through conversations with end-users, community organizations, and other stakeholders. The features of a potential technology-based solution that can address the problem are identified. Further, a proof-of-concept hardware/software prototype of the solution and/or a proposal for a more thorough solution is developed. Through this process, requirements for more robust energy frameworks and research questions that this study aims to address in *Parts II*, *III*, and *IV* are identified.

Part II presents threshold-based energy management as an energy access framework for different resource-constrained environments.

- *Chapter 5* presents stability studies for threshold-based energy management.

- *Chapter 6* presents an application of threshold-based energy management to community-scale microgrids through numerical simulations and a hardware-in-the-loop experiment.

Part III presents models for optimizing thresholds and applies the threshold-based energy management framework to the context of low-income prepaid electricity customers.

- *Chapter 7* presents a mixed-integer linear program-based optimization model for home energy management for prepaid electricity customers.
- *Chapter 8* presents a linear program-based optimization model that can be implemented using simple computation hardware and only daily average demand forecasts.

Part IV presents Picogrid, a low-cost experimental platform that can be used for hardware validation of energy access frameworks and energy education.

- *Chapter 9* presents the Picogrid platform's hardware and software features.
- *Chapter 10* presents a cloud-based solution for remote access to the Picogrid platform. Additionally, it presents a real-world example of how the Picogrid platform was used in a community workshop.

Chapter 11 summarizes the contributions of this study and presents avenues for future work.

1.4 Background Papers and Reports

The following papers and reports relate to contributions that fall within the scope of this thesis († equal contribution):

- V. Balan†, **M. Marathe**†, and G. Venkataramanan, "A Cloud-Based Solution for Remote Access to a Microgrid Experimental Platform," accepted to the *2024 IEEE International Conference on Power Electronics Drives and Energy Systems*, Surathkal, India

- **M. Marathe** and L. A. Roald, "Energy Management for Prepaid Customers: A Linear Optimization Approach," *2024 IEEE International Conference on Communications, Control, and Computing Technologies for Smart Grids*, Oslo, Norway, 2024

- **M. Marathe** and G. Venkataramanan, "Picogrid: An experimental platform for prosumer microgrids," *2023 IEEE Energy Conversion Congress and Exposition*, Nashville, Tennessee, 2023, pp. 718-725

- **M. Marathe** and L. A. Roald, "Optimal Energy Rationing for Prepaid Electricity Customers," *2023 IEEE Belgrade PowerTech*, Belgrade, Serbia, 2023, pp. 01-06

- **M. Marathe** and G. Venkataramanan, "Distributed Optimal Scheduling in Community-Scale Microgrids," *2021 IEEE Energy Conversion Congress and Exposition (ECCE)*, Vancouver, BC, Canada, 2021, pp. 833-840

- B. Bondi†, S. Bradshaw†, **M. Marathe**†, and W. Keenan†, "Electric Little Free Library: Solar Kiosks for Energy Access," 2022. smplabs.wisc.edu/electric-little-free-library

- **M. Marathe** and A. Manur, "Energy Resilience for Home Healthcare.", 2020, smplabs.wisc.edu/nsf-icorps/.

The following papers and reports constitute background contributions informing this thesis and are not included in this document († equal contribution):

- P. Kourtza†, **M. Marathe**†, A. Shetty†, and D. Kiedanski, "Identification of medical devices using machine learning on distribution feeder data for informing power outage response." To appear in the Tackling Climate Change with Machine Learning workshop at NeurIPS 2022 (Proposals Track), `arxiv.org/abs/2211.08310`, 2022.

- D. Sehloff, **M. Marathe**, A. Manur, and G. Venkataramanan, "Self-Sufficient Participation in Cloud-Based Demand Response," IEEE Transactions on Cloud Computing, vol. 10, no. 1, pp. 4–16, 2021.

- A. Manur, **M. Marathe**, and G. Venkataramanan, "A Distributed Approach for Secondary and Tertiary Layer Control in DC Microgrids," *2020 IEEE Energy Conversion Congress and Exposition (ECCE)*, Detroit, MI, USA, 2020, pp. 1284-1291

- A. Manur, **M. Marathe**, A. Manur, A. Ramachandra, S. Subbarao, and G. Venkataramanan, "Smart Solar Home System with Solar Forecasting," in 2020 IEEE International Conference on Power Electronics, Smart Grid and Renewable Energy (PESGRE2020), pp. 1–6, IEEE, 2020.

Part I

Field Experiences

Energy access is not limited to the technology that underlies energy infrastructure. Multiple factors such as user experience and the prevalent socioeconomic factors influence the success and sustainability of energy access solutions. The complexity of the problem and the dearth of meaningful and definitive publications within traditional literature calls for detailed investigative methods to address these problems. This part summarizes three different fieldwork efforts undertaken to understand these challenges and presents proof-of-concept solutions to address some of them as well as proposals for more thorough analyses. These proof-of-concept efforts can be considered 'low-fidelity' or 'jugaad' prototypes [17] that provide preliminary insights into the problem by engaging with stakeholder communities. Some of this work was performed as a part of team projects and has been identified in the text. The objective of the chapters in this part is to provide context for the assumptions made, requirements considered, and research questions addressed in the investigations and frameworks presented in Parts II, III, and IV. The research questions identified in each chapter of this part are collectively summarized at the end of the part. Each chapter explores energy access through a different lens as summarized below.

Energy access for rural communities is explored through the lens of communities in rural India. This is based on fieldwork undertaken by the author with a team prior to graduate school. Based on this fieldwork, a model to propose an optimal energy mix for a rural Indian household using different energy sources, viz. electricity, kerosene, and wood is designed and results from numerical simulations are presented.

Energy resilience and home healthcare is explored through the lens of individuals in the United States who are dependent on in-home medical devices. Over 100 interviews were conducted by the author and team with stakeholders through the National Science Foundation's Innovation Corps program. Insights from these conversations include the end-user archetype and factors influencing their concern for power outages. A need for in-home energy backup is identified. Based on these insights, a proposal for a table-top exercise is presented to further understand the detailed energy requirements of the medically fragile community. A load scheduler for medical loads connected to an in-home

energy storage system is designed and validated through numerical simulations.

Energy access and homelessness is explored through the lens of people experiencing homelessness in Wisconsin. Insights from field visits and interviews conducted by the author and team are discussed. The hardware prototype development and deployment process for the Electric Little Free Library, a potential solution for this application, is described. The successful field deployment of this solution led to a legislative change in the City of Madison's zoning laws which legalized the use of Electric Little Free Libraries. This project acts as a roadmap for community engagement, prototype development, and legislation for other cities and communities to undertake similar projects.

Chapter 2

Energy Access and Off-Grid Rural Communities

The author was a part of a team from the National Institute of Engineering, Mysuru and University of Wisconsin-Madison that visited villages in different parts of India to study existing microgrids and study the feasibility of setting up microgrids in villages with unreliable or no access to electricity [18]. The team also set up solar home systems in two urban and one rural household [19]. This work inspired the following proof-of-concept optimization model to compute the optimal energy mix to be used in a rural household powered by a microgrid. The author acknowledges contributions by Aayushi Singh to the literature review and in determining parameter values for the case study. The requirements and research questions for energy frameworks identified from this fieldwork are presented in the concluding section of Part I.

2.1 Introduction

Despite the rapid growth in electrification in recent years in rural India, there is heavy dependence on kerosene for lighting. Kerosene is known to pose numerous serious health risks such as lung impairments and burns [20]. However, studies have found 9% of electrified households surveyed across six states in 2018 to rely on kerosene as their primary fuel.

One of the main reasons behind the use of kerosene as primary fuel even with an electricity connection being present has been dissatisfaction due to unreliability in electricity supply [21]. Villages in remote areas and forest reserves cannot be connected to the main power grid as running power lines to such areas is either not economical or not permitted in nature reserves. Such villages are often electrified through off-grid microgrids based on solar PV and storage. Problems of unreliability are seen in the case of such remote microgrids as well [22]. India experiences monsoon for about four months and there can be multiple days with continued poor solar irradiation due to cloud cover. The batteries in such microgrids get drained and this compromises the reliability of electricity supply. To address this problem, systems are often oversized and the electricity rate of such systems without subsidies can be as high as ₹50/kWh which is almost 10 times the rate paid by grid-connected customers [23]. This leaves residents with no choice but to resort to unclean fuels such as kerosene and firewood.

The driving question of this study is as follows: *How to reduce dissatisfaction with energy service (electricity+kerosene+wood) in an off-grid village supplied by a solar PV and storage based microgrid without oversizing it?* This study proposes a model to account for multiple energy carriers in a typical rural Indian community, taking into account multiple parameters such as cost of each energy carrier, weather, and indoor pollution. The model answers the question of what energy mix should each household use in order to minimize cost of energy while maintaining healthy limits on air quality without exceeding electric power use limits. A case study of an off-grid village powered by a solar PV+storage based microgrid is discussed. The PV+storage capacity is designed such that it is 'just enough' - it does not account for autonomous operation, i.e., it cannot supply loads for more than a day without adequate sunlight. Each house uses kerosene, firewood, and electricity from the microgrid to meet its illumination and cooking demands.

The model uses the energy hub concept [24] which has been used to model power flows in multi-energy carrier systems. An energy hub is defined as "a unit that provides the basic features in- and output, conversion, and storage of different energy carriers". This concept

has been used to model energy use in urban residential entities with in-home combined heat and power units, plug-in hybrid electric vehicles, time-of-use electricity pricing, thermal energy storage, demand response, and other modern day technologies [25], [26]. It has also been used to model community microgrids [27], [28]. However, a majority of these studies incorporate high-end technologies, with power consumption in the kW to MW range, and are based in the urban context. This study is set in the context of rural off-grid communities powered by microgrids with power consumption in the order of 10s of watts per house. Section 2.2 presents the modeling considerations for representing residential energy use as an energy hub. Section 2.3 outlines the optimization problem. Section 2.4 presents results from a case study of an off-grid village powered by a PV+storage based microgrid.

2.2 Rural Household as an Energy Hub

Consider a rural house with energy inputs in the form of electricity, kerosene, and wood as shown in Figure 2.1. Wood and firewood will be used interchangeably in this study and both refer to the wood used for cooking. Unlike the conventional energy hub models, the loads are modeled in terms of end-use function instead of electric/thermal parameters. The two loads are illumination (L_i) measured in terms of lux.hours or $lx.h$ and cooking (L_c) measured in terms of $person.meal$, i.e., the energy required to make one meal for one person. The inputs are electricity (P_e) in Wh, kerosene (P_k) in grams or g, and wood (P_w) in g. Note that the inputs and loads are in terms of energy or mass and not power. The inputs are converted to outputs through devices such as lamps and stoves and these devices are modeled as converters. The first converter represents light emitting diode (LED) bulbs with a converter efficiency (η_{ei}) equal to the ratio of useful $lx.h$ generated to Wh consumed. The second converter represents kerosene pressure lamps with a converter efficiency (η_{ki}) given by useful $lx.h$ generated to g of kerosene consumed. The third converter represents a kerosene kitchen stove with a converter efficiency (η_{kc}) equal to $person.meals$ cooked to g of kerosene consumed. The fourth converter represents an earthen stove used to burn

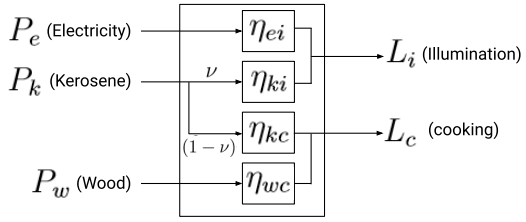

Figure 2.1: Rural house modeled as an energy hub

firewood with the converter efficiency (η_{wc}) given by the ratio of $person.meals$ cooked to g of wood consumed. The dispatch factor ν represents the ratio of kerosene consumed by lamps to the total kerosene consumed and $(1-\nu)$ represents the ratio of kerosene consumed by the stove to the total kerosene consumed. The energy balance is represented by Equation 2.1.

$$\begin{bmatrix} L_i \\ L_c \end{bmatrix} = \begin{bmatrix} \eta_{ei} & \nu\eta_{ki} & 0 \\ 0 & (1-\nu)\eta_{kc} & \eta_{wc} \end{bmatrix} \begin{bmatrix} P_e \\ P_k \\ P_w \end{bmatrix} \tag{2.1}$$

2.3 Optimization Problem Formulation

$$\min_{\mathbf{n}_i^k, \mathbf{n}_i^e, \mathbf{w}_i^k, \mathbf{w}_i^w} \quad \sum_i (\alpha^k \mathbf{n}_i^k + \alpha^e \mathbf{n}_i^e) T_i + \alpha^{kc} \mathbf{w}_i^k + \alpha^w \mathbf{w}_i^w \tag{2.2a}$$

$$\text{s.t.} \quad E^k \mathbf{n}_i^k + E^e \mathbf{n}_i^e \geq E N_i \qquad \forall i \tag{2.2b}$$

$$\frac{\mathbf{w}_i^w}{\beta^w} + \frac{\mathbf{w}_i^k}{\beta^k} \geq 2N_i \qquad \forall i \tag{2.2c}$$

$$\frac{1}{N_i V}(\mathbf{n}_i^k c^k \frac{T_i}{24} + \mathbf{w}_i^w c^w \frac{T^{cw}}{24} + \mathbf{w}_i^k c^{ck} \frac{T^{ck}}{24}) + C^a \leq C^{max} \qquad \forall i \tag{2.2d}$$

$$\mathbf{p}_{mn} = -\mathbf{p}_n + \sum_{r:n \to r} \mathbf{p}_{nr} \tag{2.2e}$$

$$\mathbf{q}_{mn} = -\mathbf{q}_n + \sum_{r:n \to r} \mathbf{q}_{nr} \tag{2.2f}$$

$$|\mathbf{v}_n|^2 = |\mathbf{v}_m|^2 - 2(R_{mn}\mathbf{p}_{mn} + X_{mn}\mathbf{q}_{mn}) \tag{2.2g}$$

$$\mathbf{p}^s \leq P^{max} \tag{2.2h}$$

$$\mathbf{n}_i^k, \mathbf{n}_i^e, \mathbf{w}_i^k, \mathbf{w}_i^w \geq 0, \quad \mathbf{n}_i^k \tag{2.2i}$$

Parameters

α^k := cost of using kerosene per lamp per hour

α^e := cost of using electricity per LED bulb per hour

T_i := duration of illumination demand in house i

α^{kc} := cost of kerosene per unit mass

α^w := cost of wood per unit mass

E^k := luminous flux per kerosene lamp

E^e := luminous flux per LED bulb

E := minimum luminous flux necessary per person

N_i := no. of residents in house i

β^w := amount of wood necessary to cook one person.meal

β^k := amount of kerosene necessary to cook one person.meal

V := volume of a typical room in a house per capita

c^k := PM2.5 emission rate per kerosene lamp

c^w := PM2.5 emission rate per unit wood burnt in stove

T^{cw} := typical duration of cooking with wood per person.meal

c^{ck} := PM2.5 emission rate per unit kerosene burnt in stove

T^{ck} := typical duration of cooking with kerosene per person.meal

C^a := ambient PM2.5 concentration in areas using kerosene lamps

C^{max} := upper limit on PM2.5 concentration according to health guidelines

R_{mn}, X_{mn} := resistance and reactance of line mn respectively

P^{max} := maximum power rating of microgrid

Variables

$\mathbf{n}_i^k$:= no. of kerosene lamps used in house i

$\mathbf{n}_i^e$:= no. of LED bulbs used in house i

$\mathbf{w}_i^k$:= mass of kerosene used for cooking in house i

$\mathbf{w}_i^w$:= mass of wood used in house i

$\mathbf{p}_{mn}, \mathbf{q}_{mn}$ = active and reactive power flows from bus m to n respectively

$\mathbf{p}^s$:= power supplied by microgrid

$\mathbf{p}_n, \mathbf{q}_n$:= active and reactive power injections at bus n respectively

$\mathbf{v}_n$:= voltage at bus n

The optimization problem is given by 2.2. The problem minimizes the cost of energy for a given day and the decision variables are the number of kerosene lamps, number of LED bulbs, mass of kerosene, and mass of wood used on the day. Equation 2.2(a) gives the objective function in terms of cost of energy in ₹. Equations 2.2(b) and 2.2(c) are a modified form of Equation 2.1. In the context of the illumination load, it is assumed that the number of spots to be illuminated with minimum useful lux is equal to the number of residents of the house, as indicated in 2.2(b). It is assumed that 2 meals per person per day are cooked in each house, and hence the cooking load is given by $2N_i$ as shown in 2.2(c). Upper limits on 24 hour average indoor pollution in terms of PM2.5 concentration

(concentration of particulate matter with width less than $2.5\mu m$) is given by 2.2(d). The amount of PM2.5 released due to using $\mathbf{n}_i^k$ kerosene lamps for T_i hours averaged over 24 hours $\mathbf{n}_i^k c^k T_i/24$. The next two terms represent the same quantity for wood and kerosene used for cooking respectively. It is assumed that the number of rooms in each house equals the number of residents N_i. The average amount of PM2.5 released during 24 hours due to the kerosene and wood is divided by $N_i V$ which is the number of rooms multiplied by the volume of a room in a typical rural house. This gives the average increase in PM2.5 concentration due to these fuels which is then added to C^a, a conservative estimate of the ambient concentration in regions which use kerosene or wood. LinDistFlow constraints are given by 2.2(e)-(g). The limit on the amount of electric power that can be drawn from the microgrid is given by 2.2(h), since it is not oversized to account for additional days of autonomous operation without adequate sunlight.

The driving question of the study is to reduce dissatisfaction with energy supply. This study does not claim 24x7 electricity supply through the microgrid but provides information about when to expect a disruption and resort to other fuels like kerosene. It uses the battery state of charge to determine the amount of power that can be supplied through the microgrid during the illumination demand duration. If this power is not enough, it recommends adequate number of kerosene lamps to be used to satisfy the demand while maintaining limits on indoor pollution. It calculates this optimal energy mix on a daily basis so that residents can plan ahead and purchase kerosene and/or collect firewood. This can result in reduced dissatisfaction due to uncertainty around electricity supply among families, and can prevent them from totally switching to kerosene and firewood as their primary source of fuel.

(a) PV panels (b) Distribution wires

Figure 2.2: Microgrid in the village of Shisawli

2.4 Case Study

2.4.1 Setup

This section presents the results of a case study based on the village of Shisawli, near the city of Mumbai in western India. The author was a part of team that visited this village through a microgrid field study project [18]. It is an off-grid village of 43 houses and is powered by a PV+storage based microgrid, set up by the energy service company Gram Oorja, as shown in Figure 2.2. Each house has been provided with 5W LED bulbs and power outlets. The parameter values for the energy hub model for this case study are given in Table 2.1. Village-specific parameters are either approximated based on the conversations the author had with residents during the field visit or are obtained from different sources in literature as indicated. The minimum luminous flux necessary per person (E) is assumed to be 200 lx/lamp, a value between E^k and E^w, and can be modified according to the requirements of the tasks being performed such as reading and cooking.

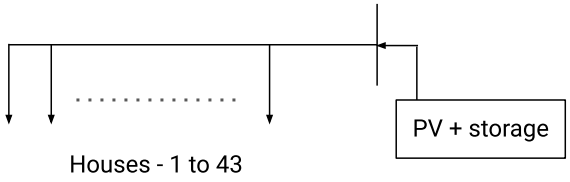

Figure 2.3: Microgrid network diagram

Parameter	Value	Reference
α^k	(65 ₹/L)(17 g/lamp-hour)(1L/800g)	[29, 30]
α^e	(5W/bulb)(0.01 ₹/Wh)	
T_i	min=2h, max=4h	
α^{kc}	(65 ₹/L)(1L/800g)	[30]
E^k	76 lx/lamp	[31]
E^e	300 lx/lamp	[31]
E	200 lx/lamp	
N_i	min=1 person, max=4 persons	
β^w	274 g/person.meal	[32]
β^k	35 g/person.meal	[32]
V	$(7.14\ m^2)(2.75\ m^3)$	[33], [34]
c^k	$(500\ \mu g/m^3)(6.34\ m^3)$	[29]
c^w	$6.3\ g/kg$	[35]
T^{cw}	1.375h	[32]
c^{ck}	0.29g/kg	[36]
T^{ck}	2h	[32]
C^a	$10\mu g/m^3$	[29]

Table 2.1: Case study parameter values

The PV+storage system capacity is assumed to be just enough to supply all the illumination load for the given duration for only one day and no additional days of autonomous operation without adequate sunlight. Accordingly the PV rating and storage capacity are calculated to be 700 W and 4 kWh respectively. The network topology is assumed to be radial as shown in Figure 2.3.

The optimization problem is implemented in Julia using the mathematical programming package JuMP [37] and the CBC solver. Results for variation in weather and the cost of wood are presented.

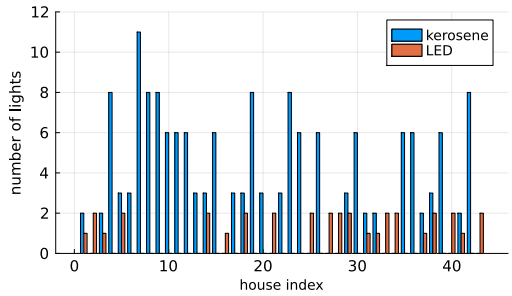

(a) 25% power output from microgrid (poor solar insolation)

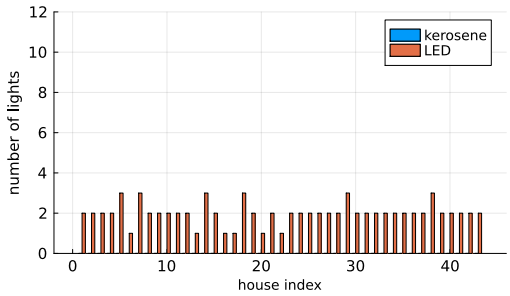

(b) 100% power output from microgrid (sufficient solar insolation)

Figure 2.4: Recommended number of lights with variation in weather: When sufficient insolation is available, no kerosene lights recommended. This agrees with the popular findings that electric lights are more economical than kerosene and do not degrade indoor air quality.

2.4.2 Variation in weather

Variation in weather is modeled as reduction in the power output from the microgrid. Figures 2.4b and 2.4a show the recommended number of lights to be used in each house for two cases - (a) when it has been cloudy and only 25% of the rated power from the microgrid can be used, (b) when there is sufficient solar insolation and 100% of the rated power from the microgrid can be used. In the 25% case, most houses use at least one kerosene lamp and at most two electric lights. In the 100% case, no house uses a kerosene lamps and all illumination load is served by electric lights. This agrees with the popular findings that electric lights are a more economical option to meet the same illumination load and do not contribute to indoor air pollution. Figure 2.5 shows the bus voltages in both the cases. The voltage drop at bus 1, i.e., the bus farthest from the PV+storage bus, in the 25% case is smaller as most of the load is met by kerosene.

2.4.3 Variation in the cost of firewood

Figures 2.6a and 2.6b show the impact of varying the cost of firewood on the recommended optimal amount of kerosene and firewood to be used for cooking in each house. Firewood does not have any rupee amount associated with it as it is generally collected from nearby forests. But it does have an opportunity cost as people spend time going to the forests

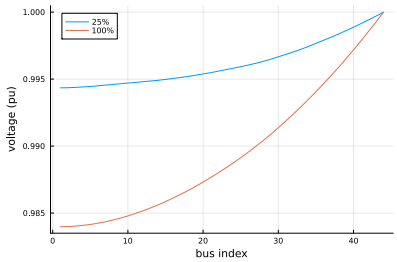

Figure 2.5: Bus voltage with variation in weather: When solar insolation is sufficient, all illumination load is served by electricity leading to more voltage drop across the radial distribution line.

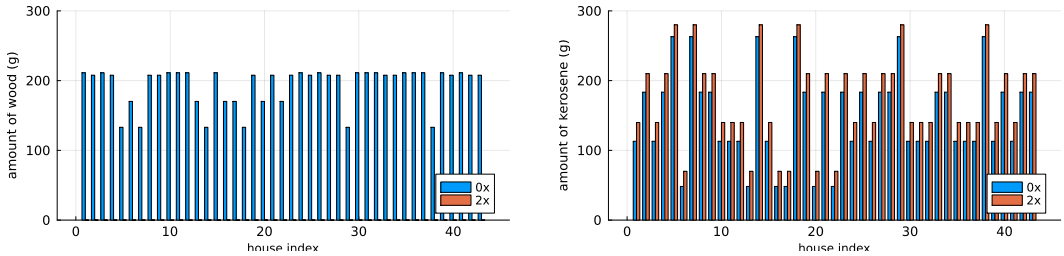

(a) Amount of firewood for cooking

(b) Amount of kerosene for cooking

Figure 2.6: Recommended cooking fuel use with variation in firewood cost

while they could be working on their farms or at other jobs. Two cases are presented. The first case assumes no cost associated with firewood ("0x") while in the second case, the rupee amount associated with firewood is such that it will cost twice the amount of money to make one meal for one person using firewood as it would by using kerosene stoves ("2x"). Figure 2.6a shows that in the 2x case, no wood use is recommended and the entire cooking load is satisfied using kerosene. Therefore, as seen in Figure 2.6b, more kerosene use is recommended in the 2x case as compared to the 0x case.

Note that in both the cases presented above (variation in weather and cost of wood), The PM 2.5 concentration limit was assumed to be 30 times the WHO Interim target-1 guideline of $75\mu g/m^3$ [38] for the problems to remain feasible. One of the reasons can be the heterogeneity in the sources of data used and the errors in the approximations. A subject of future work can be using data from a single community to generate recommendations for fuel use.

2.5 Conclusion and Future Work

This study presents a framework for last-mile delivery of energy in rural off-grid households. It presents a holistic approach for modeling energy flows in a rural household using the energy hub concept. It provides a systematic optimization-based method to balance cost, reliability, and health concerns in energy provision. It provides a-priori knowledge of resource availability and may reduce dissatisfaction with electricity supply. This can prevent households from relying only on fossil-fuels, thereby improving indoor air quality and reducing energy expenditure.

Some limitations of the model and avenues for future work are presented below. The model assumes perfect knowledge of illumination and cooking demand as well as microgrid power output. It assumes that illumination and cooking demand is constant throughout the day. Some challenges with the implementation of this model include user compliance with recommendations and availability of computation/communication infrastructure to solve the model. Future work includes studying the model performance under different scenarios varying parameters. This model can also be extended to include other commonly used energy sources such as dung and biogas. The presented framework is modeled as an operation problem. The problem can also be addressed as a planning problem to provide recommendations such as optimal sizing for the PV + storage microgrid, whether a house should invest in a kerosene stove or an earthen firewood stove, and the number of LED bulbs and kerosene lamps that a household should purchase. Further, the model can account for non-energy costs such as user inconvenience, health, and other socio-economic factors.

Chapter 3

Energy Resilience and Home Healthcare

In the United States, the number of power outages due to extreme weather events has doubled in the last two decades while the duration and frequency of outages is at their highest [12]. This number is expected to further increase as climate change-driven extreme weather events increase and continue to hamper the operation of the aging power grid. Reliable and resilient delivery of electricity is a challenge and this can compromise delivery of many essential services including healthcare. This challenge is compounded by the recent shift towards delivering healthcare at home, i.e., *home healthcare*, a trend that was accelerated through the global COVID-19 pandemic. Nation-wide, there are at least 4.4 million people who rely on in-home electricity-dependent medical devices and services, such as ventilators, oxygen concentrators, and feeding pumps [39]. This number represents only Medicare beneficiaries and there are estimated to be millions of more such individuals covered by other insurances. It is estimated that between 70,000 to 180,000 children fall into this category as well [40]. A home healthcare patient can be dependent on multiple electricity-powered in-home medical devices, and a power outage can pose severe health hazards. Energy resilience and healthcare have been studied in-depth separately. Their interdependence, especially in the context of in-home delivery of healthcare, remains a

largely unexplored space.

Existing solutions for powering medical devices during outages include fuel-based generators, but they are often unsuitable considering the risks with carbon monoxide poisoning, fuel availability and storage, and are not an option for those living in apartments. Solar photovoltaic (PV) and battery based solutions, can overcome some of these problems. The Energy Assurance Kit (EAK), an energy assurance platform based on microgrid technology for powering critical infrastructure during outages, was developed by former students from the research group of which the author is a member. It is the size of a suitcase, has in-built battery storage, can be powered through solar panels, and has a monitoring and control platform that provides a portal for external connection to electricity loads, fuel-based generators, and phone-charging ports [41], [42]. It has the capacity to become a self-organizing electrical energy network with assured availability of power [43]. Solar and battery storage based systems have been used extensively for remote electrification in developing economies [44]. The EAK and its underlying technology have been used to power an office building in India [18] and to power solar home systems for households with unreliable or no access to electricity [19]. The author was a part of a team that applied to the National Science Foundation's Innovation Corps (I-Corps) [45] program in order to explore the EAK's application in the context of home healthcare in the United States and understand the problem and the nuanced requirements through conversations with different stakeholders. The award supports academic groups looking at commercializing their research by training them in the basics of the Business Model Canvas [46, 47] and populating this canvas through inputs from potential customers and other stakeholders through the customer discovery process [48]. Through this process, a technology developer "gets out of the building" and talks to potential end-users to determine if there is a problem that their technology addresses and if yes, then how pressing is this problem, what value does the technology deliver, who in the ecosystem will pay for it, etc. The customer discovery process helps the developer understand the different aspects of the business model canvas for their technology.

The insights from I-Corps are summarized in the following section. A detailed report of the insights can be found in [49]. This is followed by a proposal for a table-top exercise to understand detailed and nuanced requirements of the medically fragile community. Further, a load scheduler, an add-on for the EAK to improve its utility, is presented.

3.1 Insights from the NSF I-Corps Program

There can be different underlying conditions that can require an individual to receive healthcare at home. Since this space is vast, the team focused on two groups which were perceived to have the greatest need - children who have undergone a tracheostomy and their families ("trach children" and "trach families" respectively) and mobility impaired adults. This section will present insights in the context of trach families. Trach children can use some or all of the following devices for their day-to-day health needs - ventilator, oxygen concentrator, suction machine, humidifier, feeding pump, nebulizer, pulse oximeter.

3.1.1 Top Concerns

The team would begin an interview with trach families by asking about their top three concerns. Some of the recurring themes are presented: (1) Medical device malfunctioning or getting disconnected, (2) Medical emergencies such as formation of mucus plug and ability/inability of the parents and caregivers to take appropriate action or find help in time, (3) Power outage, when it occurs, is a very unexpected emergency. Rigorous training in the hospital to home transition phase or in the individual care plan is not available. (4) Preemptive concern and anticipatory anxiety. There is a large amount of uncertainty and a feeling of helplessness in their day-to-day lives which can be very challenging.

It is necessary for the EAK or any product catering to this end-user group to take into account these nuanced concerns. While studying end-user requirements, it is essential to speak their language and understand their context.

3.1.2 Concern around power outages

It was found that the concern associated with power outages can vary in intensity across trach families. Some of the factors which can determine this include: (1) Past experience with outages – If a family has experienced a power outage, they will be more concerned and invest in being prepared for an outage. (2) Locality – Rural areas in general are more prone to outages and are slower to get power restored after an outage as compared to urban areas. Families living in rural areas are more prepared for outages. (3) Proximity to family, friends – Family and friends serve as a backup option for trach families if they live close enough to drive quickly to, but far enough or served by a different utility so that they are not affected by the same power outage. In such a case, the trach family may not be as concerned and may not invest in in-home energy backup. (4) Awareness of emergency preparedness – If the family has had either first hand experience with emergency preparedness through their profession (emergency management services, power companies, scouting), or through family and friends, then they are more likely to be concerned and invest in preparation for power outages. (5) Number of devices they depend upon, their criticality, how long they can go without them influences the level of concern for power outages.

3.1.3 End-user archetype

Developing an end-user persona was one of the exercises during the I-Corps program. The end-user persona can be useful to develop features for the EAK and other solutions for the end-user. The team developed such a persona for a typical trach mother “Tracie the Trach Mom”: Meet Tracie the Trach Mom, she is 35 years old and the CEO of an ICU-like setup at home. Her child requires a suite of devices - ventilator, oxygen concentrator, nebulizer, feeding pump, humidifier, and refrigeration for medication. During natural disasters or power outages, she does everything to avoid the hospital, more so with the COVID-19 pandemic. Her medical team provided a checklist for emergency preparedness which is vague and generic for making decisions around energy backup. A gas generator

is not feasible, she lives in an apartment and the fumes will be dangerous. After the last power outage, she jerry-rigged marine batteries and bought car inverters, but did not really understand if it would work for her child's devices. Her ecosystem includes the home healthcare agency and hospital, insurance providers, durable equipment provider, utilities, government representatives, and social media support groups. Her purchasing decisions are heavily influenced by the different entities in her ecosystem. Her day-to-day life is full of uncertainties and preemptive concerns. She is a self-taught expert, resilient, and can go to great lengths to ensure the health and well-being of her child. She wants to make the space around her trach child resemble that of children without a serious medical condition. She wants to take her child for walks around the block, modify the feeding pump to look like a Skip Hop lunchbox, drive to and shop at the local Target store, and go on vacations just like other families. Her trach mom friends on Instagram help her identify products that can enable her to do these activities and reduce the uncertainty." The end-user persona highlights the lack of context-aware energy backup solutions for such mothers and their families.

3.1.4 Critical devices

Devices that are critical for a medically fragile individual need not be high technology or even necessarily medical devices. A refrigerator is a critical device for a diabetic patient since it is necessary to store insulin. It is critical even for a trach child to store its feeds and medicines. An air conditioner may be critical for a patient susceptible to heat stroke. Through conversations, it was observed that devices fall into two categories: life sustaining (e.g: ventilator to aid in respiration), and life supporting (e.g nebulizer to administer drugs).

3.1.5 Energy management and lack of information

While driving to doctor's appointments, families often use car chargers for the patient's devices. However, car chargers do not have the capacity to power certain devices and

families are often unsure of what devices can be safely plugged in. There is no clear indication for how long the internal batteries of an in-home medical device will last. An interviewee exclaimed, “Found out through usage that the ventilator batteries last for shorter than what they are rated for!”. Backup batteries may not have an indication of the state of charge. Even if they do, this does not translate to how many hours the device can be used. This is critical as it determines when the family will have to evacuate to a place that has power such as a hospital. A trach mother used an app to show how fast the oxygen tank will run out for a given flow rate. This implies that translation of engineering metrics like state of charge into something more user-friendly like time duration for powering a device is essential. An apt example of this is a power outage experience that a trach mother narrated in her interview. Her child needed to use a suction machine and it had a backup battery. However, she did not use the machine during the outage and chose to manually provide suction to her child using a suction tube. She said that she was not sure if they had charged the backup battery and it showed no indication of the state of charge. She wanted to save the battery until it was absolutely necessary, for example to drive to the hospital or a location with power. “The pack says 45 minutes of backup - does it actually have 45 minutes of backup?”. She added that it was too much effort to go to the living room to find the suction machine with battery backup and get her child hooked on to that. She did not want to leave her child’s side because she was afraid that a trach plug might form by the time she got the machine with battery backup set up. She found the manual suction tube to be the easiest option, closest to where they were in the house, something that she knew how to use, and did not demand that she move away from her child. These attributes provide important context for the EAK or any product that is designed for this end-user group. This example shows that it was not the availability of energy but the information about how long it will last that was more important. Also, battery management appears to be a top issue across the board - for batteries in medical devices as well as for batteries in consumer devices.

3.1.6 Key takeaways

- A medically fragile family is burdened with multiple medical and financial uncertainties. If a product can reduce the uncertainty in terms of electricity supply, it can add value and help them regain a sense of control.
- Range anxiety is a major concern around backup batteries sold with the medical devices. It was found that information about how long the energy backup would last was essential for the family to be comfortable in using the backup.
- The extent of concern around power outages depends on a number of factors such as number of critical medical devices, proximity to a hospital, apartment/home owners, rural/urban locality, etc.
- Existing solutions often follow the one-size-fits-all approach, i.e., a single solar PV and battery based solution may be designed for use in camping, recreational vehicles, or in a household with no home healthcare patient. They are not designed taking into consideration that medically fragile households are like mini-ICUs and have different requirements ranging from form factor and portability to insurance coverage and alarm fatigue.
- It was found that there is a lack of awareness around existing energy products among the families interviewed.
- Coverage of energy backup through insurance varies greatly across providers as well as states. The most likely payer for a solution like the EAK may be utilities and community choice aggregators, particularly in regions prone to power outages and public safety power shutoffs.

There does not appear to be a single entity solely responsible for energy resilience for home healthcare. The problem surfaces and is tackled through a reactive approach during focusing events like large scale power outages due to hurricanes and wildfires. It is necessary to take a proactive approach to meet the needs of this vulnerable community. A single product like the EAK may not meet these needs entirely, but can be a part of a larger reliable and sustainable energy framework.

3.2 Table-Top Exercise

Through the I-Corps interviews it was observed that a more rigorous study would be necessary to understand the response and needs of medically fragile families during a power outage. To this end, in one of the I-Corps interviews, an emergency manager at a hospital recommended conducting a table-top exercise with medically fragile individuals and their caregivers. A table-top exercise is a discussion of plans and responses to an emergency (in this case a power outage) by presenting stakeholders with different scenarios while sitting around a table, i.e., in a low-stress environment [50]. It is necessary that the design choices used in developing energy solutions be informed by the needs of the community that will use the solution. The table-top exercise aims at addressing some of these factors. This section presents a proposed outline for this project. It is a community-engaged project which will require multiple community partners and needs to be reviewed by the relevant review boards before execution.

3.2.1 Objectives

The scope of the project is families with medically fragile children residing in the United States. The first objective of the project is to study the needs and responses of medically fragile families reliant on electricity-dependent in-home medical equipment during power outages, specifically: (1) Devices to be powered, (2) In case a backup source is present, how do they ration the available energy for their critical devices, (3) Amount of time they will spend at home before vacating to a place with power, (4) Which place are they most likely to vacate to? (e.g. hospital, fire station). The second objective is to find how the following factors influence these needs and responses: (1) Underlying medical condition – medical devices to be used depend on the medical condition, (2) Support groups on social media, (3) Past experience with outages – often families with such experience are better prepared for such scenarios, (4) Locality – rural areas are more prone to outages and are slower to get power restored after an outage as compared to urban areas, (5) Proximity to family/friends – they serve as a backup option if they stay a short drive away but

have power during a localized outage, (6) Awareness of emergency preparedness – either first hand through their profession (emergency management services, power companies, scouting), or through family/friends, (7) Household income and health insurance, (8) Type of housing – e.g., apartment, house

3.2.2 Methodology

Emergency response training generally involves the following activities [50]. (1) Orientation and Education Sessions – to answer questions and concerns, (2) Tabletop Exercise – a discussion of plans and responses with all stakeholders sitting around a table, i.e., in a low-stress environment, (3) Walk-Through Drill – actual performance of emergency response actions, (4) Functional Drills – to test specific functions like medical response and notification procedures, not necessarily at the same time, (5) Evacuation Drill – participants evacuate by walking along the evacuation pathway, (6) Full-Scale Exercise – an emergency simulation as close to reality with all stakeholders in action

Tabletop exercises are shown to help participants test their resilience-based capacities, their ability to leverage partnerships, and other assets during such times [51]. The project uses the tabletop exercise for the purpose of studying responses and needs during a power outage. The experiences and needs of the community are at the center of the project and the exercise is not formulated to be a training from electrical engineers on how the families should respond to power outages. Subsequent work can be informed by the gaps and issues that the community identifies through this exercise.

A few potential scenarios and questions to be discussed during the exercise in the context of trach children and their families are presented. They can be suitably modified for children with other medical conditions. Trach children use a host of in-home medical devices such as ventilator, oxygen concentrator, nebulizer, feeding pump, humidifier, and suction machine. The people involved in the exercise would be the primary caretakers, most often the trach parents. The questions presented below may not necessarily be posed verbatim and may need to be rephrased on a case-by-case basis to ensure that the

interviewees are not subjected to any stress or discomfort.

Scenario 1 – Outage without prior warning: It is 6 p.m. on a cold winter evening when the power suddenly goes out.

- What is the first thing that you do?
- How long can your child go without the devices that do not have an internal battery?
- How do you contact the utility? (phone/website/radio news)
- For families that possess backup generator/battery pack - Do you switch this on right away? Are there any problems to switch on the backup quickly? Which devices do you power with the backup and for how long?
- If no information is available from the utility, how long will you shelter at home?
- What will your course of action be if you find out that the power will not be back for another hour/3 hours/6 hours?

Scenario 2 – Outage with prior warning: It is in the news that your locality may experience an unplanned power outage for up to 24 hours in the next three days due to a tropical storm or that there may be a planned outage for up to 24 hours in the next three days due to wildfires. In both cases, you have not been asked to vacate because of the storm/wildfire.

- How do you prepare for such an event? (items you purchase)
- Do you plan to vacate right away to a place that will have power supply or will you shelter in place?
- What factors do you consider while making a decision about vacating/sheltering in place?

3.2.2.1 Benefits

The exercise can help energy engineers better understand the nuanced requirements of medically fragile families. This understanding can help them design better, context-aware, resilient energy solutions. Table-top exercises help in identifying both strengths and vul-

nerabilities in emergency preparedness [52], and this can benefit the end-users as also their medical and support teams. Table-top exercises can help participants to take actions to clarify areas of uncertainty and develop more effective plans to deal with emergencies [53].

Although the exercise does not involve literally switching off power to the child's devices, a hypothetical discussion about a power outage can be stressful for the family. It may also make them recall some of their past outage experiences. Careful designing of the scenarios and questions in order to minimize this stress is necessary.

3.2.3 Implementation

This section includes some considerations for implementing this project.

Partners: As this is a multi-disciplinary project between human factors design and healthcare along with energy engineering, experts from these fields may be consulted in designing and conducting the exercise. A group of participating families will also be consulted to ensure that the questions/scenarios are appropriate and if they would recommend any additional ones.

Recruitment: One of the ways of recruiting participants can be by partnering with three to five children's hospitals across the country to ensure a variety in underlying medical condition, income group, and location.

Compensation: Participants can be compensated monetarily through gift cards.

Location: Even before the global COVID-19 pandemic, medically fragile families do not prefer indoor in-person interactions in order to minimize the risk of infections. Families will be given an option to participate in this exercise virtually or in-person according to their preference.

3.2.4 Outputs

After the exercise, the participating families would be asked for recommendations on how they would like to see the data and findings from this project to be published. In addition, some of the outputs can be: (1) A distilled easy-to-read version of the insights on the

project's social media handle. Since such families are seen to be active on social media, this can be an easy way to share this information. (2) Recommendations for additions to the emergency preparation one-pager that home healthcare agencies and hospitals give to medically fragile families. (3) A system requirements specification sheet for developers of energy backup solutions for medically fragile families. (4) A research article

3.3 Load Scheduler for the EAK

Medically fragile families use multiple in-home medical devices such as ventilators, feeding pumps, oxygen concentrators, and suction machines. Through the I-Corps program, it was found that during a power outage, families prefer to shelter in place instead of vacating to a fire station or a hospital. Some of the commonly mentioned reasons were that in the hospital, they may not be able to use their in-home devices and may have to head to the emergency room (ER) which can have a heavy copay. Devices in the ER are different from in-home devices and the staff may take time to set up the device settings according to the child's comfort. Nurses are more comfortable operating hospital equipment than the patient's in-home equipment. If the outage is due to a natural disaster like a hurricane, hospitals can be inundated with patients and the staff may not have the time to ensure these settings are according to the child's comfort. Hospitals and other public places can also increase the chances of infections for the medically fragile individual. A backup battery pack, like the EAK, can provide energy for a limited amount of time during an outage so that the family can shelter in place. Families prefer to maximize this 'at-home time' during an outage due to aforementioned reasons. They also need to know the duration of this at-home time as it helps them plan for a potential evacuation. Off-the-shelf battery packs do not provide this information and do not have the capacity to perform optimal load management to maximize this time.

This section presents a load scheduler for the EAK. It is implemented by solving a scheduling problem in the General Algebraic Modeling System (GAMS) [54]. It uses the on-board sensors and relays of the EAK. To minimize computation requirements of

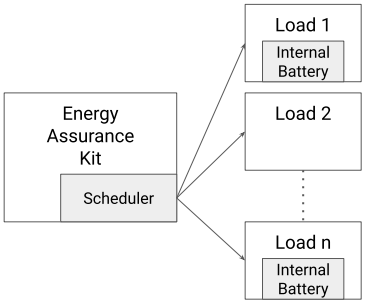

Figure 3.1: Medical load scheduler block diagram

the EAK, the optimization can be implemented on the cloud. The EAK can implement the threshold-based energy management framework presented in Chapter 5 which ensures that it will maintain basic operational sufficiency even when there are delays or failures in communication with the cloud computation platform.

3.3.1 System Configuration

As shown in Figure 3.1, the user will connect their loads to the EAK which can be considered as a battery pack external to the loads. Some medical loads also have internal batteries. External battery packs in the affordable range often have limited power output compared to the total power rating of all appliances such families need during an outage. The scheduler has to optimally schedule each load and decide whether to power it through the external battery or to let it draw power from its internal battery so as to not exceed the power and energy limits of the external battery pack. In line with this, the power output limit of the external battery pack used in this problem is less than the total power rating of the loads to be powered.

Objective: Given the specifications of loads and the external battery, along with three scenarios representing uncertainty in demand for certain loads, the scheduler has to maximize the at-home time during an outage and generate a load schedule.

3.3.2 Model Description

Load Classification: The loads considered are - ventilator, suction machine, oxygen concentrator, humidifier, and mini-fridge. Loads are classified as continuous use loads and deferrable loads. $\mathcal{C}$ is the set of continuous use loads. These loads are critical and have to run continuously. The loads which fall under this category are ventilator and suction machine. $\mathcal{D}$ is the set of deferrable loads. These loads have periodic energy requirements, i.e., they need to be on for a particular duration every hour. The loads which fall under this category are oxygen concentrator, humidifier, and mini-fridge. Additionally, there is one uninterruptible load, i.e., it has to be powered only for a specific period of time but cannot be interrupted in between this period. It is assumed that there is uncertainty in the demand for this load and is considered using different scenarios. Parameter P_s is the power demand of the uninterruptible load in scenario s. Parameter $y_{s,t}$ is the switching state of the uninterruptible load in scenario s at time t. It equals 1 if load has to be on and 0 if off. It is assumed that this load has to be switched on 3 hours into the outage. The uninterruptible loads considered in the three scenarios are - television (to watch news related to the outage), sump-pump (to drain the basement in case of a hurricane related outage), and a feeding-pump (for feeding the medically fragile patient). It is important to note that the loads under each category can differ from patient to patient. Furthermore, there may be loads that have different usage characteristics and do not fall under any of the considered categories. This model serves as an example for the assumed use case and can be extended to incorporate additional features.

Switching States: The binary variable $\mathbf{x}^i_{a,t}$ indicates whether load a is connected to its internal battery at time t, i.e., it equals 1 if connected and 0 otherwise. Similarly, the binary variable $\mathbf{x}^e_{a,t}$ indicates whether load a is connected to the external battery (EAK). Constraint 3.2 ensures that the load is connected to at most one battery. The set of all time steps in the horizon is represented by $\mathcal{T}$ and ΔT is the length of each timestep.

External battery specifications: Constraint 3.3 ensures that the power drawn by all loads at each instant t under each scenario s is less than the maximum power draw from the external battery P^{max}. Constraint 3.4 ensures that the energy drawn from the external battery over all intervals under each scenario is less than the energy content of the external battery at the beginning of the outage E^{max}.

Internal battery specifications: Some loads in different sets can have internal batteries. The set of loads that have internal batteries is denoted by $\mathcal{I}$. The number of backup hours provided to load a by its internal battery is B_a. Constraint 3.5 ensures that each appliance a is not connected to its internal battery for more than the duration B_a.

Load behavior constraints: Continuous use loads cannot be switched off for some duration and then switched on again. This is ensured by Constraint 3.6. Continuous use loads are assumed to have a higher priority than deferrable loads. Therefore, any of the continuous use loads being off implies that none of the deferrable loads can be on. This is expressed in Constraint 3.7. Deferrable loads need to be on for a particular duration every hour. The set of time intervals corresponding to the beginning of a new hour is denoted by $\mathcal{H}$. The fraction of an hour the deferrable load has to be on for is represented by F_a. The number of intervals of deviation from this requirement per hour per deferrable load is denoted by the positive variable $\mathbf{e}_{a,h}$. This is expressed in Constraint 3.8.

Objective function: If any of the continuous loads have to be turned off, that instant is the end of the 'at-home time' denoted by the variable $\mathbf{z}$. It is expressed in the maximin form such that it is less than the time for which each of the continuous use loads are on as expressed in Constraint 3.9 and the objective function maximizes $\mathbf{z}$. Even though the continuous use loads are more critical than deferrable loads, when at home, the family needs the deferrable loads to a certain extent as well. The deferrable load constraint is implemented as a soft constraint using the error term $\mathbf{e}_{a,h}$ which is a positive variable introduced in the constraint and the negative of this term is maximized through the

objective function. As the objective has two parts – maximizing the at-home time and minimizing the error in the deferrable loads constraint, a weighted sum of the two (with weights λ_c and λ_d respectively) is used as the objective function. N_z is a normalizing term and is an upper bound on the at home time evaluated as $N_z = \frac{E^{max} + \sum\limits_{a \in \mathcal{I} \cap \mathcal{C}} B_a P_a}{\sum\limits_{a \in \mathcal{C}} P_a} + 1$. N_d is a normalizing term and is evaluated as $N_d = \frac{n_D n_H F_a}{\Delta T}$, where n_D is the number of deferrable loads and n_H is the number of elements in set $\mathcal{H}$.

$$\text{maximize} \quad \lambda_c \frac{\mathbf{z}}{N_z} - \lambda_d \frac{\sum\limits_{a \in \mathcal{D},\, \mathcal{H}} \mathbf{e}_{a,h}}{N_d} \tag{3.1}$$

$$\text{subject to} \quad \mathbf{x}^i_{a,t} + \mathbf{x}^e_{a,t} \leq 1 \qquad \forall a,\ \forall T \tag{3.2}$$

$$\sum_a \mathbf{x}^e_{a,t} P_a + y_{s,t} P_s \leq P^{max} \qquad \forall T,\ \forall s \tag{3.3}$$

$$\sum_{a,t} \mathbf{x}^e_{a,t} P_a \Delta T + \sum_T y_{sT} P_s \Delta T \leq E_{MAX} \qquad \forall s \tag{3.4}$$

$$\sum_t \mathbf{x}^i_{a,t} \Delta T \leq B_a \qquad \forall a \in I \tag{3.5}$$

$$(\mathbf{x}^i_{a,t} + \mathbf{x}^e_{a,t}) - (\mathbf{x}^i_{a,t-1} + \mathbf{x}^e_{a,t-1}) \leq 0 \qquad t >= 2,\ \forall a \in \mathcal{C} \tag{3.6}$$

$$\sum_{a \in \mathcal{D}} (\mathbf{x}^i_{a,t} + \mathbf{x}^e_{a,t}) \leq (\mathbf{x}^i_{a,t} + \mathbf{x}^e_{a,t}) \qquad \forall T, \forall a \in \mathcal{C} \tag{3.7}$$

$$\sum_{t=h}^{h+1/\Delta T} (\mathbf{x}^i_{a,t} + \mathbf{x}^e_{a,t}) \geq \frac{F_a}{\Delta T} - \mathbf{e}_{a,h} \qquad \forall t \in \mathcal{H},\ \forall a \in \mathcal{D} \tag{3.8}$$

$$\mathbf{z} \leq \sum_T (\mathbf{x}^i_{a,t} + \mathbf{x}^e_{a,t}) \Delta T \qquad \forall a \in \mathcal{C} \tag{3.9}$$

$$\mathbf{x}^i_{a,t},\ \mathbf{x}^e_{a,t} \in \{0,1\},\ \mathbf{e}_{a,h} \geq 0 \tag{3.10}$$

3.3.3 Results

The model is used to generate a load schedule for an 8 hour outage for a total number of intervals = 48 and $\Delta T = 1/6$ hours. Load data is given in Table 3.1 and $P^{max} = 400$ W, $E^{max} = 1000$ Wh, $F_a = 0.17$ h for all three scenarios, $\lambda_c = 0.3$, $\lambda_d = 0.7$. Figure 3.2 shows the generated schedule. Salient events are marked and described below.

Table 3.1: Specifications of loads served by the load scheduler

Load	Power (W)	Backup Time (h)
continuous use loads		
ventilator	200	6
suction machine	150	1
deferrable loads		
oxygen concentrator	350	-
humidifier	250	-
mini-fridge	100	-
uninterruptible loads		
television	150	-
sump-pump	350	-
feeding-pump	120	-
Total	1050	

- A - The suction machine is the first continuous use load to be switched off (neither powered by the internal nor external battery). Therefore, the time it is switched off is the at-home time = 4.5 h
- B - As P^{max} = 400 W, only a limited number of loads can be powered by the external battery simultaneously. For example, in the case of event B, the suction machine and concentrator (rated at 150 W and 350 W respectively), cannot draw power from the external battery at the same time. Therefore, for the duration the concentrator is on, the suction machine is connected to its internal battery.
- Deferrable loads (concentrator, humidifier, mini-fridge) are staggered to ensure the maximum power limit of the external battery is not exceeded.
- Each of the internal batteries get 100% utilized. The external battery utilization (amount of energy utilized) is seen to be 93.3%, i.e., there is over 6% energy remaining. The energy needed by the uninterruptible load in the worst case scenario(feeding-pump) is $120W * 3 * 1/6h = 60Wh$ which is 6% of the total energy capacity of the external battery. This verifies that the scheduler saves the amount of energy necessary to cater to the uninterruptible load in the worst case scenario.

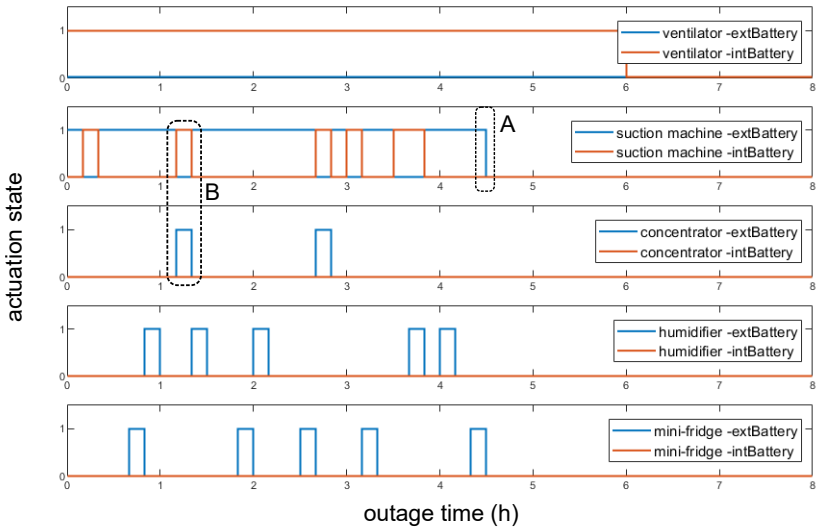

Figure 3.2: Switching state of medical devices during the outage

3.3.4 Conclusion

An electric load scheduler for an external battery pack to maximize the at-home time during an outage was implemented and the optimal at-home time with the corresponding load schedule was generated. The load scheduler takes into consideration the nuanced requirements of the use case and can be an add-on for the EAK for energy management and uncertainty mitigation. With optimal scheduling, the external battery pack with a maximum power output of 400 W was able to run 5 devices with a total power rating of 1050 W (over 2.5 times the maximum power output of the battery pack). Without the optimal scheduler, the caregiver must manually determine which loads can connect to the external battery and which should rely on internal batteries during the outage. This additional burden may shorten the time they can safely shelter at home, potentially forcing evacuation to a fire station or hospital. This, in turn, can increase admissions to such facilities that are often already overburdened during emergencies. Furthermore, manually managing the appliances can hinder the caregiver's ability to provide adequate care for the medically fragile individual or to contact emergency services, potentially leading to life threatening consequences.

It is important to note that this is a simplified model of the complex process of electric

load use. Electric processes such as battery charging-discharging efficiencies, medical factors such as load criticality, and human factors such as determining the relative priorities for critical and non-critical loads contribute to the complexity. Some of the modifications that can be made to the model so that it can represent this process more closely include: (1) The model can account for internal battery charging along with device power draw. (2) A source such as solar PV can be added to charge the external battery. The intermittency of solar and its dependency on weather parameters will be an added uncertainty to the optimization problem. (3) Along with uninterruptible loads, demand uncertainty can be included for other load types as well. (4) The user experience can be improved through a software interface and by allowing the user to add more loads online and change the type and criticality of a load. (5) Finally, it is necessary to implement this in hardware and deploy it in a user's home to validate its utility and improve its features.

3.4 Conclusion and Future Work

The intersection of home healthcare and energy resilience is an area that is unexplored in engineering as well as healthcare research. Energy resilience of the medically fragile community is a chronic and widespread problem. This problem often comes into focus in the aftermath of a disaster. Rather than this reactive approach, proactive steps need to be taken to ensure that this community's needs are met. With increase in extreme weather events due to climate change and the aging power grid, it is essential to find distributed, immediate, plug-n-play solutions that do not rely on just the legacy power grid. Solutions also need to be aware of the nuanced requirements of this community and cannot be one-size-fits-all. The table-top exercise can help gain further insights on the requirements of the community. The solar PV and battery storage based EAK with add-on features like the load scheduler can be a candidate solution to fit some of their requirements. It is important to note that a single product like the EAK or the load scheduler will not solve the problem entirely, but can be one of the pieces within a larger energy resilience framework.

Some ideas for future work include:

- Quantification of medical emergencies due to power outages: It is necessary to get data on hospital admits due to power loss to quantify the size of the problem. These may be recorded as "social admits". Some existing studies include [55–57].
- Location and number of medically fragile individuals: Information on the number of people using in-home medical devices and their locations is important for planning power outage response. Data about Medicare beneficiaries is available through the HHS emPOWER map [39], but it is estimated that there are millions more on other insurances. A proposed approach is to implement load disaggregation on distribution feeder data to identify the number of medical devices used downstream [58]. The author has contributed to this work as one of the first authors.
- Energy backup and factors in the ecosystem: The effect of various sociotechnical, geographical, and medical factors on the benefits of energy backup for a medically fragile family needs further investigation. Some examples of these factors include past experience with outages, rural/urban location, proximity to family/friends, awareness for emergency preparedness, number and criticality of devices.
- Energy awareness and education: The I-Corps interviews revealed that it is challenging for non-experts to make decisions around energy backup. An energy education and awareness add-on to the EAK or a precursor to an energy backup solution that improves energy literacy can be useful. A candidate solution can be the load scheduler in the form of a smartphone app to study energy needs during different outage scenarios. A candidate hardware solution can be a platform like the Picogrid presented in Part IV.
- Energy efficiency and healthcare: Through interviews, it was found that the intersection of energy efficiency and health could be a more established research area in the paradigm of cross-platform problems [59]. Researchers can leverage insights from this field when exploring the intersection of energy resilience and healthcare.

Chapter 4

Energy Access and Homelessness

Unreliable or no access to electricity can have multiple reasons that do not necessarily pertain to the reliability of the power grid. Even though all homes in the United States have been connected to the power grid, people who do not have a permanent home do not have reliable access to electricity. There over 500,000 people nation-wide that experience homelessness on a single night [60]. About 65% reside in homeless shelters and 35% or about 200,000 people are unsheltered. The presented work focuses on charging infrastructure for cellphones for people experiencing homelessness and other underserved communities. Studies show that houseless populations own cellphones, use them for health and social needs, and this access can bring about a sense of empowerment [61], [62]. A study showed that even those who reside in shelters can have problems accessing charging infrastructure for their cellphones [63]. The ideal goal would be to address the root cause of inaccessibility to electricity which is homelessness. As this problem is complex and may have stretched timelines, it is necessary to look at the immediate steps and plug-n-play solutions that can address this problem.

The Great Lakes Community Conservation Corps (GLCCC) [64] is an organization based out of Racine, WI which works with veterans experiencing homelessness and disadvantaged youth. They aim to address climate change, advance greener living, and offer education and job skills training. GLCCC recognized that their trainees often did not

have a permanent residence and hence a safe place to charge their personal electronics. They identified a two-fold need: (1) community solar-powered charging kiosks for their trainees to charge their electronics for free; and (2) training the trainees to fabricate the kiosks to improve their employment potential and for them to serve as green ambassadors. GLCCC received a grant from the Wisconsin Office of Energy Innovation to address these needs and reached out to UW-Madison for technical assistance in Spring 2021. The author has worked with a UW team, and with GLCCC and other partners on needs assessment, development of solar-powered phone charging kiosk prototypes, and deployment and data analysis. For more details, refer to the project's web page: smplabs.wisc.edu/electric-little-free-library.

4.1 Problem Identification and Scoping

The author and team visited the GLCCC facility in Racine in the summer of 2021 to interact with their trainees and understand the problem (Figure 4.1a). It was clear through these conversations that cellphones were important for their day-to-day activities like scheduling healthcare appointments, job interviews, school work, driving and navigation, and communication with friends and family. A trainee told us "my phone is like my lifeline". The conversations also revealed that they had gone to great lengths to keep their cellphones charged through public charging infrastructure and it was not always convenient. The public library had charging outlets but parking there was not free. Some trainees said that they had mobility constraints and could not walk more than a few blocks for accessing outlets. They would often ask the GLCCC trainers if they could plug in their cellphone at their facilities. Another trainee said that they would try to charge their phone at outlets present on the exterior of houses in the neighborhood and added that "That was the only way I could get off the street. You cannot book appointments or do your work without a cellphone." Through this field visit, it was clear that (1) cellphones are a critical need, (2) access to charging infrastructure is limited and inconvenient, (3) their efforts to keep their cellphones charged demonstrate that the need for charging infrastructure is

(a) Field visit to GLCCC, Racine

(b) Solympics: Summer Solar Makeathon

Figure 4.1: Racine field visit and the summer solar makeathon

acute and crucial.

The team then introduced the concept of public solar-powered phone charging kiosks and gathered feedback on required features and locations or environments where such kiosks will be useful. Some of the locations that came up were bus stops, laundromats, and parks. The team organized a makeathon at UW-Madison called "Solympics" for students to ideate and prototype solar-powered kiosks for different environments (Figure 4.1b). A unique feature of the makeathon was that trainees from GLCCC (i.e. the end-users) were present during the event to offer immediate feedback on useful features and design considerations. The winning entry of the makeathon was the Electric Little Free Library (eLFL). A Little Free Library (LFL) is a public book-case and is a part of a world-wide non-profit movement to promote public book exchange [65]. An eLFL is an LFL with an add-on solar panel and charging electronics. The team went on to develop the makeathon model into a field-ready prototype.

4.2 Prototype Development and Deployment

The eLFL prototype is shown in Figure 4.2. The team used commonly available off-the-shelf components for the power circuit and control circuits. The power circuit includes a 50W 12V solar panel, 20Ah 12V Li-ion battery, 10A 12V charge controller, and two 12V/USB converters with 2 USB outlets each. The control circuit includes a microcon-

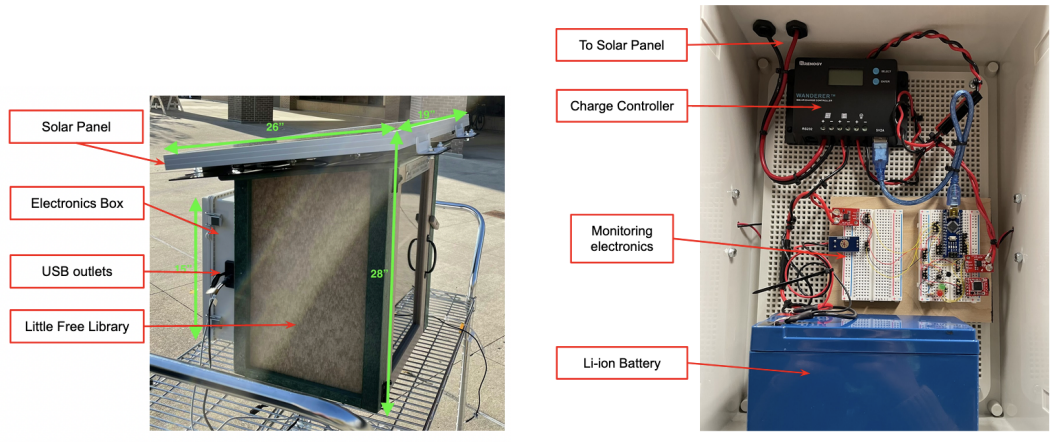

(a) External structure (b) Inside the electronics box

Figure 4.2: Electric Little Free Library prototype

troller which reads data from sensors and writes it to a data logger. A majority of the electronics is placed inside the electronics box which is mounted to the back of the LFL and the solar panel is mounted on the top.

The power circuit is shown in Figure 4.3. The PV panel feeds in to the charge controller. The battery is connected to the charge controller through a fuse. A current sensor and voltage sensor monitor its current and terminal voltage respectively. The two 12V/USB converters are connected to the charge controller through separate fuses. A current sensor monitors the total current drawn by the two converters. The control circuit is shown in in Figure 4.4. The voltage and current sensors give analog outputs. A magnetic switch sensor is placed near the door of the LFL and acts as a door sensor, i.e., to check if the door is open or closed. The real-time clock module interfaces the microcontroller via I2C and runs on a coin cell to keep time even if the microcontroller switches off. The microcontroller sends data to the data logger using serial communication. The two indicator LEDs (green and red respectively) indicate the state of the battery voltage. If it is greater than 12V, the green LED is ON indicating that the battery is operating at safe voltage levels with enough charge. If it is less than 11.5V, the red LED switches ON indicating the battery is at deep discharge levels. The data from sensors is read into the microcontroller and logged into the SD card.

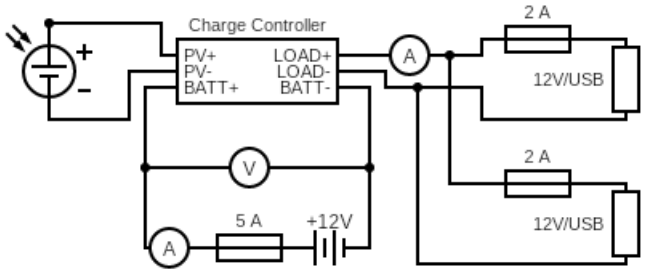

Figure 4.3: Electric Little Free Library: power circuit

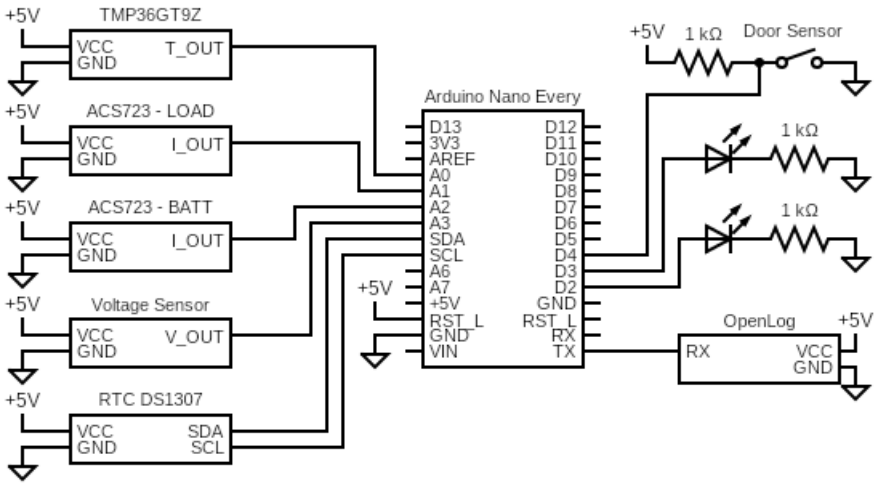

Figure 4.4: Electric Little Free Library: control circuit

(a) GLCCC, Racine (image source: The Journal Times)

(b) Lisa Link Peace Park, Madison

Figure 4.5: Electric Little Free Library deployments

The first prototype of the eLFL was deployed at the GLCCC facility in Racine in Spring 2022 (Figure 4.5a). The author was a part of the UW-Madison Energy Analysis and Policy capstone project that deployed the second prototype in Madison for 30 days in April-May 2022 (Figure 4.5b). The goals of the capstone project were to assess the energy needs for underserved communities in Madison, test the feasibility of an eLFL to serve these needs, and make recommendations for the replicability of such a project to other cities [66]. The team conducted over 20 interviews with homeless shelters, city agencies, utilities, as also potential end-users around the deployment location. The following section presents key insights from these two deployments and multiple conversations with stakeholders.

4.3 Results, Discussion, and Continuing Work

Usage: Data from the Madison eLFL was actively monitored and it was found that the average number of phone charges per day was 1.6 charges with the maximum charging days occurring over weekends. The average time per charge per day over the course of the deployment was 17.3 minutes. The library door was opened an average of 3.7 times per day. These numbers show that the charging as well as the library portion of the eLFL was actively used over the course of the 30-day deployment.

Features: The charging cables from both the prototypes went missing within a few days of installation. Along with more secure cables, future prototypes need to be vandalism-proof and also provide secure storage to cell phones while they are being charged through time-based locking compartments. Along with free access to clean electricity, access to free WiFi was a common recommendation across stakeholders.

Legislative Impact: The team had conversations City of Madison Council members including Alder Patrick Heck and found that LFLs do not fit the city's zoning codes. For large-scale deployment of eLFLs, an amendment permitting their use would have been necessary. In order to permit the use of eLFL's and other public kiosks, Alder Heck sponsored an ordinance to amend several sections of Chapter 28 of the Madison General Ordinances to create "Mission Boxes" as a permitted use in various districts. A Mission Box is defined as "a structure constructed or authorized by the owner of a parcel for the purpose of providing free items to the public, including, but not limited to, books, food, clothing and home goods." Electric Little Free Libraries can be viewed as mission boxes for clean energy and literacy. The ordinance passed in October 2022. More details can be found on the City of Madison web page [67]. The project was featured in the State of Wisconsin Clean Energy Plan, May 2023 [68].

Contributions: The project has generated documentation that can act as a roadmap for other cities, communities, and individuals to set up eLFLs. For insights and recommendations on technology, field deployment, and community engagement refer [66]. For a reference on amending zoning codes to allow mission boxes (and in turn eLFLs), refer City of Madison's zoning text memo [67].

Continuing work: After this phase of the project, multiple groups of UW-Madison students and researchers have furthered various aspects of the project.

- A team worked with GLCCC trainees and high school students in Racine to make multiple eLFLs, meeting the two-fold need of electricity access and job skills training

identified by GLCCC at the beginning of this project.

- Students identified suitable sites in Madison for eLFLs using a GIS (Geographic Information System) framework considering variables such as meeting zoning requirements, avoiding areas with air pollution, adequate access to solar, proximity to community gathering spots (including homeless resources), and bus stops with large footfall [69].
- A team of students received funding of $5,000 from the City of Madison and Bloomberg Philanthropies' Youth Climate Action Fund [70] to install four eLFLs at the locations in Madison identified by [69].
- Furthermore, there is ongoing research to identify optimal locations across the state of Wisconsin by maximizing coverage of census tract population weighted by Social Vulnerability Index (SVI) [71] and energy burden given a set budget of eLFLs. The initial optimal placements were shared with GLCCC for implementation with 10 eLFLs located in Milwaukee and Racine counties each (personal communication with one of the authors of the work, Rebecca Taylor, October 2024).

The Electric Little Free Library provides free access to clean electricity to people experiencing homelessness and underserved communities. It also serves as a platform for clean energy education and job skills training. It is important to note that the eLFL does not address the root cause of homelessness and may not be a comprehensive solution for energy access for such communities. It is, however, a good fit for being a part of a larger framework for energy access and a symbol for increasing awareness about clean energy as well as energy equity.

Chapters in this part have presented field experiences that help to understand three contexts of energy access and identify research questions. Proof-of-concept prototypes of solutions that can address some of the questions have been presented and pathways for future work have been identified. The research questions that were identified in each context which inform the frameworks and investigations presented in Parts II, III, and IV are summarized below.

Energy access for rural communities

- Hardware heterogeneity: Hardware that is locally available and economical is not uniform across vendors.
- Topology independence: Households may not want to join a microgrid until they observe that the participating households are benefiting from the project. Similarly, participating households may not want to remain a part of the project for the months when they travel elsewhere for seasonal jobs.
- Intermittent remote communication: Communication infrastructure such as the cellular network has intermittent or no connectivity in remote rural communities.
- Multi-objective driven management of limited energy: Objectives include minimizing deep discharge of batteries to reduce frequency of replacements, managing loads with different time-varying priorities, minimizing health risks due to unclean fuels.
- Uncertainty mitigation: Users want to know how much energy is available through a microgrid or a solar home system so that they can plan on budgets for other needs such as kerosene.
- Hardware experimental platforms: Field deployment can present multiple challenges which may not come up in simulation environments in the lab. Hardware-based experimental platforms are necessary to minimize failures in the field.

Energy resilience and home healthcare

- Multi-objective driven management of limited energy: Medically fragile families want to increase the time they spend at home during a power outage before evacuating.

Each medical device has a different priority which can change with time.

- Uncertainty mitigation: Families want to be certain of the amount of time their energy backup can power their critical loads.
- Energy education platforms: There is a lack of awareness among families about energy requirements and hence backup system sizing can be challenging. Education tools such as system sizing tools and outage simulators can act as a useful precursor for in-home energy backup.

Energy Access and Homelessness

- Energy education platforms: Community organizations such as GLCCC are interested in energy education platforms for job skills training and for enabling individuals to become clean energy ambassadors. There is interest from high school and college students in engaging with such platforms.
- Hardware experimental platforms: Field deployment of the prototype brought forth many hardware challenges from electronics to mounting. A hardware component in energy research and educational platforms is critical, particularly if the goal is field deployment.
- Hardware heterogeneity: If the field prototypes have to be low-budget, the design needs to be compatible with hardware from different vendors.

Proof-of-concept solutions and proposals presented in this chapter such as the optimal energy mix model, the table-top exercise, load scheduler for medical devices, and the Electric Little Free Library attempt to address some of these questions. These questions inform the frameworks presented in the following parts.

Part II

Threshold-Based Energy Management

Chapter 5

Stability Study

This chapter introduces threshold-based energy management, building upon the prior work on Self-Organizing Local Electrical Energy Network (SOLEEN) within the scope of microgrids and solar home systems. Microgrids and solar home systems deployed for energy access in remote communities experience unique technological and socioeconomic challenges. Control frameworks for such energy access solutions need to function with heterogeneous hardware, minimal technical expertise for maintenance, limited information about network topology, fit low budgets, and adapt to user preferences. SOLEEN was presented as a control framework for such lean deployments and shown to satisfy these requirements through simulation and experimental studies. This study presents the underlying mathematical framework and proof of stability of threshold-based energy management for prosumer entities with time-invariant parameters. We show that such entities converge to an equilibrium where supply-demand balance is maintained. Stability of entities as they switch from one set of time-invariant parameters to another is illustrated through numerical simulations. Additionally, we present rules for isolated and interconnected entities to avoid unstable operating conditions.

5.1 Introduction

5.1.1 Motivation

Microgrids and solar home systems (SHS) are being used as solutions for energy access in remote communities and can be a potential solution to provide for the 685 million people without access to electricity [6]. In addition to providing remote access to clean energy, microgrids offer indirect benefits such as fostering economic growth, improving health outcomes, and aiding women empowerment [11, 72]. The success of microgrid and SHS projects hinges on a few common technological and socioeconomic themes [10]. Operation and maintenance of the equipment is a challenge since there is heterogeneity in the locally available hardware and a lack of skilled technicians in remote areas. Appropriately sizing the system capacity depends on estimation of the demand for electricity in a community. This is challenging, particularly if the community was formerly unelectrified [73]. Systems are also seen to experience demand-supply imbalance during operation [19]. Getting access to data and sending corrective set points from a remote central controller in real-time may not be possible due to unreliable communication infrastructure in remote areas. In addition to these technological challenges, socioeconomic factors also influence project success and solutions need to be cognizant of this context [74]. Community-engagement in the ownership and maintenance of the project is essential for sustained operation. Upfront costs and tariff structures need to be affordable for rural households with limited means and this can necessitate innovations in financial models [75]. Furthermore, households may not want to join a microgrid until they observe that the participating households are benefiting from the project. Similarly, participating households may not want to remain a part of the project for the months when they travel elsewhere for seasonal jobs. This means that the microgrid control framework needs to be agnostic to the changing network topology. Therefore, these challenges present the following requirements on microgrid and SHS-based energy access solutions:

1. works with locally available heterogeneous hardware and minimal technical expertise for maintenance

2. supports ad-hoc prosumer microgrid formation and works without detailed information about network topology
3. works with high latency communication infrastructure
4. fits low budgets in terms of upfront and recurring costs
5. adapts to user preferences and local socioeconomic requirements

5.1.2 Background

Microgrid control paradigms and solutions have addressed some of these requirements. The use of primary control approaches based on local measurements that do not require communication between entities [76] has become well-established. Secondary and tertiary control approaches often require central control, high speed communication between entities, and system-wide measurements. This becomes challenging in small-scale microgrids deployed for remote or rural electrification, since communication infrastructure may not be reliable and may not meet the timing requirements of the power system [77]. Centralized control is associated with multiple challenges including single-point failure, ownership, and financing. Studies have proposed distributed secondary and tertiary control strategies but they often employ consensus algorithms, i.e., need communication between neighbors or need high-end power converters capable of accepting power quality set-points [78–80]. Simple converter topologies specifically catered to the remote microgrid/SHS context with minimal communication, cost, skilled maintenance requirements have been proposed in [81–83] but these solutions still require additional hardware beyond that available commercially off-the-shelf.

A rural community microgrid deployment, particularly in developing economies, works on thin budgets where high-end power converters or communication channels are not affordable [23]. In the context of this 'lean deployment', the only control handles available at each household or entity are switches for loads, sources, including import/export with the network. Self-Organizing Local Electrical Energy Network (SOLEEN) presented in [43] is a framework for distributed secondary layer control. Since it uses only these switches

as control handles, it satisfies requirements 1 and 4. It has been shown through simulations and hardware experiments that it satisfies requirements 2 and 3 in that it maintains operational sufficiency of each entity, i.e., maintains the energy content of the battery at each entity within given bounds, without central control or communication or information about network topology. A tertiary layer can be overlaid on SOLEEN to meet the custom objectives of each participating household in the microgrid as shown through numerical simulations and hardware-in-the-loop experiments [84] (and Chapter 6), thereby contributing to meeting requirement 5. SOLEEN has also been proposed as a way to maintain energy resilience of individual households participating in demand response programs [85]. Previous studies illustrate the use cases of SOLEEN through numerical simulations and hardware experiments. However, they lack a discussion on the detailed operation and analytical model, and they fail to provide comprehensive comments on the framework's stability. This study aims to bridge this gap.

5.1.3 Threshold-based energy management

Threshold-based energy management is based on the SOLEEN control paradigm. Each household or entity in the network is assumed to have some form of energy storage in addition to loads and sources. Each entity can exchange energy with the network through two separate channels for import and export. The import channel is treated as a source and the export channel is treated as a load. The discrete energy manager (DEM) in each entity measures the state of charge of the storage and actuates loads and sources. A block diagram of an entity, adapted from [43], is shown in Figure 5.1.

The primary goal of threshold-based energy management is to ensure that the energy content of each entity in the microgrid remains within predefined limits. Each load and source is assigned a threshold. If the local energy content is greater than the threshold assigned to a load, the DEM switches the load on; otherwise, it is switched off. On the other hand, if the local energy content is greater than the threshold assigned to a source, the DEM switches the source off; otherwise, it is switched on.

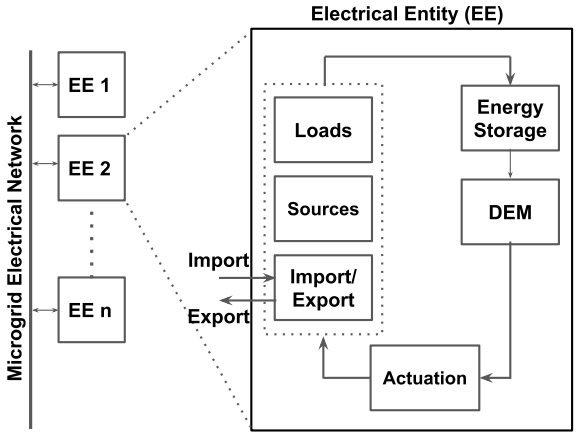

Figure 5.1: Illustration of an entity in a self-organizing local electrical energy network

5.1.4 Contributions

In this study we present the underlying mathematical framework for stability of threshold-based energy management. We show that not only does it maintain the energy content within predefined limits but also ensures that entities converge to an equilibrium that ensures demand-supply balance. We validate the framework through numerical simulations and present rules and recommendations for operation of isolated and interconnected entities. The contributions of this study are:

- proof of stability of an entity with constant-power sources and loads and constant thresholds
- numerical simulations to demonstrate stability while switching between two systems with constant-power sources and loads and constant thresholds
- rules for operation of isolated and interconnected entities

5.1.5 Organization

Section 5.2 outlines the key terms, definitions, and operating rules of the framework and presents two systems which will be used to illustrate results through numerical simulations. Section 5.3 presents proofs for an entity with a finite number of constant-power sources and loads and for an entity with an infinite number of sources and loads with an

infinitesimally small constant power rating. Section 5.4 demonstrates the stability of an entity while switching between two systems with constant-power loads and sources and constant thresholds through numerical simulations. Rules for operating isolated and interconnected entities are presented in Section 5.5, which is followed by a brief concluding section.

5.2 Model

Consider a single entity with energy content x and maximum capacity of storage X. This study presents analysis for x being energy content of a battery, but this can also represent any cumulative variable such as the monetary amount in a prepaid energy wallet, the amount of fuel in a tank, etc. Let the entity have N^s number of sources with each source j supplying power p_j^s, N^l number of loads with each load k consuming power p_k^l. Each source and load is assigned a threshold in terms of the energy content of the storage. We assign a threshold x_j^s to source j and a threshold x_k^l to source k. The only control handles the framework uses are the binary switching states of sources (u_j^s) and loads (u_k^l), determined by equations (5.1) and (5.2) respectively.

$$u_j^s = step(x_j^s - x) \tag{5.1}$$

$$u_k^l = step(x - x_k^l) \tag{5.2}$$

Here, the $step()$ function is defined as $step(y) = 1$ if $y \geq 0$ and 0 otherwise. It follows that, a source is switched on if the energy content of the storage is less than or equal to its threshold and is switched off otherwise. A load is switched on if the energy is greater than or equal to its threshold and is switched off otherwise. Equation (5.3) gives the expression for the rate of change of energy or power input to the storage.

$$\dot{x} = \sum_j p_j^s u_j^s - \sum_k p_k^l u_k^l = \sum_j p_j^s step(x_j^s - x) - \sum_k p_k^l step(x - x_k^l) \tag{5.3}$$

In order to illustrate the results in this section, we define two systems. All power and energy values are in per unit.

System 1: $N^s = 3$, $N^l = 3$, $X = 1$, source and load specifications given in Tables 5.1 and 5.2 respectively.

Table 5.1: System 1: source specifications

j	p_j^s	x_j^s
1	0.15	0.9
2	0.2	0.8
3	0.2	0.7

Table 5.2: System 1: load specifications

k	p_k^l	x_k^l
1	0.1	0.1
2	0.2	0.2
3	0.3	0.3

System 2: $N^s = 50$, $N^l = 50$, $X = 1$

Source specifications: $p_j^s = 0.01 \quad \forall j,\ x_j^s = 0.5 + \frac{(0.9-0.5)j}{N^s}$

Load specifications: $p_k^l = 0.01 \quad \forall k,\ x_k^l = 0.1 + \frac{(0.5-0.1)k}{N^l}$

Systems 1 and 2 are modeled in MATLAB and numerical results are used to illustrate and validate the analytical models presented in the following sections.

5.3 Stability Study

In this section, it is assumed that the power consumed by loads and supplied by sources remains constant and all thresholds are fixed. We offer comments on operation and stability of systems with time-varying power input/output and time-varying thresholds in Sections 5.4 and 5.5.

5.3.1 Preliminaries

5.3.1.1 Monotonicity

Let all the N thresholds ($N = N^s + N^l$) be arranged in ascending order from x_1 to x_N. If x_i is a threshold corresponding to a load then

$$\dot{x}|_{x_{i-1} \le x < x_i} - \dot{x}|_{x_i \le x < x_{i+1}} = p_k^l \ge 0 \tag{5.4}$$

If x_i is a threshold corresponding to a source then

$$\dot{x}|_{x_{i-1}<x\leq x_i} - \dot{x}|_{x_i<x<x_{i+1}} = p_s^l \geq 0 \tag{5.5}$$

From Equations 5.4 and 5.5, it follows that

$$\dot{x}|_{x_{i-1}<x<x_i} - \dot{x}|_{x_i\leq x<x_{i+1}} \geq 0 \tag{5.6}$$

The phase plane plot of $\dot{x}$ against x for System 1 is shown in Figure 5.2. It is a non-increasing function which crosses the x-axis at $x = x_3^l := x_d$.

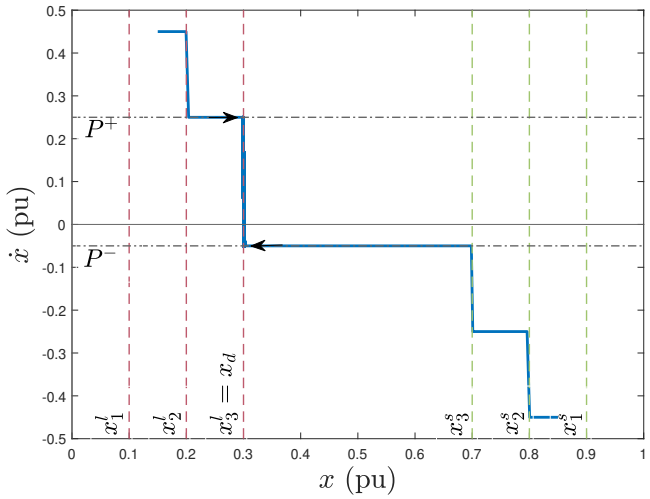

Figure 5.2: Phase-plane plot for System 1: system converges to $x = x_d$

5.3.1.2 System design considerations

For all $x < x_1$, all sources will be active and all loads will be inactive, whereas for all $x > x_n$, all loads will be active whereas all sources will be inactive. Therefore, as long as the system is designed such that there is at least one load and at least one source with a non-zero power rating, we have

$$\dot{x}|_{x<x_1} = \sum_j p_j^s > 0 \quad and \quad \dot{x}|_{x>x_n} = -\sum_k p_k^l < 0 \tag{5.7}$$

If it is assumed that the power consumed by loads, power supplied by sources, and all thresholds are constant, and since $\dot{x}$ is a monotonically non-increasing function of x, changes in $\dot{x}$ can take place only at a threshold. It follows that there exists a unique threshold $x = x_d$ such that

$$\dot{x}|_{x<x_d} > 0 \quad and \quad \dot{x}|_{x>x_d} < 0 \tag{5.8}$$

It follows that, for a given set of constant-power sources and loads with constant thresholds:

1. x_d is unique
2. x_d is time-invariant

5.3.2 Continuous variation

Consider a system with a large number of loads and sources, each with an infinitesimally small constant power rating. The discontinuous plot depicted in Figure 5.2 degenerates to a continuous straight line intersecting the x-axis at $x = x_d$. Since the loads and sources of System 2 have a small power rating and are large in number, System 2 is a good approximation of such a system and its plot of $\dot{x}$ against x resembles a straight line as shown in Figure 5.3a. We use the global invariant set theorem to comment on the stability of such a system.

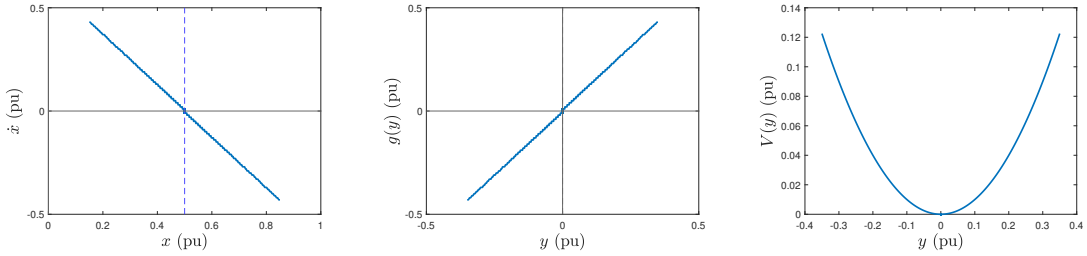

(a) Phase plane plot: system converges to $x = x_d$

(b) Plot of g(y) against y where $yg(y) \geq 0 \quad \forall y$

(c) Lyapunov function $V(y) = y^2$

Figure 5.3: System 2: phase plane and Lyapunov function plots

Let us define a new variable $y := x - x_d$ and $\dot{y} + g(y) = 0$. The plot of $g(y)$ against y is a straight line passing through the origin; the plot for System 2 is shown in Figure 5.3b.

Therefore, we have $yg(y) \geq 0 \quad \forall y$. Consider the Lyapunov function $V(y) = y^2$ (Figure 5.3c). The following conditions are satisfied:

1. $V(y) \to \infty$ as $||y|| \to \infty$
2. $\dot{V}(y) = 2y\dot{y} = -2yg(y) \leq 0 \quad \forall y$

Let $\mathbf{R}$ be the set of all points where $\dot{V}(y) = 0$ and $\mathbf{M}$ be the largest invariant set in $\mathbf{R}$. From the above conditions and since this is an autonomous system with $g(y)$ continuous, the global invariant set theorem is applicable and it follows that all solutions globally asymptotically converge to $\mathbf{M}$ as $t \to \infty$ [86]. The solutions to $\dot{V}(y) = 0$ are $y = 0$ or $g(y) = 0$, i.e., $y = 0$ is the only point in set $\mathbf{R}$. At $y = 0$, $\dot{y} = 0$ and so that is an invariant set. Therefore, the system globally asymptotically converges to $y = 0$. Note that $g(y)$ need not be a straight line or a monotonic function for this result to hold. As long as conditions (1) and (2) above are satisfied, the system will globally asymptotically converge to $y = 0$.

Figures 5.4a and 5.4b show the plot of x against time for System 2 for different initial conditions. The system is seen to converge to $x = x_d = 0.5$ (which corresponds to $y = 0$) in finite time.

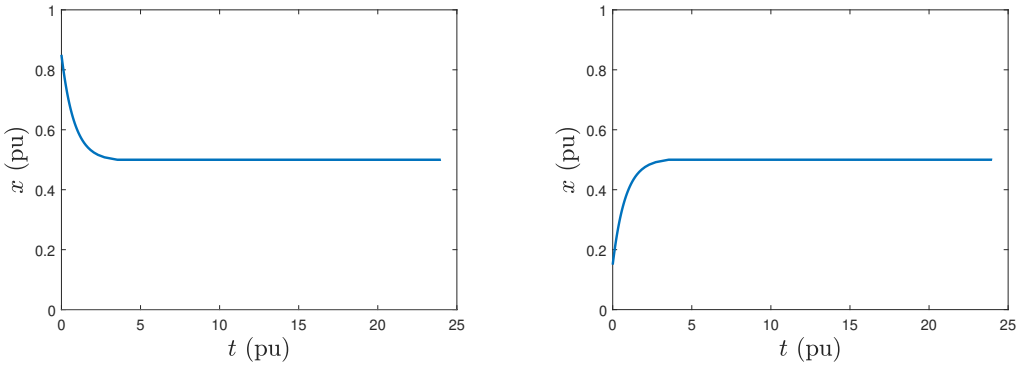

(a) Initial condition $x = 0.85$ (b) Initial condition $x = 0.15$

Figure 5.4: System 2: x against time for two different initial conditions; system converges to $x_d = 0.5$ in both cases

5.3.3 Discontinuous variation

In the case of discontinuous variation, we use the sliding mode control paradigm to comment on the stability of the system. The goal of a control system is to formulate and implement a control law such that the system tracks a certain desired trajectory. The goals of the following discussion are to analyze the threshold-based energy management framework through the sliding mode control paradigm so as to validate the following hypotheses about the stability of the system operated using the framework and identify conditions when they are satisfied.

1. system reaches $x = x_d$ in finite time
2. $x = x_d$ is an invariant set

Let the sliding variable be defined as $s := x - x_d = \tilde{x}$. Since x_d is not time-varying, $\dot{s} = \dot{x} - \dot{x}_d = \dot{x}$. Therefore, $s\dot{s} = \tilde{x}\dot{x}$.

From the definition of x_d, it follows that $\dot{x} > 0$ when $\tilde{x} < 0$ and $\dot{x} < 0$ when $\tilde{x} > 0$. Therefore,

$$s\dot{s} = -|\tilde{x}||\dot{x}| = -|s||\dot{x}|$$

Let $\eta = min\{|\dot{x}|\}$ which is the minimum of $|\dot{x}|_{x=x_d^-}| = P^+$ and $|\dot{x}|_{x=x_d^+}| = -P^-$ as marked in Figure 5.2. Therefore,

$$s\dot{s} \leq -\eta|s|$$

$$\frac{1}{2}\frac{ds^2}{dt^2} \leq -\eta|s| \tag{5.9}$$

Equation 5.9 verifies the sliding condition [86]. Therefore, the system reaches $s = 0$, i.e., $x = x_d$ in finite time which is $\leq \frac{|s(t=0)|}{\eta}$ and remains at $x = x_d$. Hence, $x = x_d$ is an invariant set. This validates the two hypotheses, assuming constant-power sources and loads and constant thresholds.

Figures 5.5a and 5.5b show the plot of x against time for System 1 for different initial conditions. The system is seen to converge to $x = x_d = 0.3$ in finite time.

To limit chattering, practical implementation of such a system introduces a small amount of hysteresis around each threshold. In the neighborhood of $x = x_d$, let us assume

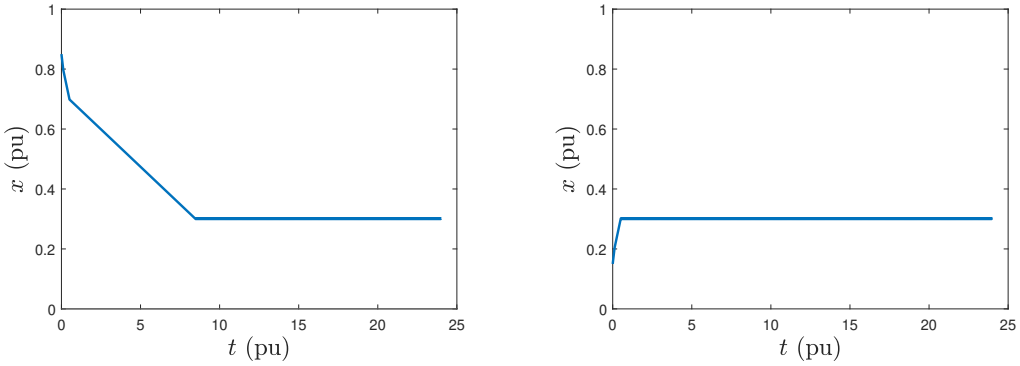

(a) Initial condition $x = 0.85$ (b) Initial condition $x = 0.15$

Figure 5.5: System 1: x against time for two different initial conditions; system converges to $x_d = 0.3$ in both cases

that the width of the dead band is Δx. The time for which $\dot{x} = P^-$ and $\dot{x} = P^+$ is given by $\Delta x/(-P^-)$ and $\Delta x/P^+$ respectively. Therefore, the average value of $\dot{x}$ in the neighborhood of $x = x_d$ is given by

$$< \dot{x} >= \frac{P^- \frac{\Delta x}{(-P^-)} + P^+ \frac{\Delta x}{P^+}}{\frac{\Delta x}{(-P^-)} + \frac{\Delta x}{P^+}} = 0$$

Therefore, around $x = x_d$, we have $< \dot{x} >= 0$, i.e., a balance between supply and demand is ensured.

This analysis for continuous and discontinuous cases reveals that the threshold-based energy management framework ensures that the system will converge to the equilibrium and ensure supply-demand balance.

5.4 Case Studies

The above discussions assumed time-invariant thresholds and constant-power sources and loads. This section presents case studies that illustrate the operation of an entity that changes from one system with time-invariant parameters to another system with time-invariant parameters, depending on different external factors.

5.4.1 Low Demand

Let us assume that System 1 represents a grid-connected household with a battery that has three wall chargers and three loads. Consider a scenario when the members of the household are away and are not using any loads. The plot of $\dot{x}$ against x is entirely above the x-axis except at $x = x_d$ as shown in Figure 5.6a and the system continues to converge to $x = x_d$ in finite time as shown in Figure 5.6b. Here, x_d is equal to the largest threshold $x_1^s = 0.9$. The system will remain there until the load demand becomes non-zero after which the equilibrium can shift to a different value of x. Note that, in this case if the initial condition is greater than x_d, the system remains at the initial condition since $\dot{x} = 0$ when $x \geq x_d$.

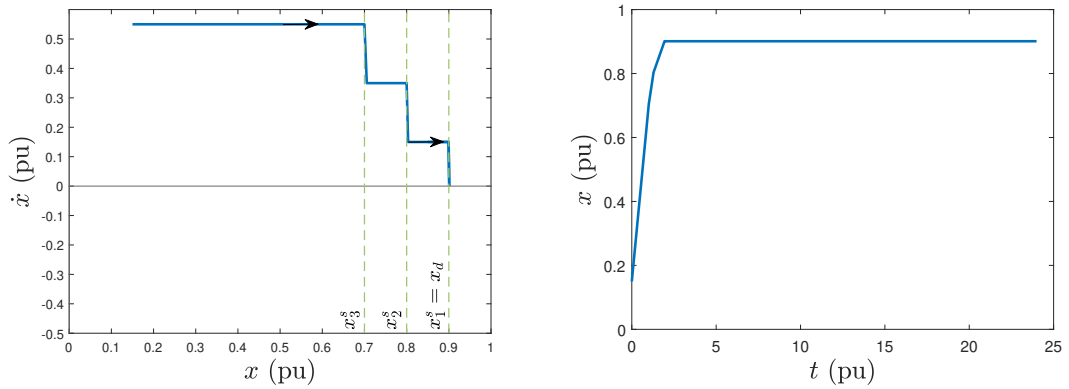

(a) Phase plane plot: system converges to $x = x_d$

(b) x against time for initial condition $x = 0.15$

Figure 5.6: System 1: Low demand case

5.4.2 High Demand

If there is a power outage, the wall chargers will not supply any power. In this case, if the household is using all the loads the plot of $\dot{x}$ against x is entirely below the x-axis except at $x = x_d$ as shown in Figure 5.7a and the system continues to converge to $x = x_d$ as shown in Figure 5.7b. Here, x_d is equal to the lowest threshold $x_1^l = 0.1$. The system will remain there until one of the sources becomes available after which the equilibrium can shift to a different value of x. Note that, in this case if the initial condition is less than

x_d, the system remains at the initial condition since $\dot{x} = 0$ when $x \leq x_d$.

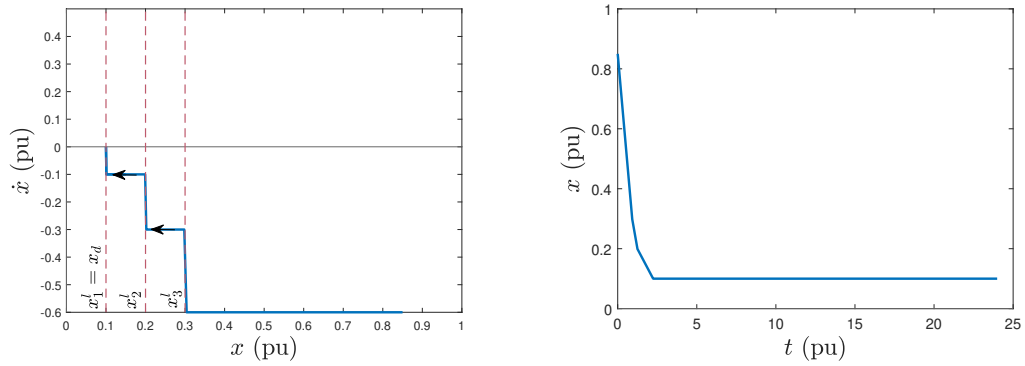

(a) Phase plane plot: system converges to $x = x_d$

(b) x against time for initial condition $x = 0.85$

Figure 5.7: System 1: High demand case

5.4.3 Increasing demand

Consider a scenario when the demand has an instantaneous increase and System 1 changes from the low demand case to the high demand case. Figure 5.8 shows the plot of $\dot{x}$ against time and the switch happens at $t = 0.2$. The system first moves towards the low demand equilibrium ($x = 0.9$). After the demand increases, the system converges to the high demand equilibrium ($x = 0.1$). This shows that the system continues to move towards the equilibrium corresponding to the current set of parameters (thresholds and load and source power).

5.4.4 Instability condition

The high and low demand cases show that the system remains stable even if the total load demand is greater or less than the total source power respectively. However, if a load/source switches roles, i.e., a load supplies power and a source starts consuming power, this can lead to instability. Consider a scenario where Source 1 in System 1 is connected to an external battery. If the external battery ends up drawing power instead of supplying power to charge the system's battery, this can lead to the system battery

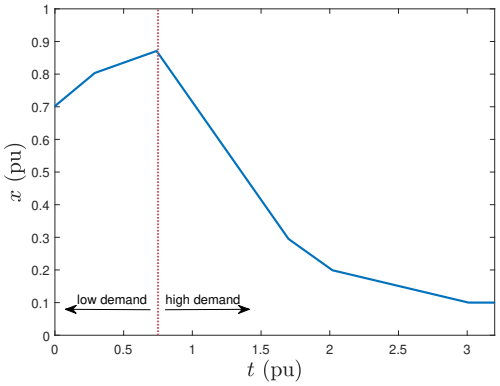

Figure 5.8: x against time for System 1 switching from low demand to high demand; system converges to the high demand case equilibrium of $x = 0.1$

getting completely drained. Figure 5.9a shows the plot of $\dot{x}$ against x when this power draw is $p_{s1} = -0.7$ and Figure 5.9b shows the plot of x against time. x is seen to become negative and continue decreasing. Practically, this would lead to the battery getting completely discharged and remain at zero state of charge.

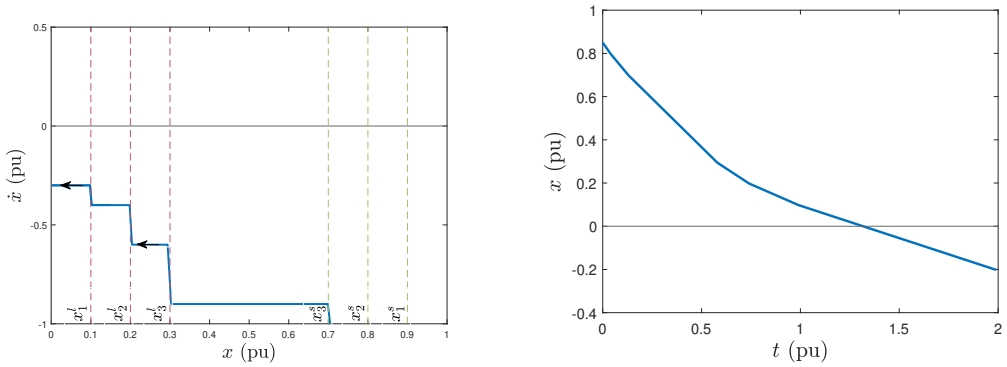

(a) Phase plane plot lies entirely below the x-axis

(b) x continues to decrease with time

Figure 5.9: System 1: Instability when a source becomes a load

The case studies reveal that a load or a source may not interchange their roles, i.e., consume or supply negative power respectively, or the system can become unstable. Furthermore, a system may consist of only loads or only sources in certain scenarios. This degenerates to the trivial case wherein the system converges to the lowest or the highest threshold respectively. As long as the chosen thresholds are within safe operating limits

of the energy storage device, these cases do not present threats to the safe operation of the system.

5.5 Rules for Operating Entities

Entities running the SOLEEN framework can be interconnected to exchange energy and each entity is observed to maintain its local energy content within predefined limits. This has been shown through Monte Carlo simulations for a 20-entity network and through hardware experiments on a 3-entity network [43]. Each entity participates in the network through two devices - import and export. The import device is treated as a source and the export device is treated as a load. In this section, we present recommendations for interconnecting entities. These are also applicable for operation of isolated entities.

Thresholds: If the power supplied or consumed by each source or load respectively as well as the thresholds vary with time, the plot of $\dot{x}$ against x may also vary with time. In this case, x_d will be a function of time $x_d(t)$. If $\dot{x}$ is plotted against x considering the power and threshold values at any given instant of time t, the relation (5.6) will still hold true at each instant. Therefore, it can be argued that $x_d(t)$ will be unique. Since the equilibrium $x_d(t)$ is one of the thresholds, the chosen thresholds should lie within the safe operating limits of the energy storage device. For example, if a battery's safe operating region is between 20% to 90% state of charge, thresholds should be picked within this range.

Bidirectional power flow: Bidirectional power flow on a load/source may lead to instability. A source or a load should not change roles, i.e., a source should not consume power and a load should not supply power since this can lead to instability as illustrated in the case studies. This is particularly important for energy exchange with the network. Separate lines for import and export are needed and unidirectionality of power flow has to be ensured on each line. In dc networks, it can be implemented by having a simple diode in series in each line as implemented in [43].

5.6 Conclusion

This study presents the mathematical framework describing the stability of threshold-based energy management and shows that entities converge to an equilibrium that maintains demand-supply balance. We prove that an entity with constant thresholds and an infinite number of sources and loads each with an infinitesimally small constant power rating will globally asymptotically converge to the equilibrium. We prove that an entity with constant thresholds and a finite number of constant-power sources and loads will converge to the equilibrium in finite time. We show through numerical simulations that if an entity's parameters change from one set of time-invariant load/source power ratings and thresholds to another similar time-invariant set, it will move towards the equilibrium corresponding to the current set of parameters. Furthermore, we present two rules for operating isolated or interconnected entities: (1) thresholds should be chosen such that they lie within the safe operating limits of the energy storage device, (2) no load/source can support bidirectional power flow, i.e., a load or source cannot supply or consume power respectively.

Stability study of entities with time-varying parameters (thresholds, power consumption of loads, power supply from sources) is a subject of future work. Additionally, a stability study of multiple interconnected entities can be undertaken. The framework can also be extended to incorporate more than one energy storage quantity. For example, for a household with battery storage and a prepaid energy wallet, the framework can be implemented through a quantity that is a function of the state of charge and the wallet amount.

It is important to note that the choice of thresholds can influence how long a particular load/source is enabled. This can affect tertiary level socioeconomic objectives of an entity beyond operational stability such as revenue generation through energy exchange or availability of a critical load. This can be achieved by overlaying a tertiary control layer on threshold-based energy management, as discussed in Chapter 6. It is also possible to choose appropriate thresholds to achieve tertiary level objectives. This is presented in Part

III which extends the concept of threshold-based energy management to prepaid wallets, i.e., the variable of interest is the wallet balance instead of battery state of charge.

Chapter 6

Application to Community-Scale Microgrids

Secondary and tertiary control of microgrids is often centralized and requires system-wide measurements and communication between entities. Such approaches can be susceptible to single points of failure especially when communication infrastructure is not reliable. Self-organizing local electrical energy network (SOLEEN) is a secondary control framework which ensures operational sufficiency of the network without any central control or communication. Higher layers of control can be overlaid on SOLEEN for optimal operation. This work presents a distributed approach for realizing tertiary control of SOLEEN-based dc community microgrids through an optimal scheduler at each entity for local loads and energy exchange with the network. The scheduler uses integer linear programming to meet the objectives of the entity such as revenue generation and maximizing service to critical loads. The model provides parameters to account for socioeconomic differences across participating entities which can result in different objectives. It is independent of network topology, variations in local power sources, making it a plug-n-play option for resource-constrained deployments in rural communities. The model is verified through computer simulations and experiments on a hardware-in-the-loop setup.[1]

[1]This chapter is based on work by the author and Giri Venkataramanan in [84]. This work was supported by the Wisconsin Electric Machines and Power Electronics Consortium.

6.1 Introduction

The paradigm of microgrids is continuing to gather attention as a means for providing electrical energy services for remote locations and emergency conditions within centralized grids. The use of primary control approaches based on local measurements that do not require communication between entities [76] has become well-established. Secondary and tertiary control approaches often require central control, high speed communication between entities, and system-wide measurements. This becomes challenging in small-scale microgrids deployed for remote or rural electrification, since communication infrastructure may not be reliable and may not meet the timing requirements of the power system [77]. Centralized control is associated with multiple challenges including single-point failure, ownership, and financing. Studies have proposed distributed secondary and tertiary control strategies but they often employ consensus algorithms, i.e., need communication between neighbors or need high-end power converters capable of accepting power quality set-points [78], [79], [80]. A rural community microgrid deployment, particularly in developing economies, works on thin budgets and high-end power converters or communication channels are not affordable [23]. To reduce upfront costs and lead time while improving resilience, interconnecting multiple modular photovoltaics (PV) + storage based solar home systems is preferred over a centralized PV array + battery bank [82]. In the context of this 'lean deployment', the only control handles available at each household or entity are switches for loads, sources, including import/export with the network.

Self-organizing local electrical energy network (SOLEEN) is a proposed control framework for distributed secondary layer control [43], useful for such lean dc community microgrids. It uses only switches for loads/sources as control handles and ensures operational sufficiency of each entity in a microgrid without any communication or central control. With the 'safety net' of SOLEEN in place, a distributed tertiary layer that may use communication with a central entity can be incorporated to improve economy of operation beyond operational sufficiency. This work presents a distributed tertiary layer in the form of a distributed optimal scheduler (DOS) for dc community microgrids based on the

SOLEEN framework. Fig. 6.1 illustrates a community scale microgrid with three electrical entities (EE) illustrating various layers of hierarchical control.

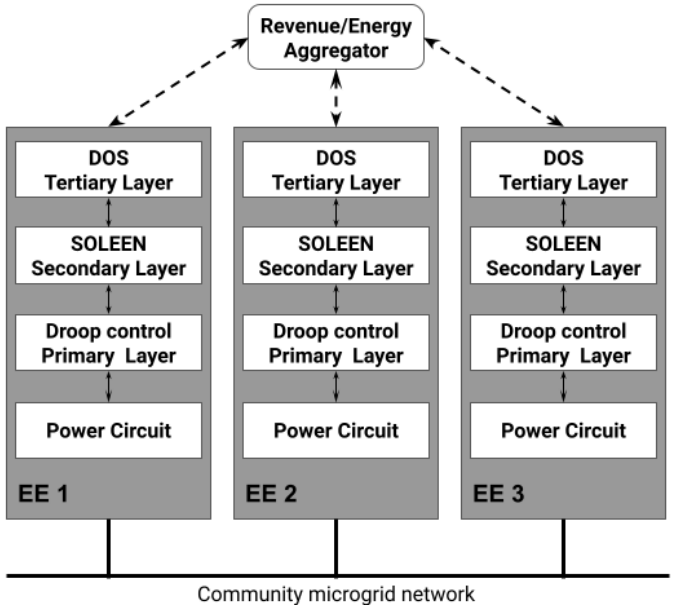

Figure 6.1: Sketch of a community scale microgrid with three electrical entities (EE) illustrating various layers of hierarchical control

A community microgrid with multiple prosumer entities and multiple owners represents operating goals different from single owner microgrids. Each entity pursues its own operating objective which may not be in complete alignment with that of others [87]. Furthermore, the overall objective function of an entity can be a combination of multiple objectives such as meeting critical demand and revenue maximization. The proposed DOS presented here uses integer linear programming to minimize the composite, versatile, and flexible cost function in order to ensure optimal operation of each entity to meet customized objectives. Each entity executes the optimization algorithm locally to schedule local loads and energy exchange with the network without any central control.

The following section summarizes the main features of SOLEEN and the distributed optimal scheduler. Section 6.3 presents the mathematical formulation of the optimization model. Section 6.4 presents computer simulation results for a modest three-entity network. Results from a hardware-in-the-loop laboratory scale experimental system are presented

in Section 6.5, followed by a brief concluding section.

6.2 Distributed Optimal Scheduling

The fundamental operational block of SOLEEN is an electrical entity (EE). An EE can be a prosumer such as a house, a building, or a commercial entity. An EE contains nominal storage and multiple electric devices (EDs) such as loads, sources, import/export channels along with a discrete energy manager (DEM). Based on the energy content of the EE, the DEM sends actuation signals and manages the different EDs. Each ED has an energy threshold - when the local energy content crosses this threshold, the DEM sends an actuation signal to the ED [43]. The EE is said to be operationally sufficient if its net energy level remains within given bounds. The controlled actuation of devices according to local energy and thresholds forms the base control loop over which higher layers of control can be overlaid. This base control loop executed in the DEM of each EE maintains the energy content within given bounds to ensure operational sufficiency, irrespective of the presence of higher layers of control.

In the context of a microgrid that is self-organizing, each entity in the microgrid optimizes 'itself' to meet its own objectives without regard to the needs of a community. Community engagement occurs in the form of participating in interconnection, and exchanging energy based on a price structure that is agreed upon by the membership in the community. In such a scenario, the EE has an added responsibility of scheduling loads, sources, and energy import/export to satisfy the objectives of the entity beyond ensuring mere operational sufficiency. Therefore, the tertiary layer controller may be viewed as a distributed optimal scheduler or DOS.

Such an approach can operate independently in the absence of any central control, real-time communication with a central entity, or between entities. If the community agrees upon a price structure that varies with the aggregate energy of the network, a central entity is necessary to determine the price of energy exchange by computing total energy content of all entities in the network. In this case, the role of this entity is limited to computing and

communicating this price to all entities, and it does not make any centralized scheduling decisions for any entity. Therefore, each entity maintains its autonomy preserving the distributed nature of the tertiary control scheme.

The scheduler uses an integer linear program for optimal scheduling and is implemented in each EE. The scheduler is overlaid on the base SOLEEN control loop. Actuation signals generated by the scheduler take a lower priority than those generated by the base loop as operational sufficiency is of higher priority than optimal operation.

The model is set in the context of a rural off-grid community, typically located in developing or underdeveloped economies. Each house or building is modeled as an EE. Each EE is assumed to have local rooftop solar PV and local storage. Its electrical appliances are classified as either critical or non-critical. All critical appliances are lumped to form the "critical load" and similarly all non-critical appliances together form the "non-critical load". All entities are interconnected so as to form a dc microgrid and enable energy exchange through an import device and an export device at each EE. Therefore, the electrical devices present in each EE are import device, export device, critical load, non-critical load, and the PV source. The scheduler generates actuation signals for the loads and the import and export devices.

A community microgrid can comprise of various types of entities broadly classified into two classes - service seekers and revenue seekers as shown in Fig. 6.2. The primary goal of service seekers is to meet their local demand and the secondary goal is to reduce expenditure on energy imports. On the other hand, the primary goal of revenue seekers is to maximize revenue generated through energy export and their secondary goal is to reduce unmet local demand. Service seekers include residential users and critical infrastructure like health clinics. Revenue seekers include commercial entities like shops and local entrepreneurs [88] who invest in high capacity solar systems with the purpose of generating revenue through energy export above and beyond serving their local loads. Both the classes of entities are expected to have critical and non-critical loads. Loads can be further classified as power and energy loads. Power loads have a constant power demand

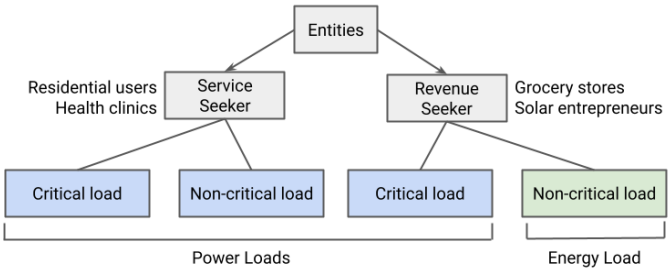

Figure 6.2: Classes of entities and loads in the community microgrid

during a certain period of the day and no demand outside of that, e.g., demand for a 40W light bulb in a residential user's house from 6:00 to 9:00 p.m. Energy loads are also constant power loads but have a total daily energy demand and can be serviced anytime during the day with interruptions, e.g., an irrigation water pump. For the purpose of this study, it is assumed that all loads of the service seeker and the critical load of the revenue seeker are power loads, whereas the non-critical load of the revenue seeker is an energy load.

6.3 Optimal Scheduler Design

The optimal scheduler illustrated here is similar to model predictive control with a window size of one time step. While the proposed approach does not need any weather forecast data, it serves as a plug-n-play model for community microgrids across different locations with varying climatic conditions, using energy price as the only proxy parameter to represent the network state. Thus, the scheduler receives a price signal p_t from the revenue/energy aggregator, and on the basis of local objectives provides switching signals for enabling the import device, export device, and the non-critical load over time step t given by $u_{i,t}$, $u_{e,t}$, and $u_{nc,t}$ respectively. The switching signals can take the values of 0 (OFF) and 1 (ON) which remain unchanged over the duration of the time step, while the scheduler computes their optimal values for the next time step.

Each entity is assumed to have three different objectives - meet critical demand, generate revenue (or reduce expenditure), and meet non-critical demand. Meeting critical

demand has the highest priority while there is a trade-off between generating revenue and meeting non-critical demand. This has to be accounted for while constructing the overall objective function of the scheduler. The scheduler has to manage a limited amount of energy while catering to these objectives. The fundamental basis for DOS is the price signal that is transmitted to all the entities, which is described further.

6.3.1 Energy Tariff

The price of energy exchange is set to depend on the aggregate energy of the entities participating in energy exchange. Larger the aggregate energy implies larger supply of energy available for exchange and hence a lower price. This negative relationship between aggregate energy and price incentivizes entities with surplus to export when most of the network is in deficit, facilitating equitable distribution and operational sufficiency. A positive relationship, on the other hand, may lead to a positive feedback system and runaway conditions. This study assumes the relation between the aggregate energy and the price to be a straight line with a negative slope and is given by (6.1). C_{max} and C_{min} are the upper and lower limits on the price, respectively, agreed upon by the community. p_t is the price at time t and $e_{i,t}$ is the energy content of the i^{th} entity at time t. The unit of p_t is monetary units per unit energy or mu/pu. The plot of energy price vs aggregate energy is monotonically decreasing and is shown in Fig. 6.3.

$$p_t = C_{max} - \frac{C_{max} - C_{min}}{E_{max}} \sum_i e_{i,t} \tag{6.1}$$

The revenue/ energy aggregator collects information about each participating entity's energy content, computes the price, and communicates it to each entity in the network, and does not make any scheduling decisions.

6.3.2 Revenue/Service Trade-off Model

In order to model the trade-off between generating revenue and meeting non-critical demand, a discrete function that penalizes revenue generation at the expense of serving

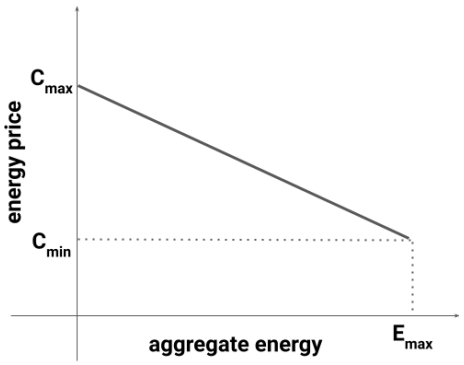

Figure 6.3: Energy price vs aggregate network energy as determined by the revenue/energy aggregator

non-critical load is defined, as $v_t = u_{i,t} - u_{e,t} + u_{nc,t}$, where $u_{i,t}$, $u_{e,t}$, and $u_{nc,t}$ represent the switching functions for import, export, and non-critical loads respectively, set to unity while they are enabled and zero otherwise. Altogether, v_t takes positive values when the states of these electric devices curtail revenue while it takes negative values when revenue is enhanced. In contrast, positive v_t indicates an increase in the service factor for non-critical loads (NCSF) and vice versa. Service factor (SF) pf a load is defined as the percentage of demand served over a day or the time-horizon of interest. These aspects are shown in Table 6.1. Adding the constraint (6.2) ensures that at most one among the import or export devices can be on, which implies that v_t can take one of four discrete values in $\{-1, 0, 1, 2\}$. With this definition of v_t, $p_t v_t$ represents the expenditure or loss of revenue due to particular choices of switching states.

Furthermore, an upper bound on the cost of unmet non-critical demand can be determined using $C_{max}\epsilon_t(-v_t)$, where ϵ_t is the fraction of the unmet energy demand of the non-critical load, over a day or the time-horizon of interest, at time t. Since the algorithm continuously makes decisions for each time step, ϵ_t can be used as a proxy for the unmet demand over the entire day or time-horizon of interest.

The cost of unmet non-critical demand is weighted using a 'greediness factor' β and discounted from the loss of revenue $p_t v_t$ to represent the total cost function to be $(p_t - \beta C_{max}\epsilon_t)v_t$. Here, small values of β would lead to maximizing revenue, where large values

of β would lead to maximizing service.

Table 6.1: Effects of various discrete switching state functions

$u_{i,t}$	$u_{e,t}$	$u_{nc,t}$	v_t	**Revenue**	**NCSF**	w_t	**CSF**
0	0	0	0	-	-	0	-
0	0	1	1	↓	↑	1	↓
0	1	0	-1	↑	↓	1	↓
0	1	1	0	-	-	2	↓
1	0	0	1	↓	↑	-1	↑
1	0	1	2	↓	↑	0	-

$$u_{i,t} + u_{e,t} \leq 1 \tag{6.2}$$

6.3.3 Critical Demand Model

While the trade-off between revenue and meeting non-critical demand is met using the cost function described above, meeting the critical demand would generally deemed to be of higher priority. Therefore, a situation when the local conditions are not sufficient to meet the critical energy demand for the day overrides the other two objectives. The scheduler detects this situation by defining an insufficiency flag $z_t = floor(E_{c,t}/e_t)$, where $E_{c,t}$ is the total unserviced energy demand of the critical load at time t projected over the time-horizon of interest, e_t is the state of energy reserve of the local storage at time t, and $floor()$ is the greatest integer function. The insufficiency flag would take the value $z = 1$ when the local energy content (or state of charge of the EE's battery) drops below a value that can serve the day's critical energy demand, otherwise $z = 0$. In this manner, the scheduler does not control the critical load directly but operates the control actions of other electric devices to ensure that the critical demand will be met, i.e., increase the critical service factor (CSF) by decreasing NCSF and revenue. The actions that hamper meeting critical demand include switching off import, switching on export, and switching on the non-critical loads. These aspects may be defined using the discrete function $w_t = -u_{i,t} + u_{e,t} + u_{nc,t}$ in a manner complementary to the definition of v_t. The

values taken by w_t are also shown in Table 6.1 alongside the other variables.

Activation of the insufficiency flag is used to add an override term Mz_tw_t to the cost function, where $M >> C_{max}$, is defined as the cost override factor in order to be effective.

6.3.4 Objective Function

On the basis of the energy tariff, revenue/service trade-off model, and the critical demand model, the overall objective function may be defined using (6.3).

$$\min_{u_{i,t},u_{e,t},u_{nc,t}} \quad (p_t - \beta C_{max}\epsilon_t)v_t + Mz_tw_t \tag{6.3}$$

Thus, the scheduler for a revenue seeker and that for a service seeker have the same objective function. The value of the greediness factor β determines whether the entity wants to lean towards making revenue or towards meeting non-critical demand.

The scheduler for a service seeker has an additional constraint given by (6.4), as the non-critical load of the service seeker is a power load. δ_{nc} is a binary constant provided by the user and acts as a 'demand schedule', i.e., $\delta_{nc} = 1$ when the user needs the load to be on and $\delta_{nc} = 0$ otherwise. The constraint ensures that the load is not switched on when there is no demand.

$$u_{nc,t} \leq \delta_{nc,t} \tag{6.4}$$

In summary, the overall objective function from (6.3), together with the constraints from (6.4), and (6.2) form the basis for the proposed DOS, which takes p_t as inputs and provides a schedule for the import, export, and non-critical load binary switching state functions.

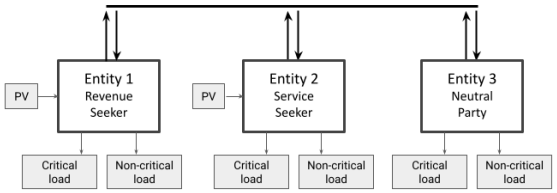

Figure 6.4: Three-entity dc microgrid network

6.4 Three-Entity Microgrid Network - Simulation Study

6.4.1 Model Setup

A three-entity radial dc microgrid network as shown in Fig. 6.4 is modeled in *MATLAB Simulink (version 2019a)* and *PLECS Blockset*. Entity 1 is modeled as a revenue seeker (RS), Entity 2 as a service seeker (SS), and Entity 3 is modeled without a tertiary layer scheduler, and is referred to as a neutral party (NP). Entity 3 has only the base SOLEEN layer whereas Entities 1 and 2 have both, a base SOLEEN layer and a scheduler. The schedulers at Entities 1 and 2 are modeled using the *YALMIP* [89] and *OPTI* [90] toolboxes for MATLAB and the solver *lpsolve* [91]. The solar PV data is taken from the research group's field site in India [19].

6.4.2 Illustrative Results

6.4.2.1 Operational Aspects

The operational aspects of the schedulers are demonstrated through a simulation for a total run time of 60 minutes. The power and energy specifications of the entities are given in Table 6.2 and the optimization parameters are given in Table 6.3, where β_r and β_s are the greediness factors for the RS and the SS respectively.

Fig. 6.5 shows the time series plots for state of charge and load profile of each entity when the schedulers are enabled and disabled. All entities have the base SOLEEN layer enabled at all times and their states of charge remain above the lower bound of 20%, irrespective of the schedulers, ensuring sufficient operation. Fig. 6.6 shows the critical and non-critical service factors (SF), and revenue generated by each entity with and without

Table 6.2: Power and energy specifications for 1hr case-study

Parameter	**EE 1**	**EE 2**	**EE 3**
Storage (pu)	2	0.32	0.8
PV (pu)	0.5	0.1	0
Critical load power (pu)	1	1.2	0.7
Critical load daily energy demand (pu)	0.1	0.12	0.28
Non-critical load power (pu)	2	1.5	0.35
Non-critical load daily energy demand (pu)	0.8	0.3	0.14

Table 6.3: Optimization Parameters for 1hr case-study

C_{max} (mu/pu)	C_{min} (mu/pu)	M (mu/pu)	β_r	β_s
50	10	10^6	0.1	1

schedulers.

Consider the operation of Entity 1. The non-critical load is served most of the time with the scheduler disabled, while it is completely curtailed when the scheduler is enabled. This is reflected in the increase in its revenue when the scheduler is enabled. Now, consider the operation of Entity 2. The non-critical demand is served longer when the scheduler is disabled but the critical demand is not met at all. On the other hand, when the scheduler is enabled, the non-critical load is curtailed and the critical demand is completely met. Entity 2 also generates a net positive revenue with the scheduler enabled as compared to a negative revenue (expenditure) when the scheduler is disabled. Entity 3 serves both, critical and non-critical demands, longer when the schedulers in Entities 1 and 2 are enabled as compared to when they are disabled. This is reflected in a decrease in revenue resulting in a net positive expenditure when the schedulers in the other two entities are enabled.

6.4.2.2 Variation in Greediness Factor

The greediness factor β (β_r for the revenue seeker and β_s for the service seeker) acts like a control handle for the trade-off between generating revenue and serving non-critical

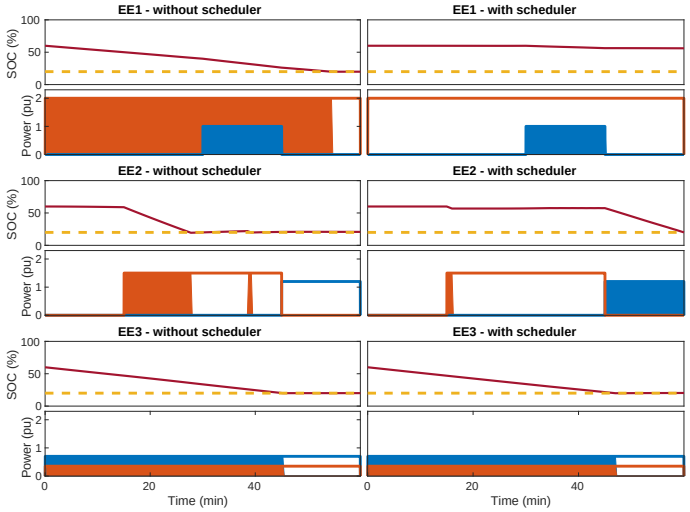

Figure 6.5: Entity-wise state of charge (SOC, top) and traces of load profile (bottom) without schedulers (left) and with schedulers (right); Critical load profile request in blue outline, solid when served, and non-critical load profile request in orange outline, solid when served. *Needs of the critical loads are fully met in all entities with DOS.*

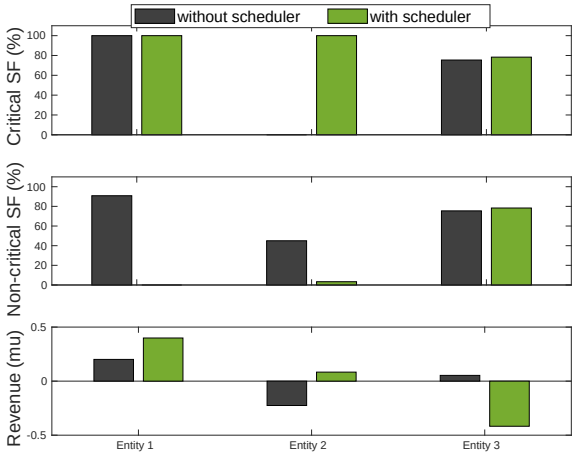

Figure 6.6: Critical service factor, non-critical service factor, and revenue with and without optimal schedulers. *Critical service factor for all entities are improved, revenue seeker gets better revenue and service seeker gets better service with DOS*

demand. The effect of β_r and β_s on service factors and revenue of each entity is demonstrated through 9 simulations on the three-entity network, one for each pair (β_r, β_s), where $\beta_r, \beta_s \in \{0.1, 1, 10\}$. The total run time of each simulation is 24 hours and the power specifications are given in Table 6.4. The schedulers in Entities 1 and 2 are always enabled and the optimization parameters are same as those given in Table 6.3, except for the values of β_r and β_s.

Fig. 6.7 shows the results of critical service factor (CSF), non-critical service factor (NCSF), and revenue for each entity. Fig. 6.7a shows that the revenue generated by Entity 1 monotonically decreases with increase in β_r as expected. This curve shifts upwards with increasing β_s. This is because an increasing β_s indicates an increasing tendency of Entity 2 to import energy. Similarly, Fig. 6.7b shows that the revenue generated by Entity 2 monotonically decreases with increase in β_s as expected. This curve shifts upwards with increasing β_r as an increasing β_r indicates a decreasing tendency of Entity 1 to export energy. In the case of Entity 3 (Fig. 6.7c), the revenue is seen to monotonically increase with β_s and the curve shifts upwards for with increasing β_r. This is because, increasing β_r and β_s indicate a reducing tendency of Entities 1 and 2 to export, respectively.

The revenue plots demonstrate inter-entity coupling in that variations in β of one entity affect the revenue generated by the other two. However, the trend of decreasing revenue by increasing the entity's own β (if scheduler present) is maintained. In each of the revenue plots, there is a larger change in revenue when β_r or β_s changes from 0.1 to 1 as compared to 1 to 10. This shows that the effect of the entity's own β and the neighbors' β diminishes as their values increase. It should be noted that the CSF for all entities is at almost 100% for all combinations of β_r and β_s. This shows that critical demand has a higher priority than revenue or non-critical demand, and is met completely irrespective of the variations in greediness factors.

There can be multiple socioeconomic reasons for revenue seekers as well as service seekers to tweak the greediness factor towards one of the two objectives on different days. For instance, a revenue seeker farmer may want to run their water pump (non-critical

Table 6.4: Power and energy specifications for the 24-hour and 5-day case studies

Parameter	EE 1	EE 2	EE 3
Storage (pu)	1	0.1	0.1
PV (pu)	2	0.2	0.2
Critical load power (pu)	0.1	0.12	0.12
Critical load daily energy demand (pu)	0.06	0.072	0.072
Non-critical load power (pu)	0.75	0.15	0.15
Non-critical load daily energy demand (pu)	0.45	0.045	0.045

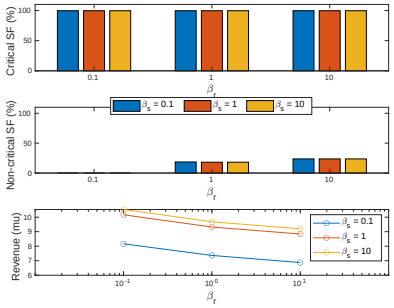

(a) Entity 1: NCSF increases with β_r, does not change with β_s. Revenue monotonically decreases with β_r, curve shifts upwards with increasing β_s; *Smaller greediness factor leads to larger revenue for the RS entity.*

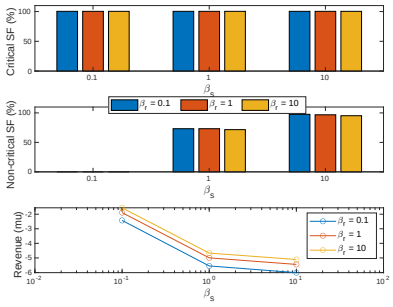

(b) Entity 2: NCSF increases with β_s, does not change with β_r. Revenue monotonically decreases with β_s, curve shifts upwards with increasing β_r. *Larger greediness factor leads to better service for the SS entity.*

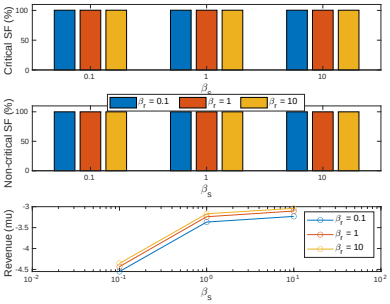

(c) Entity 3: NCSF remains unchanged at a value of 100% for all combinations of β_r, β_s. Revenue monotonically increases with β_s, curve shifts upwards with increasing β_r. *NP entity's performance is at default levels.*

Figure 6.7: Critical service factor (CSF), non-critical service factor(NCSF), and revenue for different β_r and β_s: *CSF for all entities remains at almost 100% irrespective of variation in β_r and β_s.*

load) longer on a day without rain. Increasing the value of β_r will increase percentage of non-critical demand served by reducing energy export. A service seeker residential user may want to reduce expenses at the end of the month while they wait for a pay-check. Reducing β_s will increase revenue (decrease expenditure) by compromising on serving non-critical demand.

The use of β as a user-defined control handle is demonstrated through a five day simulation, without variation in solar irradiance and with the same parameters as in Tables 6.3 and 6.4, except values of β_r and β_s. β_r is 0.1 on all days except Day 3 when it is increased to unity in order to improve the NCSF. β_s equals 10 on all days except Day 5 when it is reduced to unity to increase revenue (reduce expenditure). Fig. 6.8 shows the variation in the two greediness factors and the critical service factor (CSF), non-critical service factor (NCSF), and the revenue for each entity. On Day 3, as β_r has a higher value, it is observed in Fig. 6.8a that the NCSF of Entity 1 increases to about 60% and the revenue dips as the entity does not export as much as other days. This is reflected in an increase in revenue (dip in expenditure) by Entity 2 (Fig. 6.8b) and decrease in CSF of Entity 3 (Fig. 6.8c) on the same day as there is lower amount of energy available for import. On Day 5, as β_s has a lower value, it is observed that the NCSF of Entity 2 reduces to zero while there is an increase in revenue (dip in expenditure) due to lower imports. This is reflected in a slight decrease in revenue for Entity 1. As Entity 2 reduces its imports, there is a larger share of energy available for Entity 3 to import which is reflected as a decrease in revenue (increase in expenditure). Fig. 6.8 demonstrates flexibility the scheduler offers to a revenue seeker to tilt towards being a service seeker and vice versa by tweaking their respective greediness factors.

6.4.2.3 Variation in Solar Irradiance

The three-entity network model is simulated for a total run time of 5 days. To emulate variation in solar irradiance due bad weather, the solar data input to each entity is scaled by a weather parameter between 0 and 1, which is randomly generated on each day. The

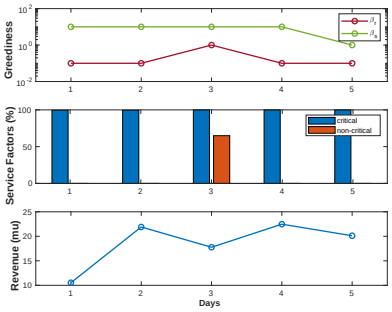

(a) Entity 1: Day 3- $\beta_r \uparrow$, NCSF$\uparrow$, revenue $\downarrow$
Day 5- $\beta_s \downarrow$, revenue $\downarrow$; *RS sought and got better service on Day 3 by trading off revenue*

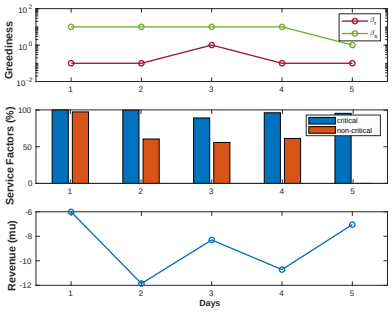

(b) Entity 2: Day 3- $\beta_r \uparrow$, revenue $\uparrow$
Day 5- $\beta_s \downarrow$, NCSF $\downarrow$, revenue $\uparrow$; *SS sought and got better revenue on Day 5*

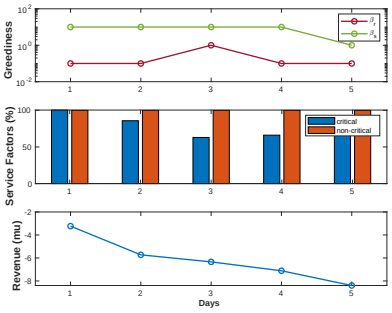

(c) Entity 3: Day 3- $\beta_r \uparrow$, CSF $\downarrow$
Day 5- $\beta_s \downarrow$, revenue$\downarrow$

Figure 6.8: Using β_r and β_s as user-defined control handles to vary service factors and revenue on a day to day basis

power and energy specifications of each entity are given in Table 6.4. The optimization parameters used are same as those in Table 6.3 except β_s equals 10. The simulation is run with and without the scheduler in Entities 1 and 2.

The weather parameter and results for the critical service factor (CSF), the non-critical service factor (NCSF), and the daily revenue generated by each entity under both cases are shown in Fig. 6.9. No significant change in CSF is observed between the two cases for Entity 1 and its value is almost 100% while its daily revenue with the scheduler is greater than that without the scheduler for most of the days. This is compensated for by a low NCSF with the scheduler. For Entity 2, there is a significant increase in the CSF with the scheduler as compared to that without the scheduler on each day, which is compensated for by a low NCSF. Its daily revenue with the scheduler is more than that without the scheduler on most days. Furthermore, even though Entity 3 does not have a scheduler, there is a slight increase in its CSF on all days in the case when the other two entities have schedulers enabled as compared to the case when they are not. This is compensated by a decrease in daily revenue. Therefore, the local optimal schedulers of Entities 1 and 2 are seen to indirectly benefit Entity 3 in terms of CSF but increase its daily expenditure as well. Fig. 6.9 demonstrates the ability of the scheduler to optimize performance without the need for PV forecast data and serve as a plug-n-play model for community microgrids across different geographies and weather conditions.

6.5 Three-Entity Microgrid Network - Experimental Study

6.5.1 Laboratory Setup

In order to establish the viability of the system in real settings, a hybrid three-entity network is emulated through a power hardware-in-the-loop (HIL) experimental setup. Fig. 6.10 shows the block diagram and photograph of the lab scale setup. Entities 1 and 2 are modeled in MATLAB Simulink as described in Section 6.4 while Entity 3 is implemented in hardware. A *Chroma DC Electronic Programmable Load Model 63201* is

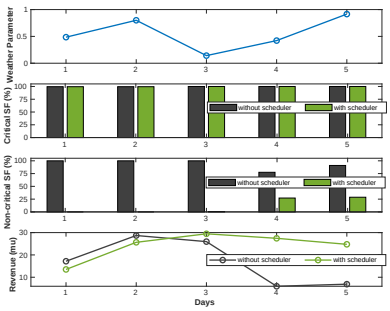

(a) Entity 1

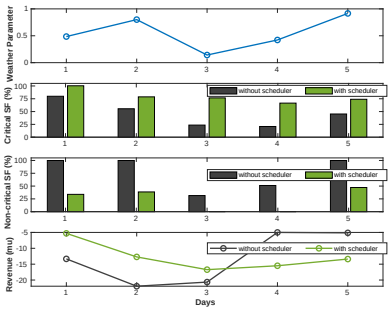

(b) Entity 2

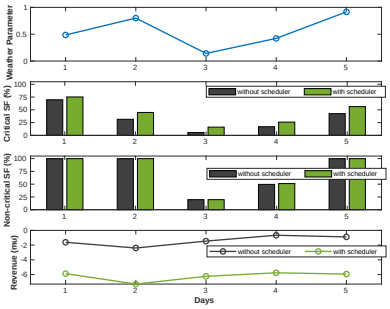

(c) Entity 3

Figure 6.9: Weather parameter, critical service factor, non-critical service factor, and revenue with and without optimal schedulers and with variation in solar irradiance; *CSF improved for all entities at the expense of NSCF/revenue*

used as the export device and a *Chroma Programmable DC Power Supply Model 62024P-40-120* is used as the import device. The MATLAB Simulink model is implemented on a 16GB RAM and 3.2GHz processor Windows PC labeled as the "Simulink Node". It communicates with the programmable load and supply via RS232. The programmable load measures the voltage of the entity's battery, sends it to the Simulink Node which computes the import/export current and sends it to the programmable source/load respectively. The DEM is a monitoring and computing platform based on the Simple Electric Utility Platform [41]. Two ac fan loads are used as the critical and non-critical load respectively and the energy exchange (import/export) is on the dc side. Entity 3 has only the base SOLEEN layer implemented locally in the DEM whereas Entities 1 and 2 have both, a base SOLEEN layer and a scheduler. The base SOLEEN layer and the scheduler are a part of the secondary and tertiary control layers respectively, which work at a time scale of minutes to hours. They are also based on energy, which is a slow changing quantity. These factors make RS232 a sufficient choice for HIL implementation of SOLEEN and the scheduler.

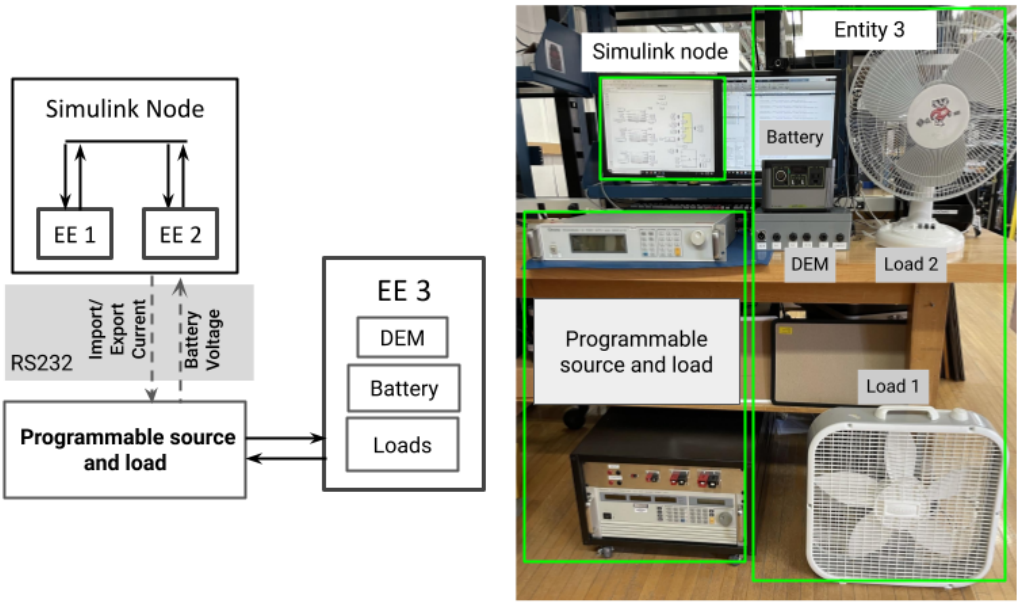

Figure 6.10: Experimental Setup

6.5.2 Experimental Results

A 60 minute HIL experiment with schedulers enabled is conducted with the same specifications as the simulation in Section 6.4.2.1, but with Entity 3 being implemented in hardware. Fig. 6.11a shows the battery voltages, export current, and revenue generated by each entity in the simulation while Fig.6.11b shows the waveforms for the HIL set-up, demonstrating excellent qualitative correlation between the simulations and the experiments, establishing the viability of implementing SOLEEN and DOS in real microgrids.

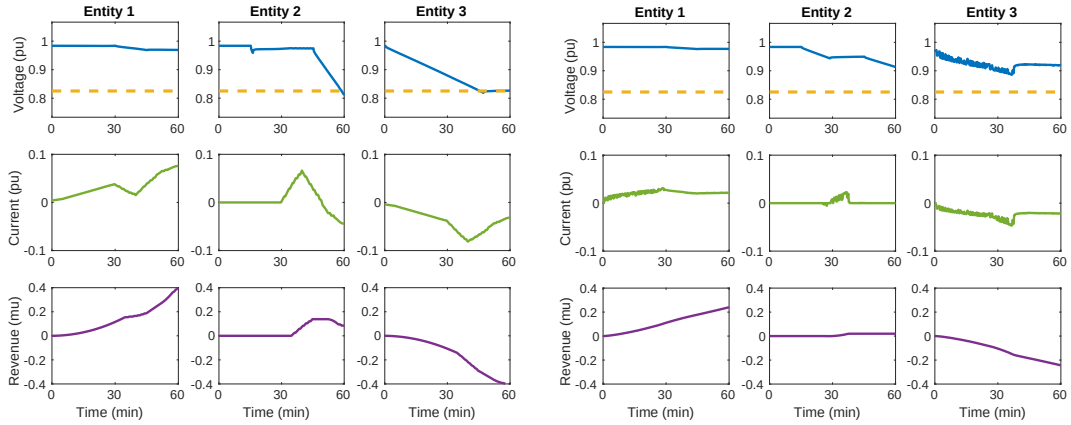

(a) Simulation (b) Hardware-in-the-loop

Figure 6.11: Simulation and Hardware-in-the-loop results: From top to bottom - battery voltage, export current, revenue

6.6 Conclusion

This chapter has presented a distributed tertiary control layer in the form of a distributed optimal scheduler which can be overlaid on the secondary SOLEEN layer. It uses integer linear programming to optimally schedule local loads and energy exchange to meet the operating goals of each entity in the community microgrid. The optimization model formulation along with simulation of a three-entity network are presented. Experimental results are presented for a lab-scale hardware-in-the-loop setup. The main features of the scheduler are:

- completely distributed; role of central entity limited to computing and communicat-

ing energy exchange price

- uses only load, source switches as control handles facilitating lean community microgrid deployment
- accounts for distinction in objectives of participating entities and the multi-objective nature of optimization within each entity
- plug-n-play, independent of network topology, source variability

Evaluation of the effect of the ratio of revenue seekers to service seekers in a larger and more diverse network, nature of pricing structure, overall system stability, scalability, and sufficiency are the subject of future work.

Part III

Optimized Threshold-Based Energy Management

Chapter 7

Energy Management for Prepaid Customers

For a large, and recently increasing, number of households, affordability is a major hurdle in accessing sufficient electricity and avoiding service disconnections. For such households, in-home energy rationing, i.e., the need to actively prioritize how to use a limited amount of electricity, is an everyday reality. In this work, we consider a particularly vulnerable group of customers, namely prepaid electricity customers, who are required to pay for their electricity a-priori. With this group of customers in mind, we propose an optimization-based energy management framework to effectively use a limited budget and avoid the disruptions and fees associated with disconnections. The framework considers forecasts of future use and knowledge of appliance power ratings to help customers prioritize and limit use of low-priority loads (electric appliances), with the goal of extending access to their critical loads. Importantly, the proposed management system has minimal requirements in terms of in-home hardware and remote communication, lending itself well to adoption across different regions, utility programs, and income groups. Our case study demonstrates that by considering both current and future electricity consumption and more effectively managing use of low-priority loads, the proposed framework increases the value provided

to customers and avoids disconnections. [1]

7.1 Introduction

7.1.1 Motivation

Reliability in the electric power systems literature typically focuses on ensuring that the infrastructure is able to supply electricity to customers on demand. However, for many low-income households, a main reason for "power outages" is inability to pay electric bills, which may prompt service disconnections. With limited disposable income, low-income customers are forced to choose between using energy or fulfilling other critical needs such as food – referred to as the "heat or eat" problem [93]. A survey showed that 20% households in the United States reduced or forwent food or medicine to pay energy costs in 2020 [14]. Further, low-income households are seen to reduce energy consumption to unsafe limits in order to limit financial stress, termed 'energy limiting behavior' [94]. A particularly vulnerable group is customers in prepaid programs, who have to purchase credits for the energy prior to use, similar to pay-as-you-go phones. These programs are often targeted towards low-income customers, who may be enrolled either voluntarily or forcefully [95]. While prepaid programs have some advantages, such as the flexibility to make multiple small payments during the month and avoiding upfront credit checks or deposits, they also present some significant disadvantages. For example, prepaid customers may pay a higher price for electricity [95]. While utilities are required to inform postpaid customers before a disconnection, prepaid customers can be automatically and immediately disconnected if their credit runs out. These unanticipated disconnections can be dangerous during extreme heat or cold events and for medically fragile customers. Furthermore, each disconnection-reconnection event can have a fixed charge as high as $75 [96]. Despite those disadvantages, it is estimated that there are between 1 to 2.5 million prepaid electricity accounts in the United States [97], [98] and several million in the United Kingdom [99].

[1] This chapter is based on work by the author and Line Roald in [92]. This work was supported by the George Bunn Wisconsin Distinguished Graduate Fellowship provided by the University of Wisconsin-Madison and the U.S. National Science Foundation under Award Number ECCS-2045860.

Prepaid metering has been observed to reduce energy consumption as compared to the more common postpaid metering plans. A study based on the SRP M-Power prepaid program in Arizona [100] showed a reduction of 12%. This can be due to a combination of the "conservation effect" (being more mindful about unnecessary consumption due to real-time feedback from the wallet balance) or because of disconnections (having no power supply for extended periods because of the inability to refill the prepaid wallet). Some studies where reduction in energy use was not due to disconnections, such as in Oklahoma [101] and Texas [102], have observed a reduction of 11% and 10% respectively, where reduction in energy use was not due to disconnections. Prepaid programs are popular among low-income households and therefore, the "conservation effect" can partially be due to energy limiting behavior [94], i.e., reducing energy usage from safe levels (e.g., by delaying switching on an air conditioner during a heat wave) in order to pay for other needs. Studies have shown that prepaid customers are more likely to show more severe energy rationing behavior than other low-income customers [103]. Low-income prepaid customers may not be able to refill their prepaid accounts with an amount commensurate with their desired use. Therefore, they have to actively ration their energy use to prevent disconnections. This presents a need for a home energy management framework which can help in effective energy rationing for this customer group, a topic that has received little attention to date.

7.1.2 Background

7.1.2.1 Purpose and scope of home energy management

The underlying assumption of energy rationing is that there is a fixed budget available for energy. As discussed in [104], home energy management systems (HEMS) generally aim to optimize one or more of the following objectives: *cost*, *well-being*, *emissions*, and *load profile*. In the context of energy rationing, we aim to minimize user inconvenience (maximize *well-being*) within a fixed energy budget (a hard constraint on *cost*). Further, [104] classify inconvenience modeling into two types: "inconvenience due to timing" (e.g.,

shifting a load from the morning to afternoon), and "inconvenience due to undesirable energy states". The latter is most closely aligned with our setting, since low-income families with a limited budget may enter the undesirable energy state where they have to forego using a load in order to preserve wallet balance for using more critical loads in the future. Therefore, the underlying assumptions of energy rationing are different from typical HEMS literature and also significantly different from demand response, which typically assumes that changes in electricity use should be nearly invisible and non-disruptive to the customer [105].

7.1.2.2 Adoption of smart home technology

Adoption of smart home technology like HEMS is known to have multiple barriers such as perceived intrusion (loss of control) and high costs [106]. A strong reason for customers to switch to or remain on prepaid programs is the increased control over their bills and flexibility in payments [107]. An energy management framework designed for such customers should therefore lead to minimal perception of loss of control. Furthermore, HEMS often rely on specific in-home communication, computing, and switching hardware for automation [108] which may be unaffordable for low-income households. An initial deposit of $100, to cover for future outstanding advances, has been found to be a significantly large upfront cost by some customers of a prepaid program (personal communication with an electric utility offering prepaid metering). Therefore, in order to ensure wide-scale easy adoption, an energy management framework designed for low-income customers needs to be minimally intrusive and implementable using minimal additional and inexpensive in-home hardware.

7.1.2.3 Home energy management and prepaid metering

Aspects of prepaid electricity service have been addressed in terms of meter technology [109, 110], power theft [111], cyber security [112] and data management [113]. However, home energy management for prepaid electricity customers remains largely unexplored.

The only study [114] we identified uses load disaggregation which may need additional hardware or high-speed internet connectivity. Only few HEMS studies explicitly account for a user-defined budget. The method proposed in [115] generates a time-based schedule for load actuation and switches each load ON/OFF, which may be experienced as intrusive. Some studies propose low-cost HEMS for solar PV and battery-based systems [116, 117], but such systems are largely unaffordable for low-income families and inaccessible for renters.

7.1.3 Contributions

We present a home energy management framework for prepaid customers for effective energy rationing, i.e., extending the use of their critical loads by reducing discretionary load usage and preventing disconnections. It can be implemented using minimal additional hardware and ensures that users have more control over their energy use. It is based on a simple threshold-based load control scheme adopted from a DC microgrid setting [43]. Rather than directly actuating loads, this framework *enables* the use of a load by comparing the money available in the prepaid account to a monetary threshold assigned to the load. We refer to the prepaid account as the *wallet* and the amount of money in the account as the *wallet balance* or just *balance*. If the balance is higher than the threshold, the load is enabled, i.e., it can be turned on if desired. As opposed to generating a load schedule or using direct load control which directly turns loads on/off, the proposed method lets the user decide when to use enabled loads. If the balance is lower than the threshold, the load is disabled, i.e., the user is notified that the load should remain off in order to preserve wallet balance for more critical loads in the future. The benefit of the proposed method is that the available budget may be more evenly spread throughout the month, and high priority loads (with lower thresholds) can be used longer. Furthermore, all loads are turned off before a disconnection occurs, thus avoiding potentially expensive disconnection-reconnection events.

While such a threshold-based method is very easy to implement, it requires careful

definition of the enabling thresholds. Thus, we formulate an optimization problem that identifies optimal threshold values while accounting for the available budget and forecasts of future electricity use. We assume that this problem is solved at regular, yet relatively infrequent intervals (e.g. daily), such that the approach lends itself well to implementation with existing in-home hardware and minimal remote communication.

In summary, this work has two main contributions. First, we design an energy management framework that incorporates user-defined load priorities and helps users optimally ration their allocated energy budget, while requiring minimal local computing and remote communication. This framework builds upon the control framework for prosumers in DC microgrids presented in [43], but extends it to (i) consider the prepaid wallet balance as a metric of available energy (ii) optimize the activation thresholds for individual loads to achieve better user satisfaction. Second, we implement our proposed method in code and demonstrate its benefit for managing household loads in a case study based on real-life energy use data obtained through the Pecan Street Dataset [118].

7.1.4 Organization

The remaining chapter is organized as follows. Section 7.2 presents the energy management framework, the optimization formulation, and comments on practical implementation. Section 7.3 presents a case study and numerical results, while Section 7.4 summarizes and concludes the chapter.

7.2 Model

In this section, we provide details on the model setup and the formulation of the optimal energy rationing problem.

7.2.1 Threshold-based energy management

The proposed energy rationing framework is an extension of the Self-Organizing Local Electrical Energy Network (SOLEEN), a control framework developed for DC prosumer

microgrids without central control or communication [43]. In the original SOLEEN design, each entity or household in the microgrid is assumed to have battery energy storage, with the battery state of charge representing available energy. Load control is done by assigning each load a threshold in terms of the state of charge of the battery. If the state of charge falls below the threshold, the corresponding load is switched off. When it is above the threshold, the load is enabled, i.e., the user can decide to switch it on or off.

Here, we adapt the SOLEEN methodology for a prepaid customer, who may not have a battery. Instead, we treat the prepaid wallet balance as a measure of the available energy and express load thresholds in terms of $ (instead of state of charge) for each load. If the $ balance falls below this threshold, the load is disabled. Due to this analogy with battery energy storage, we refer to the refilling of the wallet (in $) as a "recharge". A major difference between a battery and a prepaid wallet is that the battery has a fixed capacity and the state of charge cannot go beyond that, whereas a prepaid wallet does not have an upper limit. Furthermore, electricity demand typically follows a diurnal pattern and the battery capacity (if recharged daily, e.g., using solar PV panels) acts as a daily energy budget. In the case of a prepaid wallet, the user would not typically recharge daily. To achieve better control over enabling loads, we define a *virtual wallet* which is different from the actual prepaid wallet, which we will refer to as the *real wallet*. To match the daily pattern of electricity usage, we recharge the virtual wallet at the beginning of each day with a daily budget and compare load $ thresholds to the virtual wallet balance.

7.2.1.1 Illustrative example

Figure 7.1 shows an example of the proposed framework. The upper plot shows the balance in the virtual wallet along with the threshold for one of the loads, while the lower plot shows whether or not this load is enabled. In this example, the virtual wallet is refilled three times (at timestep 0, 960, 1920). As the wallet balance drops below the threshold, the load is disabled. After this, the considered load does not consume any power and the balance of the virtual wallet reduces less quickly (other loads with a higher priority

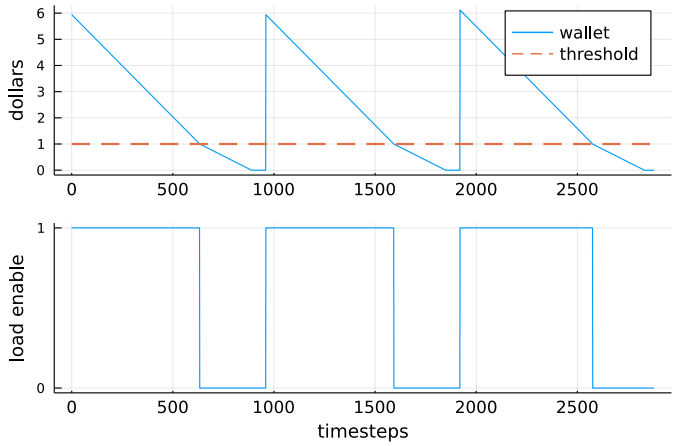

Figure 7.1: Top: Wallet balance (blue) and load threshold (red) in $. Bottom: Enable signal for the load. A value of 1 indicates that the load can be turned on, while a value of 0 indicates that the load should remain off.

continue to consume power, such that the wallet balance continues to decrease until it reaches zero and all loads are disconnected). Once the virtual wallet is recharged, the balance is above the threshold and the load is again enabled.

7.2.1.2 Determining control variables

With the threshold-based control framework, there are two main control variables that need to be determined, namely (1) how the virtual wallet is recharged as a function of the real wallet balance and (2) how to choose thresholds for effective energy rationing. To determine the daily virtual wallet recharge, we simply divide the most recent recharge amount for the real wallet by the number of days until the next recharge[2]. This uniformly distributes the latest recharge amount across all days till the next recharge. The process for determining the load enable thresholds is more sophisticated. These thresholds are obtained by solving an optimization problem as discussed below.

[2]We assume perfect information about when and what amount will be added to the real wallet. The effect of imperfect real recharge information may be addressed by more sophisticated daily virtual wallet recharge schemes, such as allocating a variable daily budget based on the fraction of the average real recharge per month that has been spent. This is a part of future work.

Table 7.1: Nomenclature

Parameters	
$\mathcal{K}$	Set of all loads
$\mathcal{T}$	Set of all time steps in the horizon
$\Delta T \in \mathbb{R}_{>0}$	Duration of time step in hours
$m \in \mathbb{R}_{<0}$	Large magnitude constant
$M \in \mathbb{R}_{>0}$	Large magnitude constant
$\epsilon \in \mathbb{R}_{>0}$	Small magnitude constant
$\alpha \in \mathbb{R}_{>0}$	Electricity rate in \$/Wh
$\gamma_k \in \mathbb{R}_{>0}$	Priority factor for load k
$P_{k,t} \in \mathbb{R}_{\geq 0}$	Demand in W for load k at time t,
$d_{k,t} \in \{0,1\}$	Indicator parameter of demand
	$d_{k,t} = 1$ if $P_{k,t} > 0$, and 0 otherwise
$Z_t \in \mathbb{R}_{\geq 0}$	Real wallet recharge at time t in \$
$X_t \in \mathbb{R}_{\geq 0}$	Virtual wallet recharge at time t in \$
Variables	
$\mathbf{z}_t \in \mathbb{R}$	Real wallet balance at time t
$\mathbf{u}^z_{k,t} \in \{0,1\}$	Real enable signal for load k at time t
$\mathbf{x}_t \in \mathbb{R}$	Virtual wallet balance at time t
$\mathbf{x}_{k,t} \in \mathbb{R}$	Threshold for load k at time t
$\mathbf{u}^x_{k,t} \in \{0,1\}$	Virtual enable signal for load k at time t
$\mathbf{a}_{k,t} \in \{0,1\}$	Actuation state of load k at time t

7.2.2 Optimization formulation

The optimization model determines thresholds for each load k at time t denoted by $\mathbf{x}_{k,t}$. The thresholds for each load are kept constant throughout each day, so the number of unique thresholds is equal to the number of loads times the number of days in the optimization horizon. The input parameters include user-defined priority order for loads, demand forecast, and recharge schedule forecast. We implement the model as a rolling horizon problem with a forecast horizon of seven days and a time step of 15 minutes. We solve the problem once daily, then use the optimized thresholds for the first day to simulate the use of loads to calculate the resulting real and virtual wallet balances. These balances, along with updated forecasts, are used as an input when we re-solve the optimization problem the next day. The resulting optimization problem is a mixed-integer linear programming problem. The nomenclature is given in Table 7.1.

7.2.2.1 Real wallet constraints

The amount of money in the real wallet gets updated according to the energy consumption in the previous time step and the recharge amount scheduled for the current time step as given by

$$\mathbf{z}_t = \mathbf{z}_{t-1} + Z_t - \alpha \Delta T \sum_{k \in \mathcal{K}} (P_{k,t-1} \mathbf{a}_{k,t-1}) \quad \forall t \in \mathcal{T} \tag{7.1}$$

Here, Z_t is equal to the recharge scheduled for the day (if any) if t is the first time step of the day and zero otherwise. The real enable signal $\mathbf{u}^z_{k,t}$ expresses whether there is money in the real wallet. If the real wallet balance $\mathbf{z}_t$ is positive, $\mathbf{u}^z_{k,t} = 1$, and otherwise is zero. This is enforced by

$$m\mathbf{u}^z_{k,t} \leq -\mathbf{z}_t \qquad \forall k \in \mathcal{K}, \forall t \in \mathcal{T} \tag{7.2}$$

$$(M + \epsilon)(1 - \mathbf{u}^z_{k,t}) \geq \epsilon - \mathbf{z}_t \qquad \forall k \in \mathcal{K}, \forall t \in \mathcal{T} \tag{7.3}$$

7.2.2.2 Virtual wallet constraints

The virtual wallet balance $\mathbf{x}_t$ is updated according to the energy consumption since the previous time step and the daily virtual recharge X_t computed from the real recharge, i.e.

$$\mathbf{x}_t = \mathbf{x}_{t-1} + X_t - \alpha \Delta T \sum_{k} (P_{k,t-1} \mathbf{a}_{k,t-1}) \quad \forall t \in \mathcal{T} \tag{7.4}$$

where X_t is equal to the recharge scheduled for the day if t is the first time step of the day and zero otherwise. The virtual enable signal $\mathbf{u}^x_{k,t} \in \{0, 1\}$ should be 1 if the virtual wallet balance $\mathbf{x}_t$ is greater than or equal to the load threshold $\mathbf{x}_{k,t}$, or otherwise zero, as expressed by

$$\mathbf{x}_t - \mathbf{x}_{k,t} + \epsilon \leq (M + \epsilon)\mathbf{u}^x_{k,t} \qquad \forall k \in \mathcal{K}, \forall t \in \mathcal{T} \tag{7.5}$$

$$\mathbf{x}_t - \mathbf{x}_{k,t} \geq m(1 - \mathbf{u}^x_{k,t}) \qquad \forall k \in \mathcal{K}, \forall t \in \mathcal{T} \tag{7.6}$$

Note that $\mathbf{x}_{k,t}$ is also constrained to be the same for all time steps t during a single day.

7.2.2.3 Actuation constraints

The actuation constraints describe whether a load is on and consuming power. The actuation state $\mathbf{a}_{k,t}$ of load k at time t is zero if there is no demand $d_{k,t}$, the virtual wallet balance $\mathbf{x}_t$ is less than its threshold $\mathbf{x}_{k,t}$, if the real wallet balance $\mathbf{z}_t$ is less than or equal to zero, or if the real wallet balance in the next time step $\mathbf{z}_{t+1}$ would be less than or equal to zero if the load is kept on (the latter condition ensures that the real wallet balance does not go negative by the next time step). In this case, $\mathbf{a}_{k,t} = 0$ as expressed by the following constraints

$$\mathbf{a}_{k,t} \leq d_{k,t}\mathbf{u}^x_{k,t}, \quad \mathbf{a}_{k,t} \leq \mathbf{u}^z_{k,t}, \quad \mathbf{a}_{k,t} \leq \mathbf{u}^z_{k,t+1} \quad \forall k \in \mathcal{K}, \forall t \in \mathcal{T}$$

If none of the above conditions are satisfied, the actuation state has to be equal to 1, i.e., $\mathbf{a}_{k,t} = 1$, as described by

$$d_{k,t}\mathbf{u}^x_{k,t} + \mathbf{u}^z_{k,t} + \mathbf{u}^z_{k,t+1} \leq 2 + \mathbf{a}_{k,t} \quad \forall k \in \mathcal{K}, \forall t \in \mathcal{T} \tag{7.7}$$

7.2.2.4 Objective function

Our goal is to maximize the value provided to the customer from using a limited (less than desired) amount of electricity. To express this, we make a few key assumptions. First, some loads bring more value, i.e., have a higher priority, as compared to others and the value of a load does not necessarily scale with its power rating. For instance, a light bulb rated at 5W can provide more value than a TV rated at 100W. Second, we assume that value is associated with whether or not a load is available when desired. Therefore, we design our objective function to account for (1) the priority assigned to each load by the user and (2) the percentage of time the load was available when desired.

We introduce the *load priority factor* γ_k to express the relative value of satisfying the demand of load k compared to other loads. It is calculated as $\gamma_k = \frac{1}{\eta_k}\frac{1}{\sum_k \frac{1}{\eta_k}}$, where η_k is a number that represents the position of the load in the priority order (lower numbers

imply higher priority). For example, if the user ranks loads k = 1, 2, 3 in the order 2, 3, 1 then $\eta_1 = 2$, $\eta_2 = 3$, $\eta_3 = 1$. Note that this is not the only way to determine load priority factor, and this was chosen since it ensures that $\sum_k \gamma_k = 1$.

Next, we define the *Service Factor* (SF_k) for each load k as the ratio of the amount of time a load was available to the amount of time it was demanded.

$$SF_k = \frac{\sum_t \mathbf{a}_{k,t}}{\sum_t d_{k,t}} \tag{7.8}$$

The service factor expresses the percentage of time the load was available when desired and is independent of the power rating of the load. For example, a light rated at 5W demanded for 6 hours and served for 3 hours will have the same service factor as a TV rated at 100W demanded for 2 hours and served for 1 hour. Both will have $SF_k = 0.5$.

The *Priority Service Factor* (PSF) is the weighted average of the service factors, where the weight is the load priority factor. Our objective is to maximize the PSF,

$$\max \quad \sum_{k \in \mathcal{K}} \gamma_k SF_k \tag{7.9}$$

7.2.3 Benchmark Cases

To compare the proposed method, we also implement a simulation of two benchmark cases:

7.2.3.1 Baseline

The baseline case does not have any energy manager and assumes that all loads are enabled as long as the real wallet balance is positive. From a mathematical perspective, this formulation only considers the real wallet update (7.1) and sets $\mathbf{a}_{k,t} = 1$ if $d_{k,t} = \mathbf{u}^z_{k,t} = 1$.

7.2.3.2 Fixed Thresholds

The fixed thresholds case uses a similar model as the one described in Section 7.2.2, except that the load thresholds $\mathbf{x}_{k,t}$ are fixed (i.e., not optimized). While there could be many

methods for computing these fixed thresholds, we choose to calculate them once at the beginning of the month as $\mathbf{x}_{k,t} = \frac{\eta_k}{N}\beta X \quad \forall t$. Here, η_k is the position of Load k in the priority order, N is the total number of loads, X is the total recharge amount for the month (in \$), and β is a positive constant less than 1. For this study, $\beta = 0.05$ was used. With this definition, lower priority loads (i.e. those with a higher η_k) are assigned higher thresholds and will get disabled before higher priority loads as the wallet balance drops.

7.2.4 Implementation through a prepaid program

A benefit of the proposed framework is that it requires minimal additional hardware, computation and remote communication, and thus lends itself well to implementation using the existing infrastructure without significant technological overheads.

A) Local computation: Prepaid programs generally install in-home displays in the customer's house that show their wallet balance [119]. The in-home display is connected to the meter and computes and displays the real wallet balance in real-time. It can be programmed to keep track of the virtual wallet as well, and since this is a simple algebraic operation, additional computation hardware may not be necessary.

B) Remote communication: Households that struggle to pay energy bills may also fall behind on internet and phone bills, thus limiting options for communication. The optimized thresholds can be computed on a remote server and communicated to the in-home display at the beginning of each day through the same communication channel that the utility uses to connect to the in-home display (e.g. the Advanced Metering Infrastructure (AMI) communication system). Since thresholds need to be communicated only once a day, communication delays can be tolerated.

C) Actuation: Direct actuation of loads in a user's home requires additional hardware such as smart switches. If users cannot afford this additional hardware or are not comfortable with an application directly controlling certain household appliances such as medical equipment, either the in-home display or a phone application can instead provide "nudges" to suggest to the user that they switch off the load to allow them to use higher priority

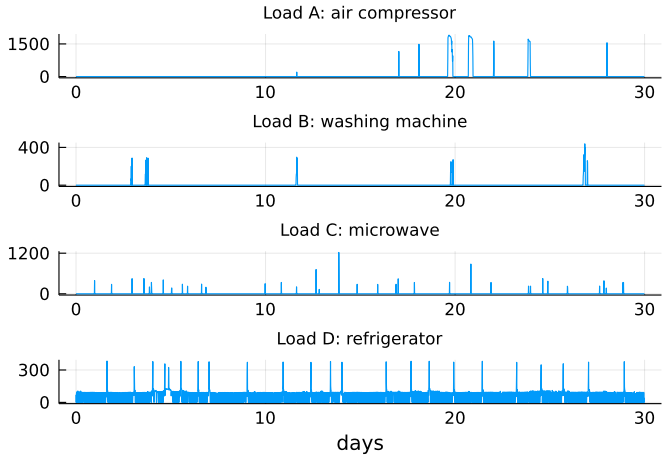

Figure 7.2: Load power demand for 30 days (W).

Table 7.2: Load data

Appliance		Energy (kWh)	Max Power (kW)	Load Priority
A	air compressor	28	1.9	2
B	washing machine	2.0	0.44	4
C	microwave	3.6	1.2	3
D	refrigerator	41	0.38	1

loads later on.

7.3 Case Study

We next demonstrate our proposed framework for optimal energy rationing with a case study. We compare the proposed optimal method against the two benchmark cases, and assess the impact of recharge frequency and overall recharge amount on the priority service factor and the number of disconnections.

7.3.1 Setup and implementation

We use load data for one month (30 days) from one house in the Pecan Street Dataset [118]. The four loads used are an air compressor (Load A), a washing machine (Load B), a microwave (Load C), a refrigerator (Load D). Figure 7.2 shows the power demand for each

load for the duration of the month and Table 7.2 summarizes the total energy demand, maximum power demand, and priority for each load.

We assume that perfect information about the current and future demand for each load as well as the recharge amount and timing is available to the model. (Effects of imperfect information are considered in Chapter 8 and user non-compliance is a part of future work.) The presented results assume either direct load actuation through smart switches or total user compliance to the load enable signal nudges given by the model, i.e., we assume that a load is only in use when the corresponding load actuation signal is $\mathbf{a_{k,t}} = \mathbf{1}$. We use an electricity rate of $\alpha = 0.16$ \$/kWh. Since this is a parameter, time-of-use pricing (i.e. time-varying $\alpha(t)$) may be incorporated without changing the complexity of the problem. The total cost of electricity for using the devices in Table 7.2 with a constant $\alpha = \$0.16/kWh$ would thus be \$11.9 [3].

The *recharge frequency* is the number of times a user recharges their wallet in a month, and typically varies between 1 and 7 per month [107]. We express the total recharge as the fraction of the total cost of desired electricity. The *recharge amount* is the total amount of money added to the real wallet over the course of the month. We express this amount as a percentage of the amount needed to cover the desired electricity use listed in Table 7.2. Thus, recharge amounts $< 100\%$ imply a need for rationing. We assume that the total recharge amount is uniformly distributed across all recharges.

The proposed optimization model and the benchmarking cases are implemented in the Julia programming language [120] (v1.6) and run on a machine with an Intel CPU @3.2GHz and 16GB memory. In the optimized thresholds case, the simulation calls the optimization model implemented using JuMP [121] and the Gurobi solver [122]. The parameter ϵ was set to 1e-6 which is equal to the default tolerance of the solver Gurobi to meet constraints. The optimization model computes new thresholds daily, using an optimization horizon of 7 days. The thresholds for the current day are then implemented in the simulation. The real and virtual wallet balances at the end of the simulated day

[3] Additionally, a transaction cost (fee associated with each recharge) and a monthly fixed cost can be included and is considered part of future work. Factors such as whether the fixed cost will be deducted from the wallet per day or upfront at the beginning of the month may influence model performance.

are then used as an input for the optimization problem the next day.

7.3.2 Comparison with Benchmark Cases

As a first investigation, we compare the performance of the optimal energy rationing framework with the baseline and fixed thresholds benchmark cases. To do this, we run each method for the full 30 days and compare the resulting service factors (SF) per load as defined by (7.8), the overall achieved priority service factor (PSF) as defined by (7.9), as well as the amount of energy consumed per load. For this evaluation, we assume a recharge amount of 70% and a recharge frequency of 5 payments per month. Figure 7.3 shows the service factor SF_k for each load and the overall PSF and Table 7.3 shows the energy use per load. We observe that the different cases lead to very different use of energy across the different loads. The refrigerator (Load D) has the highest priority, and is also the load that runs most continuously. The optimized and fixed threshold cases achieve both a service factor and energy use close to 100% for this load, while the baseline case (which experiences a prolonged disconnection) only achieves a service factor and energy use of about 85%. The air compressor (Load A) has a power demand that is much higher than other loads and the second highest energy demand. Although this load has the second highest priority, the optimized threshold case compromises serving this load to ensure better service to the higher priority Load D and the lower priority but lower energy demand Loads B and C. The baseline and fixed thresholds cases serve more energy to the air compressor, but have lower service factors for the microwave (Load C) and the washing machine (Load B). Because of this, the overall PSF in the optimized thresholds case is greater than that in the other two cases. Further, the optimized thresholds case and the baseline case fully use the allocated budget of 70% of total desired energy, whereas the fixed thresholds case only uses 68%. This is because the fixed thresholds case always has residual balance equal to at least the lowest threshold, i.e., the threshold corresponding to the highest priority load.

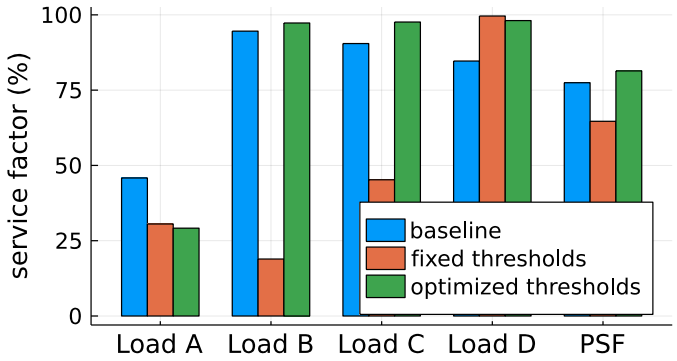

Figure 7.3: Service factor for the 4 loads and overall priority service factor (PSF) at a recharge frequency of 5 per month and recharge amount of 70%. Load priority: Load D > Load A > Load C > Load B

Table 7.3: Energy Usage per Load

Appliance		**Baseline**		**Fixed Thresholds**		**Optimal Thresholds**	
		kWh	**%**	**kWh**	**%**	**kWh**	**%**
A	air compressor	12	43	7.5	27	6.7	24
B	washing machine	1.9	95	0.34	17	2.0	100
C	microwave	3.2	89	1.8	50	3.5	97
D	refrigerator	35	85	41	100	40	98
Total		52.1	70	50.6	68	52.2	70

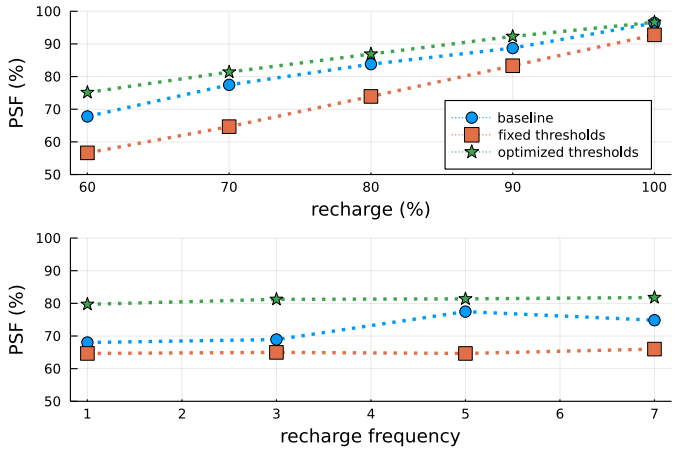

Figure 7.4: Top: PSF against recharge amount at a recharge frequency of 5 per month. Bottom: PSF against monthly recharge frequency at a recharge amount of 70%.

7.3.3 Impact of Recharge Amount and Frequency

Next, we compare the achieved PSF and the number of disconnections (i.e., how frequently the real wallet balance falls below zero and customers lose electricity supply) across different recharge amounts and frequencies.

7.3.3.1 Impact on priority service factor

The upper plot in Figure 7.4 shows the variation in the PSF as the recharge amount is varied from 60% to 100% with a constant recharge frequency of 5 per month. The PSF increases with increasing recharge amount for all three cases, as expected. Across all recharge amounts, the optimized thresholds case has a PSF greater than the baseline while the fixed thresholds case performs worse due to the residual balance that remains unused. The bottom plot in Figure 7.4 shows the variation in PSF as the recharge frequency is varied from 1 to 7 per month while keeping the recharge amount constant at 70%. The optimized and fixed thresholds cases have minimal variation in PSF even if the recharge amount is distributed across increasing number of recharges during the month because the daily virtual wallet recharge remains the same. The optimized thresholds case performs better than the baseline whereas the fixed thresholds case performs worse due to the unused residual energy.

7.3.3.2 Impact on disconnections

We further investigate the impact of recharge frequency and amount on the number of disconnections. We first vary the recharge amount from 60% to 100% while keeping the recharge frequency constant at 5 per month, and then vary the recharge frequency from 1 to 7 per month while keeping the recharge amount constant at 70%. In all of these cases, both the fixed and optimized threshold cases result in zero disconnections as all loads were disabled before the real wallet balance could fall below zero. This demonstrates that the simple threshold-based management can avoid disconnections and associated reconnection fees.

This is quite an improvement relative to the baseline case. With 5 recharges per month, the baseline case experienced 3 disconnections for recharge amounts of 60% and 70% and one disconnection for recharge amounts $\geq$ 80 %. When we fix the recharge amount at 70%, we observe that the number of disconnections increase with increasing recharge frequency. With one recharge, we only have one disconnection, with 3 recharges we have 2 disconnections and with 5 and 7 recharges we have 3 disconnections. The reason for this behavior is that the recharge amounts are distributed uniformly across the month, whereas the load is not. For low recharge amounts or high recharge frequencies, there is therefore a higher chance that the real wallet balance might drop to zero before the next recharge is made whereas for higher recharge amounts and fewer payments, these intermediate disconnections are avoided.

7.4 Conclusion

This work proposes a threshold-based energy rationing framework for prepaid customers. This framework compares a predetermined threshold with the prepaid wallet balance to decide whether a load can be used without impacting other, higher priority loads later. To determine the optimal threshold values, we formulate and solve a rolling horizon optimization problem.

The case study shows that the framework with optimized thresholds outperforms both

a baseline without energy management and a method where control thresholds are fixed solely based on load priority information. Specifically, the proposed method serves higher priority loads and reduces disconnections by curtailing lower priority loads.

The following chapter studies the effects of imperfect and/or limited forecast information. Some avenues for future work include studying the effect of incorporating fixed and transaction costs to inform overall prepaid program design. Finally, while the framework has been presented in the context of low-income households in the United States, it can be extended for other contexts such as postpaid customers on energy assistance programs and pay-as-you-go solar home system users.

Chapter 8

Addressing Imperfect Forecasts and Implementation Constraints

The previous chapter proposed an energy management framework for low-income prepaid electricity customers that requires detailed demand forecasts, which are challenging to generate for residential loads. Additionally, the framework involves solving a mixed-integer linear programming problem using an optimization solver on a remote server, which raises data privacy and cybersecurity concerns. This chapter presents a method based on a linear optimization problem that only uses average power demand forecasts as an input and can be solved to optimality using a simple greedy approach without the need for optimization solvers. We compare the model with two mixed-integer linear programming models: (1) from the previous chapter and (2) a benchmark representative of traditional home energy management systems which also requires more detailed demand forecasts and optimization solvers for implementation. In a numerical case study based on real household data, we assess the performance of the different models under different accuracy and granularity of demand forecasts. Further, we demonstrate that the proposed model can be implemented on a basic 8-bit low-cost microcontroller. Our results show that the proposed linear model is much simpler to implement, while providing similar performance under realistic circum-

stances. [1]

8.1 Introduction

Very few studies investigate energy management methods for prepaid customers. The method in [114] uses load disaggregation techniques and alerts the user to switch off a load to preserve wallet balance once it exceeds a target consumption. To perform the disaggregation, additional hardware or high-speed internet connectivity with a server may be needed. More traditional home energy management systems (HEMS) [108] generate specific load schedules to switch loads ON/OFF. This can be viewed as intrusive, and if automated, it needs expensive in-home hardware such as smart switches for actuating loads. Furthermore, to be effective, such HEMS typically need forecasts of power demand of each load at each timestep in a day. Obtaining highly accurate, granular forecasts can be challenging because of the volatile nature of household-level electricity use, which depends on various behavioral and environmental factors [124]. Additionally, imperfect and uncertain information can significantly impact the performance of HEMS [104], [125], making it necessary to analyze sensitivity of energy management methods to imperfect information. Overall, energy management methods that use lower granularity forecasts (e.g., by aggregating loads or averaging in time) may lend themselves better to practical implementation than very detailed models.

8.1.1 Contributions

To support effective home energy rationing while reducing the need for communication and computation, [92] proposed the threshold-based energy management framework. To identify optimal daily load thresholds, [92] uses rolling-horizon mixed-integer optimization with forecasts of load demand for every 15 min. However, while the thresholds optimization requires load demand forecasts, real-time measurements of load demand are not necessary

[1] This chapter is based on work by the author and Line Roald in [123]. This work was supported by the the George Bunn Distinguished Graduate Fellowship by the University of Wisconsin-Madison and the U.S. National Science Foundation under Award Number ECCS-2045860.

once the thresholds are determined. We make the following contributions beyond prior work:

First, we present a new threshold-based energy management method, which has two main features that distinguish it from the model in [92] (Chapter 7: (1) It only requires information regarding the average power demand per day, as compared to detailed power demand forecasts at each 15 min timestep. In particular, it does not require information about when certain loads will be used during the day. (2) The resulting optimization problem is a linear program (LP), which can be solved to optimality using a greedy approach, thus eliminating the need for a solver.

Next, we compare the proposed model to two benchmark models, the threshold-based model from [92] and a more traditional home energy management system that generates a switching schedule for each load at each timestep. We first qualitatively compare the practicality of implementing and using the different methods, including the computation, demand forecast information, and communication requirements. Furthermore, we perform a quantitative comparison where we run the three models on a case study based on real load data from Pecan Street Dataport [118]. We analyze the performance of the three models under different levels of accuracy and granularity of demand forecast information.

The results of our comparison show that the proposed method has a similar quantitative performance as the two benchmark models, i.e., it is able to help customers effectively manage their electric loads. Furthermore, it has significantly lower requirements for demand forecasts and communication, can be implemented using simpler hardware without optimization solvers, making it a much more viable choice for low-income customers. The model is made publicly available through a GitHub repository [126].

8.1.2 Organization

The chapter is organized as follows: Section 8.2 describes the mathematical optimization formulations for the three models. Section 8.3 compares computation, forecast information, and communication requirements for implementing the models. Section 8.4 presents

Table 8.1: Nomenclature

Parameters		**Model**
$\mathcal{K}$	Set of all loads	AFG, DFM, OBM
$\mathcal{T}$	Set of all time steps in the horizon	DFM, OBM
$\Delta T \in \mathbb{R}_{>0}$	Length of time step in hours	DFM, OBM
$\mathcal{D}$	Set of all days in the horizon	AFG, DFM
$m \in \mathbb{R}_{<0}$	Large magnitude constant	DFM
$M \in \mathbb{R}_{>0}$	Large magnitude constant	DFM
$\epsilon \in \mathbb{R}_{>0}$	Small magnitude constant	DFM
$\alpha \in \mathbb{R}_{>0}$	Electricity rate in \$/Wh	AFG, DFM, OBM
$Z \in \mathbb{R}_{\geq 0}$	Initial real wallet balance in \$	AFG, DFM, OBM
$\gamma_k \in \mathbb{R}_{>0}$	Priority factor for load k	AFG, DFM, OBM
$P_{k,t} \in \mathbb{R}_{\geq 0}$	Demand in W for load k at time t	DFM, OBM
$\bar{P}_{k,d} \in \mathbb{R}_{\geq 0}$	Average demand in W for load k on day d	AFG
$d_{k,t} \in \{0,1\}$	Indicator parameter of demand $d_{k,t} = 1$ if $P_{k,t} > 0$, and 0 otherwise	DFM, OBM
$X_d \in \mathbb{R}_{\geq 0}$	Virtual wallet recharge on day d in \$	DFM
$s^{max}_{k,d} \in \mathbb{R}_{\geq 0}$	Upper bound on enable duration of load k on day d in hours	AFG
Variables		
$\mathbf{z}_t \in \mathbb{R}$	Real wallet balance at time t in \$	DFM
$\mathbf{u}^z_{k,t} \in \{0,1\}$	Real enable signal for load k at time t	DFM
$\mathbf{x}_t \in \mathbb{R}$	Virtual wallet balance at time t in \$	DFM
$\mathbf{x}_{k,d} \in \mathbb{R}$	Threshold for load k on day d in \$	AFG, DFM
$\mathbf{u}^x_{k,t} \in \{0,1\}$	Virtual enable signal for load k at time t	DFM
$\mathbf{a}_{k,t} \in \{0,1\}$	Actuation state of load k at time t	DFM, OBM
$\mathbf{s}_{k,d} \in \mathbb{R}_{\geq 0}$	Enable duration of load k on day d in hours	AFG
$\mathbf{X}_d \in \mathbb{R}_{\geq 0}$	Virtual wallet recharge on day d in \$	AFG

case studies comparing the performance of the models using real-world energy usage data, and this is followed by a brief concluding section.

8.2 Model Formulations

This section presents the mathematical optimization formulations of the three models. A nomenclature with the notation used across models is given in Table 8.1.

The objective of all models is to maximize the value that a user can get from a limited amount of initial wallet balance. Concretely, we aim to maximize the fraction of time for which a load was ON when demanded. We refer to this as the *service factor* SF_k for

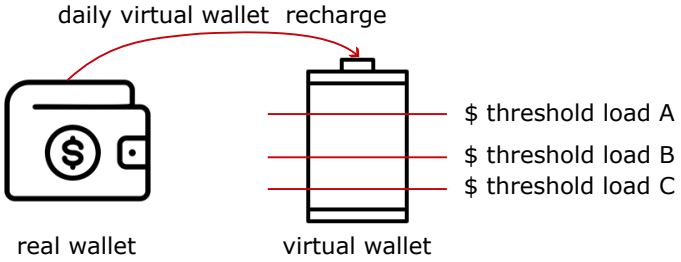

Figure 8.1: Illustration of virtual wallet recharge

load k. For example, a lamp demanded for 2 hours and served for 1 hour has a service factor of 50%. Since some loads are more critical than others, we assign a *priority factor* γ_k to each load k, where a higher γ indicates a more important load. Finally, we define the priority service factor (PSF) as the priority factor weighted sum of service factors, $\text{PSF} = \sum_{k \in \mathcal{K}} \gamma_k \text{SF}_k$. PSF is a linear measure of user convenience and well-being, and all the models presented below seek to maximize PSF.

8.2.1 Detailed Forecast MILP (DFM) model

We first summarize the DFM model from [92], which we will use as a benchmark.

8.2.1.1 Modeling considerations

The DFM model uses demand forecasts $P_{k,t}$ per load k at each timestep t and uses rolling-horizon optimization to determine the optimal thresholds $\mathbf{x}_{k,d}$, per load k per day d. The load thresholds are expressed in terms of prepaid wallet balance (i.e., in \$), as the prepaid wallet balance is a measure of how much energy is available (similar to the battery state of charge in the case of DC microgrid control [43]). However, the prepaid wallet may be recharged at infrequent and possibly irregular intervals. To avoid the balance being used too quickly, [92] defines a *virtual wallet*. This wallet is recharged with regular amounts from the actual prepaid wallet, which we refer to as the *real wallet*, and thresholds are defined in terms of the virtual wallet balances. This setup is illustrated in Figure 8.1. The DFM model based on [92] defines the the virtual wallet recharge X_d as the initial real wallet balance Z divided by the number of days in the optimization horizon.

8.2.1.2 Mathematical formulation

The mathematical formulation of the DFM problem is given as follows,

$$\max_{\mathbf{x}_{k,d},\mathbf{x}_t,\mathbf{z}_t,\mathbf{u}^x_{k,t},\mathbf{u}^z_{k,t},\mathbf{a}_{k,t}} \quad \text{PSF} = \sum_k \gamma_k \frac{\sum_t \mathbf{a}_{k,t}}{\sum_t d_{k,t}} \tag{8.1a}$$

$$\text{s.t.} \quad \mathbf{z}_t = \mathbf{z}_{t-1} + Z - \alpha\Delta T \sum_k (P_{k,t-1}\mathbf{a}_{k,t-1}) \quad \forall t \in \mathcal{T} \tag{8.1b}$$

$$m\mathbf{u}^z_{k,t} \leq -\mathbf{z}_t \qquad \forall k \in \mathcal{K}, \forall t \in \mathcal{T} \tag{8.1c}$$

$$(M+\epsilon)(1-\mathbf{u}^z_{k,t}) \geq \epsilon - \mathbf{z}_t \quad \forall k \in \mathcal{K}, \forall t \in \mathcal{T} \tag{8.1d}$$

$$\mathbf{x}_t = \mathbf{x}_{t-1} + X_d - \alpha\Delta T \sum_k (P_{k,t-1}\mathbf{a}_{k,t-1}) \quad \forall t \in \mathcal{T} \tag{8.1e}$$

$$\mathbf{x}_t - \mathbf{x}_{k,d} + \epsilon \leq (M+\epsilon)\mathbf{u}^x_{k,t} \quad \forall k \in \mathcal{K}, \forall t \in \mathcal{T} \tag{8.1f}$$

$$\mathbf{x}_t - \mathbf{x}_{k,d} \geq m(1-\mathbf{u}^x_{k,t}) \qquad \forall k \in \mathcal{K}, \forall t \in \mathcal{T} \tag{8.1g}$$

$$\mathbf{a}_{k,t} \leq d_{k,t}\mathbf{u}^x_{k,t}, \quad \mathbf{a}_{k,t} \leq \mathbf{u}^z_{k,t}, \quad \mathbf{a}_{k,t} \leq \mathbf{u}^z_{k,t+1} \qquad \forall k \in \mathcal{K}, \forall t \in \mathcal{T} \tag{8.1h}$$

$$d_{k,t}\mathbf{u}^x_{k,t} + \mathbf{u}^z_{k,t} + \mathbf{u}^z_{k,t+1} \leq 2 + \mathbf{a}_{k,t} \qquad \forall k \in \mathcal{K}, \forall t \in \mathcal{T} \tag{8.1i}$$

Here, the objective function is to maximize the PSF as given in (8.1a). Constraints (8.1b) ensure that the real wallet balance $\mathbf{z}_t$ is updated at each time step t; the initial real wallet balance Z is included in the constraint corresponding to the first time step ($t = 1$). Constraints (8.1c), (8.1d) ensure that the real enable signal $\mathbf{u}^z_{k,t}$ is 1 if there is money in the real wallet, and is 0 otherwise. Constraints (8.1e) update the virtual wallet balance $\mathbf{x}_t$ at each timestep t; the constant daily virtual wallet recharge X_d is included in the constraints corresponding to the first timestep of the day. Constraints (8.1f), (8.1g) ensure that the virtual enable signal for load k, $\mathbf{u}^x_{k,t}$, is 1 if $\mathbf{x}_t$ is greater than or equal to the threshold $\mathbf{x}_{k,d}$, and is 0 otherwise. Constraints (8.1h), (8.1i) ensure that a load k at time t is OFF,

i.e., actuation state $\mathbf{a}_{k,t} = 0$, if there is no demand, if the virtual enable signal is 0, or if the real enable signal of the current or next timestep is 0. Similarly, they also ensure that $\mathbf{a}_{k,t} = 1$ if there is demand, virtual enable signal is 1, and the real enable signals for the current and next timestep are 1. Since $\mathbf{a}_{k,t}, \mathbf{u}^z_{k,t}, \mathbf{u}^x_{k,t}$ are binary variables this is a MILP problem. The problem is always feasible if constants ϵ, m, and M are chosen such that: ϵ is as small as possible (e.g., equal to tolerance of the solver), $m \leq -Z$, $M \geq Z$.

8.2.2 Average Forecast Greedy (AFG) model

The average forecast greedy (AFG) model is the new model we propose in this work. Rather than requiring detailed load forecasts, this model only assumes knowledge of the *average* power demand $\bar{P}_{k,d}$ per load k per day d, which can be obtained by forecasting total energy consumption per load per day and dividing it by 24 h. The decision variables in the model are the *durations* $\mathbf{s}_{k,d}$ for which a load k is enabled on day d. Based on the optimal solution $\mathbf{s}^*_{k,d}$, we can algebraically compute the optimal daily virtual wallet recharge, $\mathbf{X_d}$, and thresholds per load k per day d, $\mathbf{x}_{k,d}$. The AFG model is described by the optimization model (8.2a)-(8.2c). The objective (8.2a) is to maximize the PSF. Constraint (8.2b) ensures that the total cost of energy usage for all loads remains within the initial wallet balance, while (8.2c) provides an upper bound $s^{max}_{k,d}$ for the enable duration of each load. This upper bound $s^{max}_{k,d} = 0$ if $\bar{P}_{k,d} = 0$, i.e., when there is no demand for the load on that day, and $s^{max}_{k,d} = 24$ h otherwise.

$$\max_{\mathbf{s}_{k,d}} \quad \text{PSF} = \sum_k \gamma_k \frac{\sum_d \mathbf{s}_{k,d}}{\sum_d s^{max}_{k,d}} \tag{8.2a}$$

$$\text{s.t.} \quad \sum_{k,d} \alpha \bar{P}_{k,d} \mathbf{s}_{k,d} < Z \tag{8.2b}$$

$$\mathbf{s}_{k,d} \leq s^{max}_{k,d} \quad \forall k \in \mathcal{K}, \forall d \in \mathcal{D} \tag{8.2c}$$

8.2.2.1 Solving the AFG model

Since $\mathbf{s}_{k,d}$ are continuous variables, the AFG model (8.2) is a version of a fractional Knapsack problem, which seeks to maximize the value of items in our knapsack while respecting an overall weight limit. This type of problem can be solved efficiently to optimality using a greedy approach [127]. In our problem, the "items" to be chosen are enable durations $\mathbf{s}_{k,d}$ per load per day and the "value" of each item is the respective objective function coefficient $b_k = \frac{\gamma_k}{\sum_d s_{k,d}^{max}}$. The "weight" of each item is the cost of using the load per hour for that day, i.e., $w_{k,d} = \alpha \bar{P}_{k,d}$. To solve the problem, we first compute the ratios of benefit per unit weight, $r_{k,d} = b_k / w_{k,d}$. Note that if $w_{k,d} = 0$, i.e., if there is no demand for a load on a day, we assign $\mathbf{s}^*_{k,d} = 0$. We arrange the ratios $r_{k,d}$ in non-increasing order in a vector $\mathbf{r}$. Therefore, we have $\mathbf{r}^{(i)} \geq \mathbf{r}^{(i+1)}$, where $\mathbf{r}^{(i)}$ represents the ith element of the vector $\mathbf{r}$. Next, we arrange variables $\mathbf{s}_{k,d}$ in a vector $\mathbf{s}$, parameters $s_{k,d}^{max}$ in vector $\mathbf{s}^{max}$, and parameters $\bar{P}_{k,d}$ in vector $\bar{\mathbf{P}}_{k,d}$ in the same order as that of elements in $\mathbf{r}$, such that the ith element of $\mathbf{s}$, $\mathbf{s}^{max}$, and $\bar{\mathbf{P}}_{k,d}$ map to the same load k and day d as the ith element of $\mathbf{r}$. Given these vectors, we implement the greedy solution approach summarized in Algorithm 1. Starting from the first element in $\mathbf{r}$, we assign the maximum duration $\mathbf{s}^{max(i)}$ to each variable $\mathbf{s}^{(i)}$, until we reach the element $\mathbf{s}^{(i')}$ which leads to a violation of the wallet balance constraint (8.2b). For this *marginal load* $\mathbf{s}^{(i')}$, we assign a fractional value equal to the leftover balance divided by the cost of using the load per hour, which is typically less than $s_{k,d}^{max}$ (i.e., we enable the load only for a fraction of the day). For all elements after the i'th element, i.e., those with a lower $r_{k,d}$ value, we set $\mathbf{s}^{(i)}$ to zero. This gives us the optimal enable durations $\mathbf{s}^*_{k,d}$ for each load k and day d. Note that at most one load k in one day d will have a fractional value, i.e., there is only one marginal load.

Algorithm 1 Greedy approach to solve (8.2a)-(8.2c)

sort $\mathbf{r}$ in non-increasing order
$\mathbf{s}^{(i)} \leftarrow 0 \quad \forall i$
$i \leftarrow 0$
while $\sum_i \alpha \bar{\mathbf{P}}^{(i)} \mathbf{s}^{(i)} < Z$ **do**
  $\mathbf{s}^{(i)} \leftarrow \mathbf{s}^{max(i)}$
  $i \leftarrow i + 1$
end while
$i^{'} \leftarrow i$
$\mathbf{s}^{(i^{'})} = \frac{Z - \sum_i \alpha \bar{\mathbf{P}}^{(i)} \mathbf{s}^{(i)}}{\alpha \bar{\mathbf{P}}^{(i^{'})}}$

8.2.2.2 Computing virtual wallet recharge

The daily virtual wallet recharge $\mathbf{X}_d$ is calculated as the amount of recharge needed to support the optimal enable durations $\mathbf{s}^*_{k,d}$, i.e.,

$$\mathbf{X}_d = \sum_k \alpha \mathbf{s}^*_{k,d} \bar{P}_{k,d}, \forall d \in \mathcal{D}$$

The virtual wallet is recharged by $\mathbf{X}_d$ at the beginning of the day with no further recharge during the day, and the virtual wallet balance thus reduces as the loads consume energy. Once the balance goes below threshold $\mathbf{x}_{k,d}$, the corresponding load k is disabled and not enabled again on that day.

8.2.2.3 Computing thresholds

Algorithm 2 presents the method to compute the thresholds $\mathbf{x}_{k,d}$. To compute the thresholds $\mathbf{x}_{k,d}$ for a given day d for a given load k, we distinguish three cases. First, if $\mathbf{s}^*_{k,d} = 0$ (i.e., the load is disabled for the whole day), then the threshold $\mathbf{x}_{k,d}$ is assigned a value slightly larger than the virtual wallet recharge for the day, $\mathbf{x}_{k,d} = \mathbf{X}_d + \epsilon$, where $\epsilon = 10^{-4}$. The virtual wallet balance is expected to never exceed the initial charge $\mathbf{X}_d$ and by setting the threshold higher than this value, the model expects that it will not be enabled. Second, if $\mathbf{s}^*_{k,d} = s^{max}_{k,d}$ (i.e., the load should be enabled for the whole day), then the threshold $\mathbf{x}_{k,d}$ is set to zero. This ensures that the virtual wallet balance never goes negative. Fi-

nally, we consider the threshold for the marginal load $\mathbf{s}^*_{k,d}$ (corresponding to $\mathbf{s}^{(i')}$) that has $0 \leq \mathbf{s}^*_{k,d} \leq s^{max}_{k,d}$. The threshold of this load $\mathbf{x}_{k,d}$ should be chosen such that the virtual wallet balance, which is reducing from $\mathbf{X}_d$ in the beginning of the day, reaches the threshold $\mathbf{x}_{k,d}$ after $\mathbf{s}^*_{k,d}$ hours. This can be expressed as

$$\mathbf{x}_{k,d} = \mathbf{X}_d - \alpha \mathbf{s}^*_{k,d} \sum_{n \in \mathcal{S}^{en}_d} \bar{P}_{n,d},$$

where the second term is the cost of running all enabled loads on the day, $\mathcal{S}^{en}_d \equiv \{n : \mathbf{s}^*_{n,d} > 0\}$, for the duration $\mathbf{s}^*_{k,d}$. The overall time complexity of the AFG model is very low and depends mainly on the type of sorting algorithm used. For example, if merge sort is used, it will be $\mathcal{O}(n \log n)$.

Algorithm 2 Computing thresholds

```
for d ∈ 𝒟 do
  for k ∈ 𝒦 do
    if s*_{k,d} == 0 then
      x_{k,d} ← X_d + ϵ
    else if s*_{k,d} == s^{max}_{k,d} then
      x_{k,d} ← 0
    else
      x_{k,d} ← X_d − α s*_{k,d} Σ_{n∈S^{en}_d} P̄_{n,d}
      where S^{en}_d ≡ {n : s*_{n,d} > 0}
    end if
  end for
end for
```

8.2.3 Optimal Benchmark MILP (OBM) model

We now describe a model more closely aligned with traditional home energy management systems proposed in literature. Rather than relying on thresholds, this model directly decides the activation state of each load at each time step. If given perfect forecasts of desired consumption, it produces an optimal schedule with the highest possible PSF for a given budget. Therefore, we refer to this as the optimal benchmark MILP (OBM) model,

which is given by

$$\max_{\mathbf{a}_{k,t}} \quad \text{PSF} = \sum_k \gamma_k \frac{\sum_t \mathbf{a}_{k,t}}{\sum_t d_{k,t}} \tag{8.3a}$$

$$\text{s.t.} \quad \sum_{k,t} \mathbf{a}_{k,t} \alpha P_{k,t} \Delta T < Z \tag{8.3b}$$

$$\mathbf{a}_{k,t} \leq d_{k,t} \quad \forall k \in \mathcal{K}, \forall t \in \mathcal{T} \tag{8.3c}$$

The model inputs are the demand forecasts $P_{k,t}$ per load k at each timestep t, and it determines the actuation state $\mathbf{a}_{k,t}$ per load k at time t, so as to maximize the PSF as defined by (8.3a). Constraint (8.3b) ensures that the energy usage is within the initial real wallet balance Z and constraint (8.3c) ensures that a load is actuated only when there is demand. Since $\mathbf{a}_{k,t}$ are binary variables, it is a MILP problem.

8.3 Qualitative Comparison - Computation, Communication, and Information Requirements

In this section, we compare the computation, communication, and information requirements of the proposed AFG model with the DFM and OBM models. Ideally, we want a method that limits the need for expensive local hardware, while also minimizing communication needs. We frame our discussion in the context of two possible modes of implementation, *purely local*, where all computations are performed using local in-home hardware, or *mixed mode*, where the optimization problems are solved in the cloud on a remote server and the setpoints are communicated to the local hardware.

8.3.1 Computational requirements

OBM and DFM are MILP problems with a large number of variables, which are generally hard to solve. In our test cases, the DFM problem can take up to 50 min to converge (with 30 day optimization horizon, 4 loads) on a system with a state-of-the-art commercial

MILP solver. The computational effort required to solve the problem indicates that a local implementation of the problem may be impractical or expensive. In comparison, AFG is an LP problem that can be solved to optimality with the greedy approach outlined above, making it quick and easy to solve even with simpler hardware and without optimization solvers. Therefore, it can be implemented purely locally on existing hardware (e.g., the in-home displays typically provided to prepaid customers [107]).

In order to illustrate the computational simplicity of the AFG model, we solved it on an 8-bit microcontroller. We successfully implemented a case with 4 loads and an optimization horizon of 30 days on an Arduino Nano Every, a microcontroller popularly used for lab classes and hobby electronics. It uses the ATMEGA4809 processor (8-bit, 6 KB RAM, 48 KB Flash). It generates thresholds with 7 significant figures. The retail price of the processor is under USD 2.00 (as of November 2024). Implementation on the simple processor demonstrates that the model can be implemented purely locally on inexpensive in-home hardware without the need for remote communication with a server, thus reducing data privacy and cybersecurity concerns. Another option for implementing the model is on smartphones for customers who have access and are comfortable using them.

8.3.2 Load information requirements

Load forecasting is challenging, but can be achieved using statistical and machine learning based methods [124]. The DFM and OBM models require load forecasts with a 15 min granularity for each load. Creating accurate forecasts with such granularity is a very challenging task and would require customers to either share granular historical load data with the remote server, or generate the forecasts locally and communicate them. Either option may require significant communication bandwidth or local computational power. In comparison, the AFG model only requires information regarding the total expected energy demand for each load per day, from which the average power demand can be computed. This lower granularity forecast would be significantly easier to generate, whether it is done

Table 8.2: Qualitative comparison of models

	OBM	**DFM**	**AFG**
Problem type	MILP	MILP	LP
Variables per day	$\|\mathcal{K}\|\|\mathcal{T}\|$	$\|\mathcal{T}\|(3\|\mathcal{K}\|+2)+\|\mathcal{K}\|$	$\|\mathcal{K}\|+1$
Load forecast information	per timestep per load	per timestep per load	average per day per load
Control setpoints per day	$\|\mathcal{K}\|\|\mathcal{T}\|$ binary numbers	$\|\mathcal{K}\|$ floating-point numbers	$\|\mathcal{K}\|$ + 1 floating-point numbers
Mode of implementation	mixed	mixed	purely local

locally or remotely. Furthermore, we would only need to communicate one value per load per day. Avoiding the sharing of high fidelity load forecasts is also more desirable from a privacy and cybersecurity perspective.

8.3.3 Communication of load activation information

In the *mixed mode* of implementation, the optimization problems are solved on a remote server and we need to communicate the resulting control setpoints (i.e., load activation information) to the user. For DFM, only a single threshold per load per day needs to be communicated from the remote server to the local hardware, while AFG requires that the thresholds and the virtual wallet recharge per day be communicated. For a household with $|\mathcal{K}|$ loads, this means communicating $|\mathcal{K}|$ and $|\mathcal{K}|+1$ floating-point numbers per day respectively. For OBM, the actuation states per load per timestep need to be communicated. This amounts to $|\mathcal{K}||\mathcal{T}|$ binary numbers per day where $|\mathcal{T}|$ is the number of timesteps in a day. This is a much larger number than the number of setpoints to be communicated for implementing AFG or DFM. Note that for the AFG model, the communication of control setpoints could be entirely avoided through a purely local implementation. This also proves to be useful in case the model has to be re-run with new load priority factors. For example, in case AFG notifies the user that an uninterruptible load such as a dishwasher has to be turned off in the middle of its operating cycle, the user can choose to assign a relatively higher priority factor to the load and re-run the model locally for a new set of thresholds.

An overview of the comparison is summarized in Table 8.2. We observe that the AFG model has several significant advantages from an implementation perspective. It is the least computationally expensive method, making it suitable for a purely local implementation. If implemented in mixed mode, it communicates only low-dimensional information regarding loads and control setpoints, thus reducing privacy and cyber-security concerns.

8.4 Quantitative Comparison - Case Study

We next compare the AFG model with the DFM and OBM models in a quantitative case study based on real-life energy usage data.

8.4.1 Case study setup

We use energy usage data of one household from the Pecan Street Dataset [118] as load data and "forecasts". We consider four loads, namely a refrigerator, air compressor, microwave, and washing machine in that priority order. The priority factors of the four loads are $\gamma = 0.48, 0.24, 0.16, 0.12$ respectively. The cost of electricity is assumed to be $\alpha = 0.16$ \$/kWh. Each optimization model solves a problem to obtain setpoints, for a duration of 30 days. These setpoints are then used as input to a numerical simulation for the same 30 days. This process is repeated for three months of data. The Julia programming language (v1.6) is used with the JuMP package [121] and the Gurobi solver [122] for implementing the models on an Intel CPU @3.2GHz machine with 16GB memory.

We compare the priority service factor (PSF) from the numerical simulation for AFG, DFM, OBM, and a simple baseline (BSL) of unrationed energy use, which lets a user satisfy all energy demand until the wallet balance is zero. We consider a *perfect* demand forecast, as well as an *imperfect* forecast where the order of days is shuffled. Within each type, we consider two levels of information granularity, a *detailed* forecast with 15 min power demand per load and *limited* forecast with only daily average power demand per load. To reflect the reality of low income customers who may not have enough money to cover their desired energy demand, we assume initial wallet balances that are enough to

supply 70% to 90% total energy demand. The cases and results are described in more detail below.

8.4.2 Perfect forecast

We first assume perfect forecasts of load demand, and investigate the detailed and limited information cases.

8.4.2.1 Detailed information

In this set of experiments, models know the true load demand at each 15 min timestep in the case of OBM and DFM and the true average demand per load per day in the case of AFG. With this perfect detailed information, the OBM provides a truly optimal solution since it has complete information about load demand and can decide which load to actuate at every timestep. The DFM also has information about load demand at each timestep but can only determine a threshold for enabling each load per day, thus we expect DFM to have a lower PSF than OBM. Since AFG only uses daily average power demand per load as input, we expect AFG to have a lower PSF than both DFM and OBM. In these experiments, we seek to assess the performance drop of AFG and DFM relative to OBM.

Figure 8.2(a) shows improvement in PSF over the baseline for month A, while the results for all months A, B, and C are shown in Table 8.3. Note that the DFM values are from the optimization model (and not numerical simulation) because of numerical precision issues. We observe that OBM has the highest improvement for all recharge amounts and months. The performance improvement of DFM is $0-2$ %pt. lower than OBM depending on the month and recharge level, indicating that there is some performance drop due to only having the thresholds as a control variable. The AFG model improves performance relative to the baseline case across all months, despite having significantly lower granularity of demand information. The PSF improvement is $2-6$ %pt. lower than OBM and $0.5-5$ %pt. lower than DFM, indicating that detailed load forecasts are important to achieve high performance.

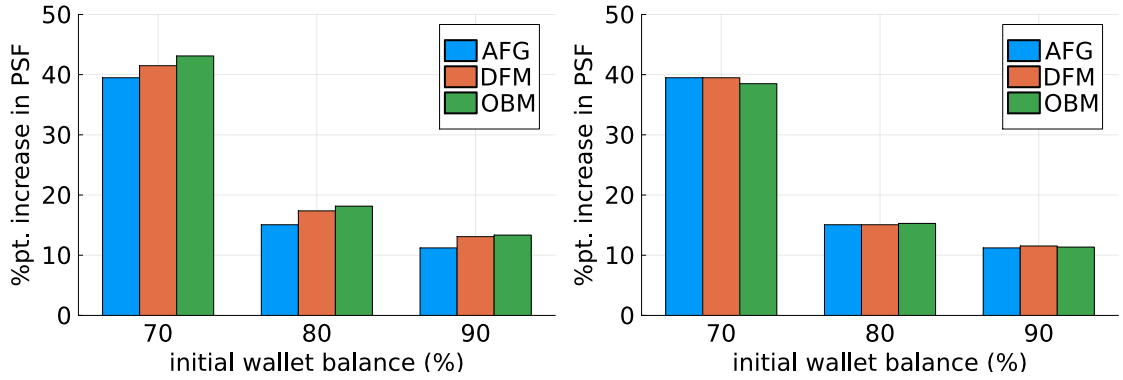

(a) Detailed information (b) Limited information

Figure 8.2: Perfect forecast: Percentage point (%pt.) improvement in priority service factor (PSF) over baseline for the proposed AFG model (blue) and the benchmark models DFM (red) and OBM (green)

8.4.2.2 Limited information

To further assess the impact of limited information, we run experiments where we provide all models with information about the average demand per load per day (i.e., the same information provided to AFG in the previous case). This is a more realistic case, with an easier to obtain load forecast. Further, in this case, the OBM and DFM have no obvious advantage over the AFG model.

Figure 8.2(b) shows the improvement in PSF over the baseline for each model for month A, with similar numbers provided for months A, B, and C in Table 8.3. AFG and DFM perform within 1 %pt. of each other in all cases, while the OBM model performs similar to the others (within 1 %pt. in most cases) or up to 4 %pt. worse in the high initial balance cases in month B. This confirms that all models perform similarly in the setting where they all are given limited information.

8.4.3 Imperfect forecast

Next, we assess performance under imperfect forecast information, generated by randomly shuffling the order of days. The order of shuffling is preserved across models.

Table 8.3: Perfect forecast: Percentage point improvement in priority service factor (PSF) over baseline for the proposed AFG model and the benchmarks DFM and OBM

data	balance	perfect detailed			perfect limited		
		AFG	DFM	OBM	AFG	DFM	OBM
A	70%	39.5	41.5	43.1	39.5	39.5	38.5
	80%	15.1	17.4	18.2	15.1	15.1	15.3
	90%	11.2	13.1	13.3	11.2	11.5	11.4
B	70%	13.7	14.6	16.8	13.7	13.6	12.9
	80%	10.6	11.3	13.4	10.6	10.5	6.97
	90%	8.35	9.01	10.5	8.35	8.33	5.99
C	70%	8.32	13.2	14.0	8.32	8.30	8.76
	80%	3.63	8.64	9.02	3.63	4.24	4.21
	90%	2.16	5.15	5.18	2.16	2.94	2.94

8.4.3.1 Detailed information

First, we provide DFM and OBM with (imperfect) 15 min demand information whereas AFG is provided with (imperfect) average power demand information per day. Figure 8.3(a) shows the PSF for each model for month A, while Table 8.4 shows the results for months A, B, and C. We observe that in month A, the AFG model outperforms the OBM and DFM models, while when considering all the months in Table 8.4, we see that PSF of AFG was sometimes lower than that of DFM. Therefore, the relative performance of the two models depends on the specific data used. The OBM model has the lowest PSF (up to 61 %pt. lower than AFG) across all months and recharge levels, because it activates loads at specific times which do not coincide with the true demand. It is also worth noting that the PSF of the baseline BSL (i.e., no control) is comparable to and sometimes higher than that of the other models in the imperfect information case. However, the user experiences a disconnection in each case with the BSL and may require the payment of reconnection fees. Further, the baseline case leaves the user with no access to power for a prolonged period of time after the disconnection, e.g., for month A the disconnection time is 17, 7, and 5 days with 70%, 80%, and 90% initial wallet balance, respectively. Furthermore, it is also likely that a more realistic implementation of the AFG, DFM, and OBM models, where setpoint optimization would be rerun frequently (e.g., daily) with information from actual usage in the previous day, would help close the performance gap with the baseline

Table 8.4: Imperfect forecast: PSF in percent and improvement in PSF over baseline BSL in percentage points in parentheses for the proposed model AFG, the benchmarks DFM and OBM, and PSF and disconnection duration (# days) for the BSL model

month	balance	imperfect detailed			imperfect limited			BSL	# days
		AFG	DFM	OBM	AFG	DFM	OBM		
A	70%	80.6 (29.2)	77.8 (26.3)	33.7 (-17.8)	80.6 (29.2)	79.1 (27.6)	70.0 (18.5)	51.5	17
	80%	80.6 (1.95)	77.5 (-1.15)	34.0 (-44.7)	80.6 (1.95)	78.1 (-0.63)	70.0 (-8.69)	78.7	7
	90%	80.6 (-4.69)	73.5 (-11.8)	34.2 (-51.1)	80.6 (-4.69)	80.6 (-4.76)	70.0 (-15.3)	85.3	5
B	70%	71.0 (3.01)	73.1 (5.08)	33.8 (-34.2)	71.0 (3.01)	76.2 (8.22)	61.9 (-6.07)	68.0	9
	80%	71.0 (-6.06)	80.5 (3.41)	35.1 (-41.9)	71.0 (-6.06)	76.3 (-0.74)	61.9 (-15.1)	77.1	6
	90%	72.9 (-12.4)	81.2 (-4.08)	36.9 (-48.4)	72.9 (-12.4)	78.6 (-6.69)	69.6 (-15.7)	85.3	4
C	70%	78.2 (-1.25)	78.7 (-0.82)	33.0 (-46.5)	78.2 (-1.25)	75.6 (-3.88)	72.8 (-6.69)	79.5	3
	80%	88.4 (1.31)	86.3 (-0.80)	34.0 (-53.2)	88.4 (1.31)	85.8 (-1.30)	73.4 (-13.8)	87.1	2
	90%	95.2 (2.26)	94.9 (1.96)	34.1 (-58.8)	95.2 (2.26)	95.2 (2.26)	73.4 (-19.6)	92.9	1

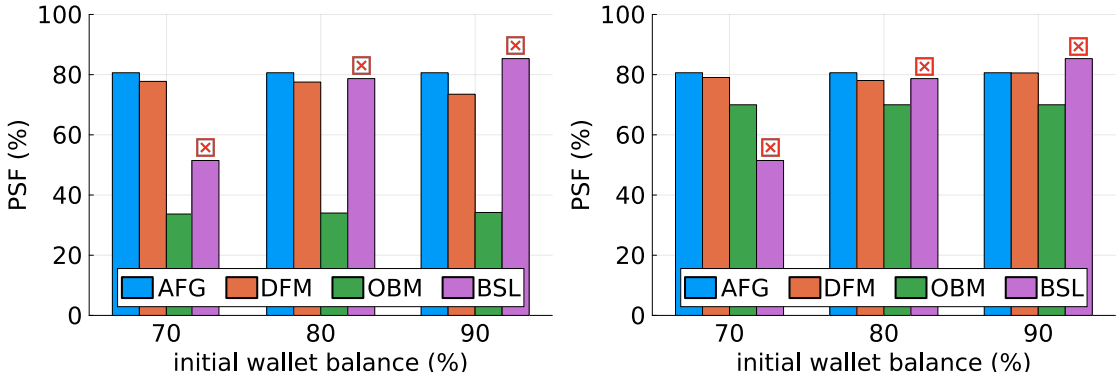

(a) Detailed information (b) Limited information

Figure 8.3: Imperfect forecast: Priority service factor (PSF) and customer disconnections (indicated by 'x' mark) for the proposed model AFG (blue), the benchmark models DFM (red), OBM (green), and the baseline BSL model (purple)

BSL model.

8.4.3.2 Limited information

Next, we provide all models only average power demand data for the shuffled days (same as what was provided to AFG in the previous case) and results are shown in Figure 8.3(b) for month A and Table 8.4 for months A, B, and C. Similar to the imperfect-detailed case, PSF of AFG is higher than that of OBM (up to 22 %pt.) and the relative performance of AFG and DFM is observed to be dependent on the specific data used as seen in Table 8.4. It can also be seen that the PSF of OBM considerably increases. This is because the forecast contains demand equaling the daily average power demand for the entire duration of 24 hours every day, which may have more overlap with the actual demand than in the previous case.

These results indicate that when all models are provided with perfect-limited information, the AFG model performs on par with DFM and OBM. With imperfect-limited information, AFG performs on par with DFM in most cases and outperforms OBM. The case study highlights that the proposed AFG model achieves comparable or improved performance compared to the benchmark models, despite being computationally simpler.

8.5 Conclusion

This study presents a linear threshold-based energy rationing model for prepaid electricity customers, which needs only daily average demand forecasts and can be solved to optimality using a simple greedy strategy. We compare this model with two mixed-integer linear programming (MILP) models which require demand forecasts at each 15 min timestep in case studies with perfect, limited, and imperfect forecast information. The proposed linear model has comparable or improved performance compared with that of the MILP models, while being computationally inexpensive. Therefore, it can be implemented on inexpensive local in-home hardware as demonstrated through implementation on a basic 8-bit microcontroller.

Some avenues for future work include modeling user noncompliance to load enable/disable signals, determining a relationship between forecast error and model performance, formulating the optimization model to incorporate uncertainty in forecasts, and studying the effects of delays in computation and communication of optimal setpoints for energy rationing. We would also like to deploy this method in a field experiment.

Part IV

Picogrid

Chapter 9

Picogrid: An Experimental Platform for Prosumer Microgrids

The microgrid paradigm is gaining momentum as one of the key pieces of technology for expanding clean energy access and improving energy resilience. Most of the interest in this pertains to distinct entities that either generate electricity or act as loads, i.e., distinct producers and consumers. Remote community microgrids and emerging transactive energy service models with interconnected prosumers do not clearly fit into this paradigm. Notwithstanding various publications that present concepts and simulations, there has been a dearth of experimental platforms to study them, due to practical challenges. This work presents the 'Picogrid' - an experimental platform particularly designed for dc prosumer microgrids. It is a low-power, low-cost hardware platform that enables interconnecting multiple prosumer entities in a bench-top setup. Each prosumer sends data to a cloud dashboard and can receive set points for optimal operation from a remote computer system, lending itself to use in a virtual lab setup. The platform enables implementation of custom power profiles based on real-world generation and demand datasets. Features of the platform are demonstrated using simulation and experimental results. [1]

[1]This chapter is based on work by the author and Giri Venkataramanan in [128]. This work was supported by the George Bunn Distinguished Graduate Fellowship by the University of Wisconsin-Madison and the Wisconsin Electric Machines and Power Electronics Consortium.

(a) Producer-consumer microgrid (b) Prosumer microgrid

Figure 9.1: A sketch of microgrid architectures

9.1 Introduction

Microgrids have shown great potential in contributing towards the clean energy transition in developed as well as emerging economies since they are key for building electricity systems that are flexible, resilient, cost-effective, and just. [129]. A microgrid with a single load-serving entity that owns generation assets and supplies multiple households, has a "producer-consumer" architecture. This consists of distinct entities for generation, storage, and loads, as shown in Figure 9.1(a). On the other hand, the "prosumer" architecture as shown in Figure 9.1(b) is useful to represent modular interconnected solar home systems in off-grid communities. Each house is a prosumer and can have bidirectional power exchange with the network. In ad hoc prosumer networks, the absence of a dedicated load-serving entity opens up questions about supply-demand balance and rate-making for energy exchange. There is a need for research and education platforms for prosumer microgrid modeling that address these factors as a part of the broader "transactive energy" paradigm [130]. Furthermore, legacy power systems curricula need to be updated to train the new workforce in microgrid technology using such platforms.

Microgrids consist of a physical energy hardware layer, a control and computation software layer, and communication links between layers. Operating frameworks for microgrids need to be developed keeping in mind the engineering requirements and limitations of the underlying equipment and software tools. Therefore, there is great value in having a hardware platform as opposed to a simulation-only platform for validating such frameworks. For instance, multi-agent systems (MAS)-based microgrid control, which is a popular op-

tion for distributed control in multi-entity prosumer networks, is often implemented in simulations, and studies recommend that the true test of such frameworks can come from rigorous hardware implementation [131]. Furthermore, microgrid laboratory courses based on hardware platforms can help in imparting the necessary skills for real-world microgrid deployment. An ideal research and education experience is offered by setting up a real prosumer microgrid in a village or a community of households. However, this is often not practically feasible since it needs a large budget, has a multi-year timeline, and needs engineers as well as community organizations to deal with the technical and socioeconomic aspects of such a community energy project respectively. The next best option is a lab-scale setup for research and education.

In this context, examples of microgrid education and experimental platforms at different scales and power levels are presented in Table 9.1. Educational institutes are setting up microgrids on their campus to meet their clean energy and resilience goals and also to use them as learning labs for students [132, 133]. At a lower power scale, hardware-based laboratory-scale microgrid platforms that incorporate multiple energy sources such as solar PV, wind, fuel cells, and diesel generators have been developed, for example see [134,135]. To incorporate more flexibility in experimenting with control paradigms and integration with simulation platforms, hardware-in-the-loop microgrid platforms have also been developed [136–138]. Several studies like [42,139,140] have developed hardware-based platforms at the power level of a single-home and have designed curricula for smart home energy management systems. Purely simulation-based coursework and platforms have also been developed [141–143]. Various microgrid test beds and experimental platforms are reviewed in [144, 145].

Hardware-based education platforms at the scale of campus-wide microgrid deployments can be high budget projects. Lab-scale setups that are developed at the power levels of real-world deployments can also be expensive and have significant operational and maintenance overheads. Nevertheless, hardware-based platforms are key for effective microgrid research and education. Furthermore, the option of conducting virtual experi-

ments on such platforms can prove to be extremely useful as necessitated by the COVID-19 pandemic and the increasing popularity of distance education programs. In summary, the aforementioned platforms do not address this gap of a low-cost experimental platform for emerging prosumer microgrid modeling needs.

Table 9.1: Comparison of microgrid education and experimental platforms

References	**Implementation**	**Power level**	**Typical hardware costs**
[132, 133]	campus microgrid	MW	$ Millions
[134, 135]	lab-scale hardware	kW	$ Tens of thousands
[136–138]	hardware-in-the-loop	kW	$ Tens of thousands
[42, 139, 140]	home energy management	W	$ Thousands
[141–143]	simulation	kW	-

9.1.1 Contributions

In this work, we present the Picogrid - an experimental platform for dc prosumer microgrids. Each prosumer entity is represented by low-power hardware and this makes it cheaper, smaller, and safer to operate tens of such prosumer entities in a lab setting. The distinguishing features of this platform are: (1) enables experiments based on community microgrids with prosumer entities, (2) is a low-cost, low-power dc hardware platform, (3) enables easy bench-top setup of tens of entities, (4) offers a cloud dashboard for visualizing sensor data, (5) can integrate with computation-heavy tools like optimization solvers running on any computer system with an internet connection, (6) supports virtual labs and remote experiments.

The hardware and software source files are made publicly available for interested researchers and educators through a GitHub repository [146].

9.1.2 Organization

The following section presents details about the platform's components and features. Section 9.3 presents three experiments that demonstrate various features of the platform. This is followed by a brief concluding section.

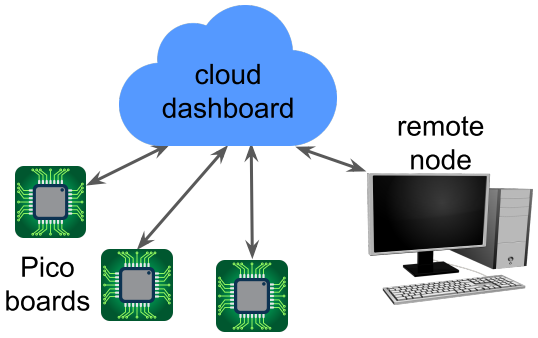

Figure 9.2: A sketch of layers of the Picogrid platform

9.2 Platform

As shown in Figure 9.2, the Picogrid platform consists of multiple layers, viz., Pico boards, a cloud dashboard, and a remote node. These layers together form a small benchtop microgrid or a "picogrid" and emulate their real-world counterparts. Pico boards emulate prosumer households. The remote node emulates DERMS (distributed energy resource management system) or a microgrid operator which provides operating set points to the prosumers. The cloud dashboard emulates the data transfer system between the prosumers and the operator. In this section, we present the utility and features of each layer and briefly discuss the unit price of a Pico board.

9.2.1 Pico board

9.2.1.1 Power circuit

Each prosumer in the picogrid is represented by a Pico board. Figure 9.3 shows the block diagram of a Pico board connected to the picogrid network. Figure 9.4 shows a photograph of a Pico board. The Pico board models a prosumer entity which can have battery storage, channels to import from and export to the network, and local devices that can either act as power sources or loads. The Pico board has 2 source channels, 3 load channels, an import channel, and an export channel, bringing the total to 7 channels. Battery storage is represented by a single Lithium-ion cell. Source channels can be connected to external

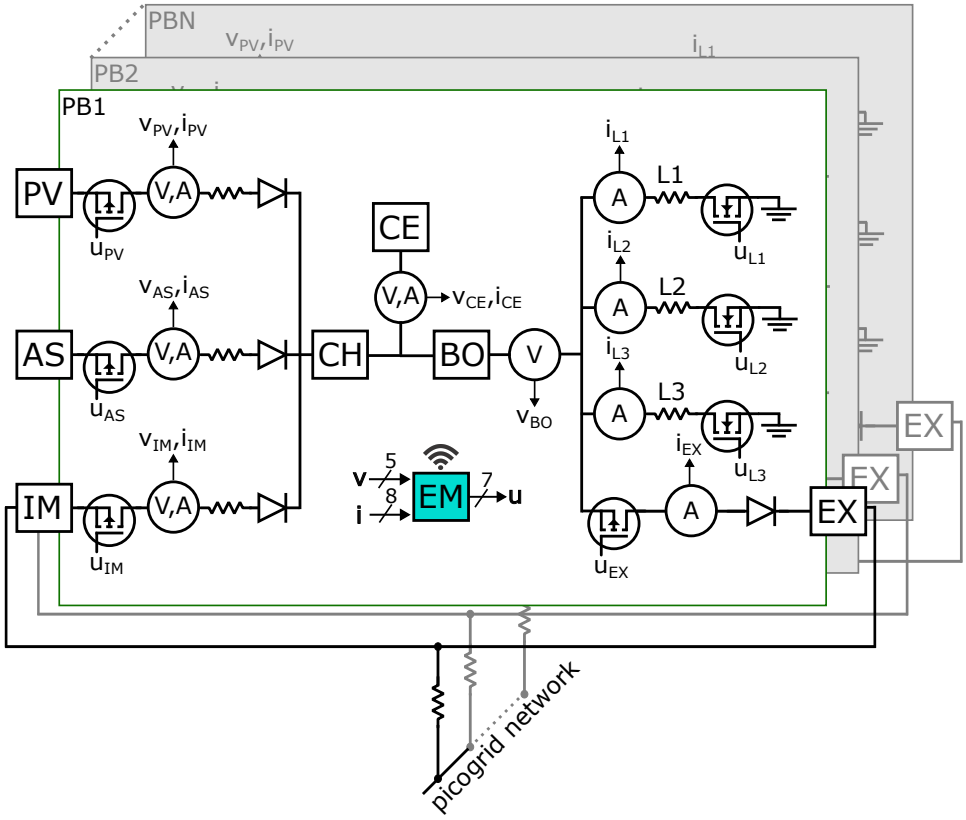

Figure 9.3: Pico board block diagram. The inputs to and outputs from the energy manager are: $\mathbf{v} = [v_{PV}\ v_{AS}\ v_{IM}\ v_{CE}\ v_{BO}]$,
$\mathbf{i} = [i_{PV}\ i_{AS}\ i_{IM}\ i_{CE}\ i_{L1}\ i_{L2}\ i_{L3}\ i_{EX}]$, $\mathbf{u} = [u_{PV}\ u_{AS}\ u_{IM}\ u_{L1}\ u_{L2}\ u_{L3}\ u_{EX}]$.
(Labels: PB = Pico board, PV = PV Source channel, AS = Auxiliary Source channel, IM = Import channel, CE = cell, CH = charger, BO = boost converter, EM = energy manager, L1 = Load 1 channel, L2 = Load 2 channel, L3 = Load 3 channel, EX = Export channel)

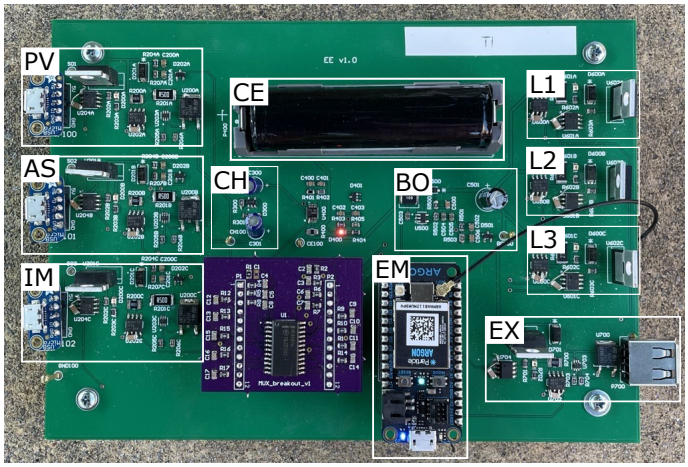

Figure 9.4: Photograph of a Pico board that represents a prosumer entity with sources, loads, storage, import/export channels, and an energy manager.

power sources rated at 1 pu nominal voltage such as a solar PV panel or a benchtop power supply. They are labeled as PV and Auxiliary Source (AS). Source and import channels are connected to a cell charger IC through a diode and a droop resistor. The nominal voltage of the cell is 0.72 pu. A boost converter boosts this voltage to 1 pu to supply to the load and export channels. An on-board resistor acts as the load at each load channel. The per unit base quantities are: voltage = 5 V, current = 0.5 A, energy = 1 Wh. The channel power ratings are: Source 1 pu, Load 0.37 pu. The cell has an energy capacity of 12.24 pu.

9.2.1.2 Control circuit

The local controller or the energy manager (EM) is implemented using the Particle Argon microcontroller. It has a WiFi module to communicate with the cloud dashboard. Particle products are packaged as PaaS (platform-as-a-service) and can effectively support scaling up of solutions [147]. All 7 channels have a MOSFET switch and the EM determines their switching state **u**. It can use pulse-width modulated gate signals to model variable load and source power profiles. The EM reads voltage **v** from 5 on-board voltage sensors (PV channel, AS channel, Import channel, cell terminals, boost converter output) and current **i** from 8 on-board current sensors (PV channel, AS channel, Import channel, cell, Load 1-3 channels, Export channel). Figure 9.5 shows 4 Pico boards with PV panels, demonstrating easy bench-top setup of multiple prosumer entities. To be sure, the system can be scaled with numerous Pico boards using framed mechanical racks, if so desired.

9.2.1.3 Power modulation

While a naturally modulated power source such as a PV source can be connected to the Pico board, in order to provide more flexibility and convenience of not being dependent on weather, a source channel of the Picogrid can be connected to a 1 pu nominal voltage source. The on-board linear charger draws a constant current of 1 pu (CC mode) until the cell reaches its regulation charging voltage and the charger switches to constant voltage

charging (CV mode). Therefore, in the CC mode, the voltage and current at the source channel are stiff (at 1 pu each). The voltage at the load channel is the voltage output of the boost converter (1 pu) and the load is an on-board resistor that draws 0.37 pu current at 1 pu voltage. Therefore, the voltage and current at the load channel are stiff. Since the voltage and current at source and load channels are stiff, the power through a channel is only dependent on the duty cycle of the channel's switch. The power through a channel at time t is given by $p_{c,t} = d_t P_c$, where d_t is the duty cycle of the gate signal and P_c is the nominal power input/output at the source/load channel. In the prototype system, $P_c = 1$ pu for the source channel and $P_c = 0.37$ pu for the load channel.

9.2.1.4 Interconnecting Pico boards

Pico boards can be interconnected to form a network or a "picogrid". Each board has dedicated unidirectional channels to import and export power as shown in Figure 9.3. The energy manager (EM) controls the switching state of the MOSFET switch while the diode ensures unidirectional power flow. The EM can turn on the import switch and turn off the export switch if the prosumer desires to import power from the network whereas it can turn on the export switch and turn off the import switch if it wishes to export power. Note that if the EM turns both switches on at the same time, current can circulate within the Pico board and therefore this should be avoided. To connect a Pico board to the picogrid, the import and export channels are shorted together and connected to the network via a resistor that models line resistance. Figure 9.11 shows three Pico boards interconnected in a radial configuration.

9.2.2 Cloud dashboard

The cloud dashboard is set up using the ThingSpeak IoT platform by MathWorks and supports REST and MQTT API [148]. Data on the dashboard is displayed in the form of data channels. There are data channels for data from sensors on Pico boards (called Pico board data channels) and for setpoints from the remote node (called setpoint data

Figure 9.5: Photograph of multiple Pico boards that fit easily on a lab bench.

channels). A screenshot of the cloud dashboard showing a Pico board data channel is shown in Figure 9.6. Pico boards can write data from on-board sensors to their data channels and can read from setpoint data channels. The remote node can read from the Pico board data channels and write to the setpoint data channels. The permissions for reading and writing are controlled through read/write API keys.

9.2.3 Remote node

The remote node is a remote device with greater computation power than the EM on the Pico boards and can generate setpoints for their operation. It can be any computer system with internet connectivity, not necessarily in close proximity to the Pico boards. It can read data from and communicate setpoints to the cloud dashboard. The cloud dashboard enables the Picogrid platform to be extended to a virtual lab setup. A remote node can be granted access to the necessary read/write API keys to read from Pico board data channels and write to setpoint data channels to observe and conduct experiments.

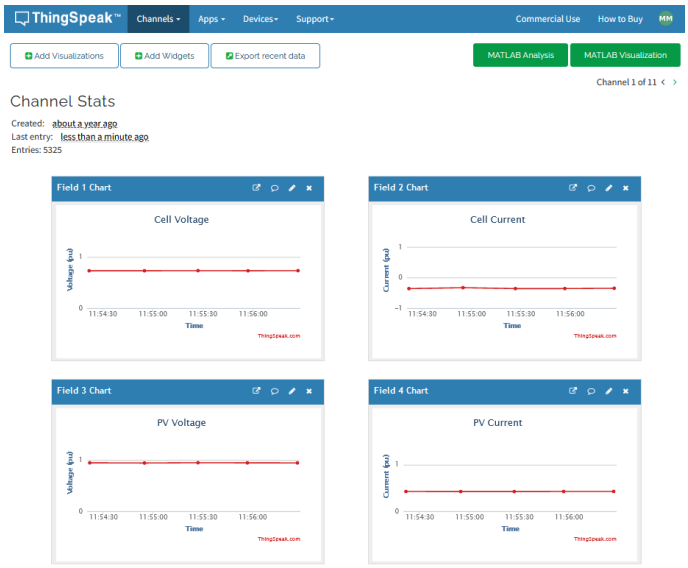

Figure 9.6: Screenshot of the cloud dashboard showing a Pico board data channel

9.2.4 Bill of Materials

The bill of materials of the Pico board can be broadly divided into 5 categories: (1) PCB manufacturing, (2) microcontroller, (3) switches, drivers, and sensors, (4) capacitors and resistors, (5) connectors. The unit cost of a board against number of units is shown in Figure 9.7. The unit cost is seen to vary from about USD 140 at a single unit to USD 80 at 1000 units (as per prices in 2023). The price point makes the platform affordable for wide-scale adoption in undergraduate and graduate coursework and research.

9.3 Experimental Results

This section presents three experiments that demonstrate features of the platform. Experiment 1 demonstrates source and load power modulation. Experiment 2 demonstrates how a Pico board can meet its objectives with local control informed by setpoints from the remote node. Experiment 3 presents interconnection of three Pico boards to form a prosumer network. A simulation model of the Pico board is developed using MATLAB Simulink and PLECS Blockset. Experimental data from Experiments 1 and 3 are used to

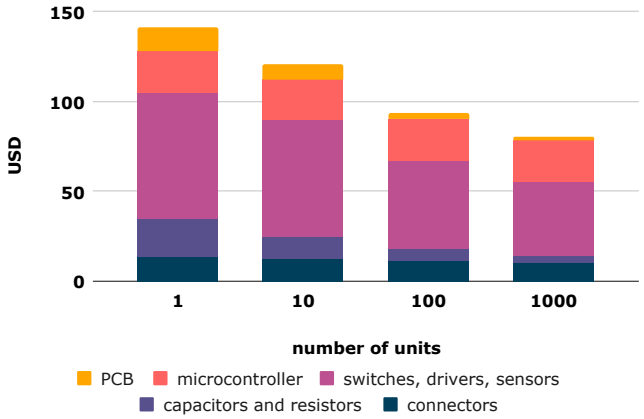

Figure 9.7: Variation in unit price of a Pico board with number of units

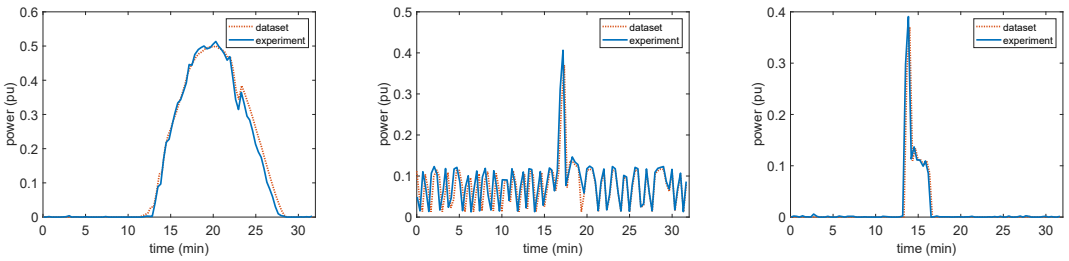

(a) PV (b) Load 1 (c) Load 2

Figure 9.8: Power variation across PV, Load 1, Load 2 obtained experimentally matches closely with that from the dataset

benchmark the simulation model. The model can be used to simulate multiple scenarios with varying parameters and can help in designing experiments for the platform.

9.3.1 Experiment 1: Source and load power modulation

This experiment demonstrates how a Pico board can emulate variable power profiles of sources and loads by modulating channel power using PWM. We use rooftop solar photovoltaic power generation data and household appliance power consumption data for two load circuits, viz. refrigerator and kitchen appliances, for 24 hours for a house from the Pecan Street Dataset [118]. This data is scaled in terms of power and time duration and is implemented on a Pico board over the duration of a 32 min experiment. PV, Load 1, and Load 2 channels are used to represent solar photovoltaic, refrigerator, and kitchen appliances data respectively.

The PV, Load 1, and Load 2 power profiles from the dataset are 24 hour time series of power values at a sampling interval of 15 min, i.e., 96 values per time series. The EM runs at a timestep of 10 s which means that the duty cycle of the switches can be updated once every 10 s. It logs data to the cloud dashboard at every other timestep, i.e., every 20 s due to limitations on the update interval. In order to run experiments in a reasonable duration of time and ensure that the cloud dashboard logs values without loss of data, we scaled down the data in terms of time such that the interval between two values in the 96 value time series is 20 s, i.e., the total duration is 1920 s or 32 min. We interpolated this 32 min time series with a sampling interval of 10 s to get 192 values. These values are used to generate duty cycles for the channel switches and are implemented in the embedded system code using look-up tables. We denote power values in this time series by $p_{d,t}$. The power values are scaled down for implementation on the Pico board. The duty cycle is obtained as $d_t = \alpha p_{d,t}/P_d$, where $\alpha \in [0, 1]$ is a scaling factor and $P_d = max\{p_{d,t}\}$. This ensures that $d_t \in [0, \alpha]$. As discussed in Section 9.2.1.3, the power through a channel at time t is given by $p_{c,t} = d_t P_c$, where P_c is the nominal power input/output at the source/load channel. $P_c = 1$ pu for the source channel and $P_c = 0.37$ pu for the load

Table 9.2: Power scaling parameters

Channel	α	P_c/P_d
PV	0.5	1.4×10^{-3}
Load 1	1	2.7×10^{-3}
Load 2	1	3.6×10^{-3}

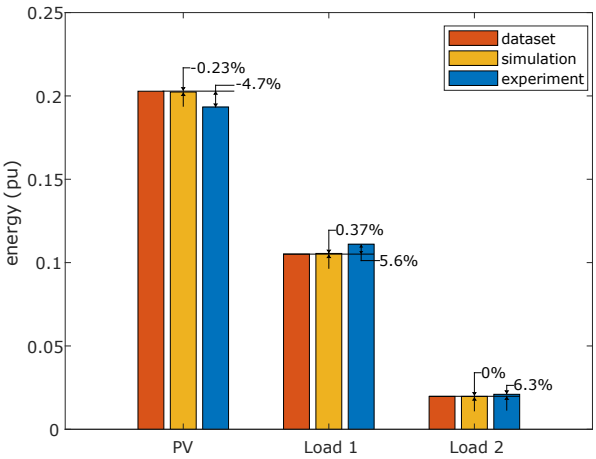

Figure 9.9: Energy supplied by PV and consumed by Loads 1 and 2. Values indicated on top of simulation and experiment bars represent percentage error with respect to the dataset

channel. The parameter values used in this experiment are presented in Table 9.2.

Power variation across channels PV, Load 1, and Load 2 obtained experimentally are plotted with the ideal values from the dataset as shown in Figure 9.8. The experimental results are seen to closely follow the variations in the values of the time series from the dataset. To quantify this, we compare the area under the curve, i.e., the energy supplied by PV and consumed by Loads 1 and 2, with values computed analytically using the dataset and simulation results. The energy supplied/consumed by a source/load channel over duration T of the experiment can be analytically calculated as $E_A = \int_0^T p_{c,t}\, dt = P_c \int_0^T d_t\, dt$. Figure 9.9 shows a bar chart that compares the energy supplied by PV and consumed by Loads 1 and 2 as obtained analytically using the dataset, using the simulation model, and through the experiment. Values displayed on the top of bars corresponding

to simulation and experimental results represent percentage error with respect to the analytically calculated value. We see that the magnitudes of simulation errors are under 0.5% and that of experiment errors are under 7%. This shows that the platform can be used to effectively model scaled down real-world generation and demand profiles.

9.3.2 Experiment 2: Setpoints from remote node

This experiment, using a single isolated Pico board, demonstrates how different layers of the platform, viz., Pico board, cloud dashboard, and the remote node, interact with each other to meet the entity's objectives. Specifically, we aim to demonstrate how the load management goals of the entity can be met by its local energy manager (EM) operating according to the setpoints received from the remote node. The experiment duration of 15 min is divided into three 5 min intervals. The goal is to keep all the three loads on in the first interval, only Loads 1 and 2 on in the second interval, and only Load 1 on in the third interval.

The EM implements a threshold-based energy management framework as presented in [43] wherein each load is assigned a threshold in terms of the state of charge (*soc*) of the on-board cell. If the *soc* exceeds the threshold, the corresponding load is switched on and if it goes below the threshold the load is switched off. The thresholds are obtained as setpoints from the remote node which is implemented on a Windows PC. The remote node runs a Julia script to compute the thresholds and sends them to the cloud dashboard using REST API. We write the script such that it reads the *soc* from the Pico board data channel at the beginning of each interval and computes and sends thresholds to the setpoint data channel. The EM reads thresholds from the setpoint data channel and implements the threshold-based energy management framework. In order to determine the thresholds per interval, we need to determine what is the maximum change in *soc* that will be possible over each interval. During the experiment, a 1 pu voltage source is connected to the Auxiliary Source channel and supplies 1 pu nominal power. Each load channel is rated to consume 0.37 pu nominal power. The energy capacity of the cell is 12.24 pu. Therefore,

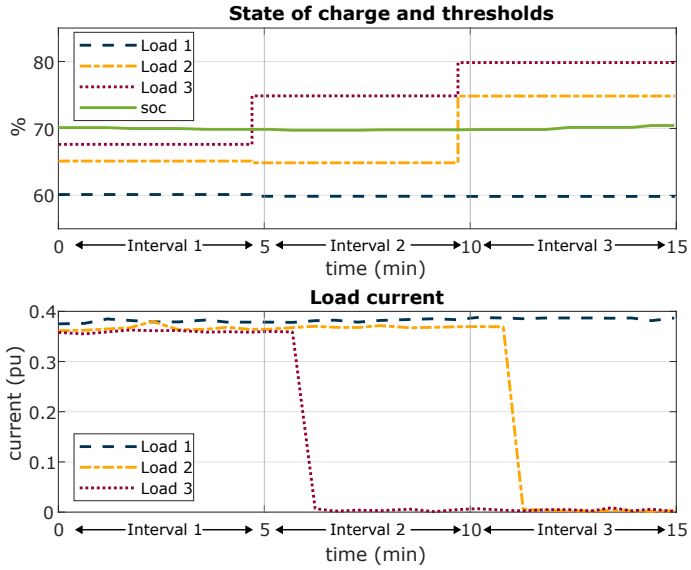

Figure 9.10: Top: State of charge (*soc*) variation and load thresholds. Bottom: Load current. Loads are switched off when the *soc* is less than their respective thresholds.

the change in *soc* over any interval will be $\leq 1\%$. We determine the threshold for Load k in an interval as $soc_o + \Delta_k$, where soc_o is the *soc* at the beginning of the interval as read from the Pico board data channel and Δ_k is chosen to be greater than 1% if the load is to be switched off and less than 1% if the load is to be switched on. Table 9.3 shows the values chosen for Δ_k.

Table 9.3: Δ_k values for each interval and load

	Δ_1	Δ_2	Δ_3
Interval 1	-10	-5	-2.5
Interval 2	-10	-5	5
Interval 3	-10	5	10

Figure 9.10 shows the *soc* and load thresholds on the top and load currents on the bottom. We can see that all three loads are on in Interval 1; Loads 1 and 2 are on and Load 3 is switched off in Interval 2; and Load 1 is on and Loads 2 and 3 are switched off in Interval 3 as expected. This experiment shows that control schemes with a combination of local and remote control can be implemented on the platform. More advanced schemes

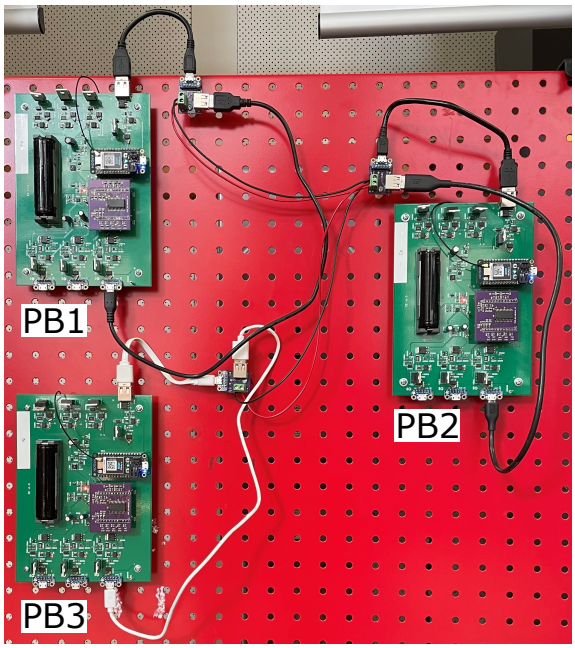

Figure 9.11: Experimental setup showing three radially connected Pico boards

such as optimization-based control can be implemented using computation resources of the remote node and can be used to generate setpoints for Pico boards.

9.3.3 Experiment 3: Three-entity prosumer network

This section demonstrates the interconnection of three prosumer entities through simulation and experimental results. The experimental results serve as a benchmark for the simulation model. Figure 9.11 shows the experimental setup. The three entities represented by Pico boards (PB1, PB2, PB3) are interconnected radially. It is assumed that Load 1, Import, and Export are the only channels that are active. The experiment runs for a duration of 32 min. The load demand is assumed to be constant at the nominal power of the channel (0.37 pu). The load demand schedule (user schedule) for Load 1 across the entities is as follows: PB1 8-16 min, 24-32 min; PB2 0-16 min, PB3 16-32 min. Each entity implements threshold-based energy management presented in [43]. Across all entities, Load 1 is assigned a threshold of 20%, i.e., if the state of charge (*soc*) of the cell is less than 20%, the load is switched off, and if it is greater than 20%, the load follows the

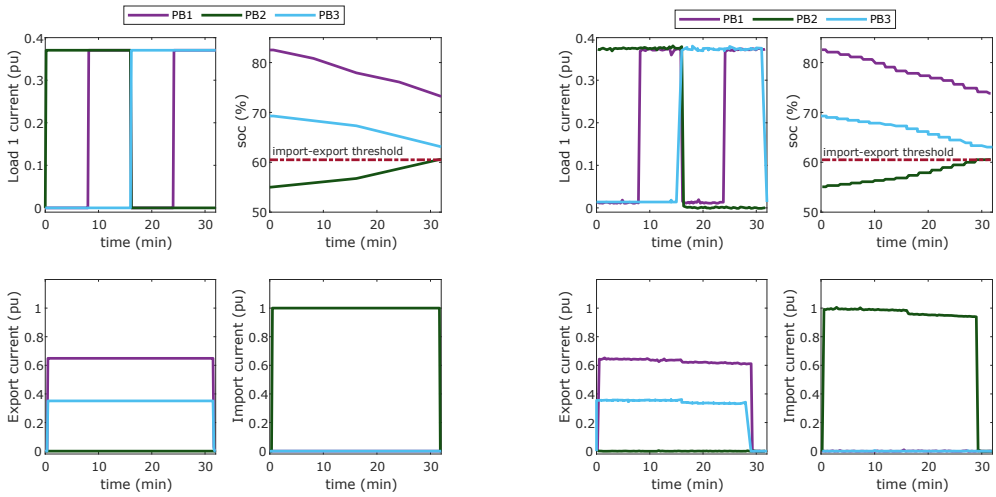

(a) Simulation (b) Experiment

Figure 9.12: Simulation and experimental results (clockwise from top left in each sub-figure: Load 1 current, state of charge, Import current, Export current) for a network of three prosumers. Plots show that the simulation model can effectively represent the behavior of the hardware.

user schedule. Import and Export are both assigned a threshold of 60%, i.e, if the *soc* is less than 60%, Import is switched on and Export is switched off, and if it is greater than 60%, Import is switched off and Export is switched on.

Simulation and experimental results are shown in Figure 9.12. Load current plots show that load schedules are followed in the simulation and the hardware. The *soc* of no entity goes below 20% over the duration of the simulation or the experiment and therefore, loads follow the user schedule as expected. Measurement errors in current sensors lead to a slight mismatch in the *soc* computation between the simulation and the experiment. In the simulation, the *soc* of PB2 stays just below 60% until the end of the experiment and so PB2 continues to import current as seen in the Import current plot. The *soc* of PB1 and PB3 are always above 60% and therefore they continue exporting to PB2 as seen from the Export current plot. Since the line resistances in series with PB1 and PB3 are of different values, their export current values also differ. In the experiment, the *soc* of PB2 reaches 60% by minute 29 and so Import is switched off. Even though the *soc* of PB1 and PB3 remain above 60% and their Export channels remain on, since no entity is importing,

Table 9.4: Error in change in state of charge for each entity in the experiment as compared to that in the simulation is found to be under 6 %

Quantity	Error in change in *soc* (%)
PB 1	−5.77
PB 2	−0.375
PB 3	1.31

the Export currents of PB1 and PB3 also go to zero. The percentage error in change in state of charge for each entity in the experiment as compared to that in the simulation is shown in Table 9.4. It is observed to be under 6 %. Overall, the experimental results are in congruence with simulation results and this can be improved by better calibration of on-board current sensors.

We observe that the simulation model can effectively represent the behavior of the hardware. The simulation model can be used to simulate multiple cases with different parameters for better design of hardware experiments. This experiment also demonstrates that multiple Pico boards can be interconnected to form a prosumer network or a picogrid.

9.4 Conclusion

This chapter presents the Picogrid, an experimental platform for prosumer microgrid research and education. It is a low-power, low-cost platform which enables interconnection of multiple prosumer entities on a bench-top setup. Features of the platform such as implementation of control schemes based on a combination of local and remote control, implementation of scaled down real-world generation and demand profiles, and interconnection of multiple prosumers to form a network is demonstrated through simulation and experimental results. The platform has the potential to be extended to form a hardware-in-the-loop setup where high-power entities modeled in a simulation software on the remote node interface multiple of Pico boards. Hardware-in-the-loop experiments are using the Picogrid platform are presented in Chapter 10.

The Picogrid platform has been designed to implement secondary and tertiary level

control schemes which expect the system response to be of the order of several seconds to minutes. It cannot be used for testing primary control schemes which expect system responses to be under seconds, e.g., modeling transients due to interactions between different power electronic converters. Being a dc platform, it also cannot be used to model ac system dynamics. However, some of these aspects can be incorporated with potential increases in cost and size of each Pico board and is a subject of future work.

Chapter 10

Custom Cloud-Based Solution for Remote Access to the Picogrid

Hardware validation of energy access and energy management paradigms, such as microgrids and distributed energy resource management systems, is crucial for bridging the gap between simulation-based research and real-world applications. However, there are significant barriers for using hardware experimental platforms including high costs, lab space requirements, and maintenance challenges. Additionally, users must typically be physically present with such platforms to effectively conduct experiments. This work presents a cloud dashboard designed for conducting remote virtual experiments on the 'Picogrid', the existing low-cost open-source experimental microgrid hardware platform presented in the previous chapter. This enables researchers who build the hardware platform to rent it out to remote users for specific durations, facilitating remote experimentation through a hardware-as-a-service model. The approach significantly reduces the burden of developing and maintaining the hardware infrastructure for researchers, and makes hardware validation more accessible. Multiple users can simultaneously run experiments on their allocated hardware instances from any location worldwide, with minimal resource setup. Additionally, the dashboard enables educators to offer virtual laboratory exercises to remote students. Three experiments involving remote third-party users demonstrate applications of

the proposed cloud dashboard, in conjunction with the hardware platform, as a research and educational tool for smart solar home systems, virtual power plants, and demand response schemes. Furthermore, the platform was used in a real-world setting, during a community meeting in Holyoke, MA, to demonstrate demand-response schemes and understand the potential barriers that the community may face in participating in such utility programs. [1]

10.1 Introduction

The advent of inexpensive computing hardware, coupled with excellent software platforms have enabled digital simulation to become a ubiquitous practice in power system engineering. This approach is extensively used to study various upcoming energy paradigms such as microgrids, swarm electrification, distributed energy resource management systems, demand response, and virtual power plants. On the other hand, some of the time-sensitive dynamics, physical uncertainties, cyber-physical interactions, and human mediated aspects continue to be challenging to study using numerical simulations on software. One needs to resort to a hybrid approach that is often termed as hardware-in-the-loop simulation to accurately model and understand such aspects [151]. Thus, hardware validation is deemed necessary for translating the research concepts to real-world applications.

Hardware experimental platforms generally require high initial costs, needing large lab space, and adequate resources for maintenance. In order to address this, [128] presented an accessible open-source solution called the 'Picogrid', a low-cost dc prosumer (producer-consumer) microgrid hardware platform. It is a low-power sandbox for research and education, and lowers the barriers to entry for hardware validation. Another potential limitation of hardware platforms is the requirement for users to be physically present to conduct experiments. Internet of Things (IoT) and cloud-based technologies are emerging as a solution to remotely access physical hardware, enabling researchers to make their

[1] This chapter is based on work by the author, Varun Balan, and Giri Venkataramanan in [149]. This work was supported by the Wisconsin Electric Machines and Power Electronics Consortium. The community meeting at Holyoke, MA was in collaboration with a team at the University of Massachusetts Amherst and was a part of a larger project undertaken by their team [150].

hardware experimental platforms available through a hardware-as-a-service model [152]. Leveraging cloud computing services also offers multiple advantages such as rapid infrastructure deployment and modification, automated failure recovery, scalability, security, cost efficiency, and use of artificial intelligence and machine learning insights [153].

Various IoT and cloud-based software have been used in experimental platforms for microgrids, smart grids, and energy management. These include out-of-the-box IoT products developed for hobbyists, makers, and educators such as Mathworks ThingSpeak [154], Arduino Cloud [155], and ThingsBoard [156]. A simple cloud dashboard, developed using ThingSpeak, for the Picogrid platform was presented in [128]. While such out-of-the-box solutions are developer-friendly and do not require extensive experience in cloud software development, they do have some notable drawbacks. Firstly, they involve high fixed costs, meaning users must pay a predetermined fee regardless of their actual usage levels. Furthermore, these solutions impose limitations on customization, data transfer rates, and data storage. These constraints hinder their effectiveness in enabling the underlying hardware to be offered through a hardware-as-a-service model. On the other hand, using software from cloud service providers such as Microsoft Azure [157], Amazon Web Services [158], and Google Cloud [159] to build custom solutions from their suite of services offers greater flexibility and scalability. In this work, we present a customized solution developed using services offered by the cloud service provider, Microsoft Azure, and the IoT platform, Particle Cloud, that makes remote access to the Picogrid [128] more affordable and user-friendly.

10.1.1 Contributions

We make the following contributions beyond prior work. First, we present a custom cloud dashboard developed using services from Microsoft Azure and Particle Cloud for the Picogrid hardware. Its features include (1) remote monitoring of sensor data, (2) sending setpoints to control the hardware, and (3) secure authorized access, enabling researchers and educators who build the Picogrid hardware to offer it for virtual remote

experimentation through a hardware-as-a-service model, which was not possible using the platform in [128]. This allows users, without the resources to build the hardware, to access it remotely for a desired duration. It enables them to focus on validating their models in hardware without spending time and resources on setting up the infrastructure. Next, we demonstrate the utility of the dashboard through three experiments: (1) smart solar home system (experiment conducted on on-campus hardware by two third-party users from an off-campus location), (2) virtual power plant (a hardware-in-the-loop experiment demonstrating aggregate control), (3) demand response (a hardware-in-the-loop experiment conducted with hardware at two different locations by two third-party users in conjunction with a simulation model running at a third location). The cloud dashboard software is made publicly available through the Picogrid GitHub repository [146].

10.1.2 Organization

Section 10.2 discusses the architecture and pricing of the custom cloud dashboard, Section 10.3 presents experimental results, Section 10.4 presents a real-world example of how the Picogrid platform was used in a community workshop, and it is followed by a brief concluding section.

10.2 Platform

10.2.1 Overview of the Picogrid platform

We first present a brief overview of the Picogrid platform presented in [128] (and Chapter 9). The Picogrid platform consists of three layers: Pico boards, cloud dashboard, and a remote node. The Pico boards are 7" $\times$ 5" circuit boards, each representing a prosumer entity such as a household in a community microgrid. As shown in Figure 10.1, each Pico board contains an on-board cell for energy storage, two source channels, three load channels, and an import and export channel to exchange energy with other Pico boards. A Wi-Fi enabled microcontroller (Argon by Particle) is used to implement local energy

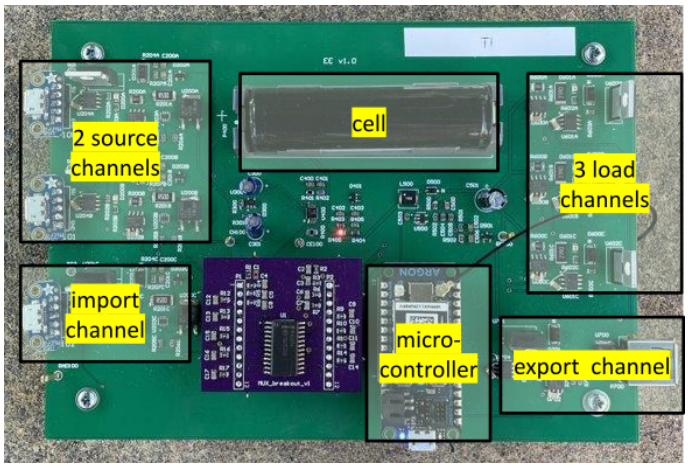

Figure 10.1: Photograph of a Pico board, highlighting important components

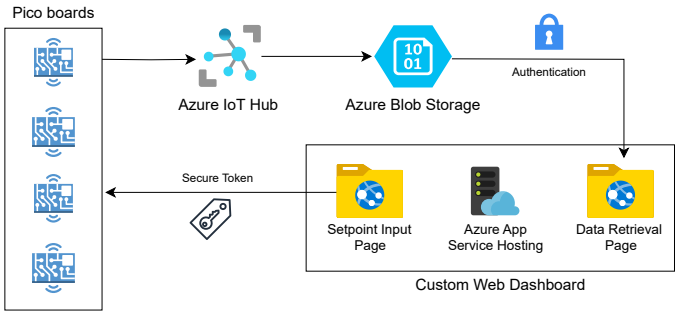

Figure 10.2: Sketch of data pipeline between Pico boards and cloud dashboard

management, read on-board sensor values, and communicate with the cloud dashboard. Channels have a power semiconductor that can be controlled using pulse-width modulation to implement custom power profiles. Source channels are connected to an external dc power supply. The remote node is any computer system with an internet connection and can represent a microgrid operator, aggregator, or load serving entity. The cloud dashboard acts as a data transfer system between the remote node and Pico boards. This work presents a custom cloud dashboard designed to address the flexibility and cost limitations of the out-of-the-box dashboard discussed in [128].

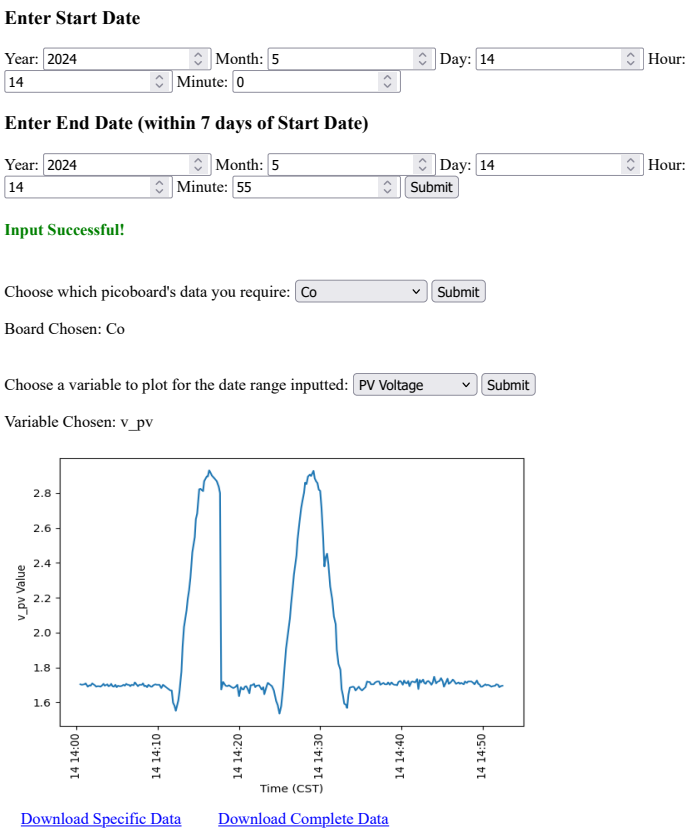

Figure 10.3: Screenshot of Data Retrieval Page: Waveform of selected quantity (PV Voltage) during the selected interval (14:00-14:55 May 14, 2024) from the selected board (Co).

10.2.2 Custom Cloud Dashboard

In this section, we describe the new custom cloud dashboard proposed in this work. The requirements from the cloud dashboard are: (1) extract data from the hardware platform between specific time frames in which users run their experiments, (2) send setpoints from the dashboard to the hardware with minimal latency to allow dynamic changes during experiments, (3) secure access to the dashboard to prevent unauthorized third-parties from sending setpoints or accessing sensor data.

10.2.2.1 Architecture

As seen in Figure 10.2, Azure IoT Hub is used as the bridge between the Wi-Fi enabled microcontrollers on Pico boards and Microsoft Azure Storage Blobs (cloud data storage).

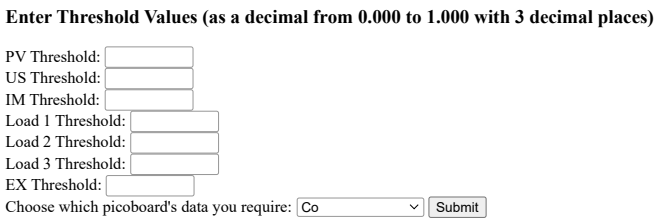

Figure 10.4: Screenshot of Setpoint Input Page for selecting threshold levels for Photo-Voltatic (PV) and Utility Source (US) channels, import (IM) and export (EX) channels, and load channels (Load 1 to 3)

The microcontrollers are configured to read sensor data on the Pico boards and send to Azure IoT Hub at each timestep. The length of the timestep, i.e., the resolution of data, can be chosen based on user requirements and budget. The smallest timestep supported by Particle microcontrollers is one second. The custom web dashboard was built with Python and the Flask web framework for users to interact with the Picogrid platform. The application was hosted on the web using Azure App Service. Only authorized users are allowed to access the dashboard and security configurations can be set as desired. Figure 10.3 shows the data retrieval page of the dashboard. The application pulls data from Azure Blob Storage based on user filters of start/end date (the time duration allotted to them for running experiments) and the specific instance(s) of Pico boards assigned to them. Users can choose to plot data from specific sensors and download data in CSV format for further processing. The application also allows sending setpoints to control the operation of the Picogrid platform directly using an API token and sending an HTTP POST request to the Particle microcontroller using the Particle Cloud Functions feature. The maximum supported frequency is 10 requests per second. For example, if the user wants to implement a threshold-based load control scheme for dc microgrids, as presented in [43], the control setpoint for each load and source channel is a threshold in terms of the on-board cell's state of charge (soc). A source channel is switched on if the soc is less than its threshold, and is otherwise switched off. On the other hand, a load channel is switched on if the soc is greater than its threshold, and is otherwise switched off. Figure 10.4 shows the page of the dashboard which can be used to send thresholds as control setpoints for

each channel. The proposed solution allows multiple users to access the cloud dashboard simultaneously, with each user being able to access data from the Pico boards assigned to them during their allotted experiment time frame.

10.2.2.2 Pricing

There are four services that are used to create the cloud dashboard and can be billed according to use, with each having a "freemium" model. This offers flexibility, customization, and cost savings since users can choose which tiers to purchase in each service according to their use cases.

i) Azure IoT Hub: The Azure IoT Hub pricing depends on (1) the number of devices connected to the IoT Hub, (2) the frequency of sending data from the boards to the IoT Hub, and (3) the size of each data packet sent (message meter size). In the free tier pricing of IoT Hub, up to 500 devices can be connected. There is a daily limit of 8000 messages (for all the devices combined) with each having a meter size of 0.5 KB. In case the limit of 8000 messages is not enough, buying a higher tier of Azure IoT Hub for $10 per month would allow 400,000 messages per day with a 4 KB message size.

ii) Azure Blob Storage: The Azure Blob Storage offers scalable data storage in the cloud. Pricing in the default tier is $0.018/GB of data per month.

iii) Particle Cloud: For sending setpoints to Pico boards using Particle Cloud Functions, there is a limit of 100,000 data operations (function calls) per month in the free tier which can be upgraded if necessary.

iv) Azure App Service: The cost associated with the web server to host the application using Azure App Service is about $10 per month.

In our Picogrid hardware setup, there are 3 Pico boards each with 13 sensors collecting data at about every 15 seconds. The boards are typically used for 3 hours everyday. The free tier of Azure IoT Hub and Particle Cloud is sufficient for our hardware requirements. Storing one year of data collected from the setup in Azure Blob Storage will cost under $0.02 annually. The web server to host the application costs about $10 per month. There-

fore, the total costs associated with the cloud dashboard have been limited to less than $121 per year, of which $120 is just for hosting the web application. Hosting it on a local server would eliminate this cost, and the annual cost of the data pipeline would be under $1. On the other hand, the academic research license of ThingSpeak (out-of-the-box platform used in [128]) has a fixed cost of $275 per unit per year (all prices as of May 2024). Although ThingSpeak offers a plug-n-play platform, our custom cloud solution provides a more cost-efficient alternative that scales according to the usage levels. Furthermore, our solution enables creation of custom web dashboards to suit the needs of the end users.

10.3 Experimental Results

This section presents three experiments that demonstrate use cases of the proposed cloud dashboard integrated with the Picogrid platform. Two of these experiments involve third-party remote users. For each experiment, we outline the learning objectives, i.e., what students or researchers are expected to gain, followed by a detailed description of the experimental setup and a discussion of the results. The power ratings of the channels on the Pico boards used are: Source channel – 1 pu, Load channel – 0.37 pu. The cell has an energy capacity of 12.24 pu. The per unit base quantities are: voltage = 5 V, current = 0.5 A, energy = 1 Wh.

10.3.1 Smart Solar Home System

The aim of the experiment is to demonstrate the operation of a smart solar home system. It was conducted on on-campus Pico boards by two remote third-party users using the cloud dashboard.

10.3.1.1 Learning Objectives

The target student group for this experiment is senior undergraduate students. The learning objectives of the experiment are: (1) Explain smart charging methods, for a house with rooftop solar and battery storage in order to reduce the electricity purchased from the grid,

(2) Distinguish between critical and non-critical loads, (3) Demonstrate a smart charging scheme for a house with rooftop solar and storage modeled on the Picogrid platform.

10.3.1.2 Setup

The users were given remote access to one Pico board each for the duration of the experiment. The experiment duration was 20 minutes, with the first half representing "daytime" and the second half representing "nighttime". On each board, both source channels were connected to a 1 pu dc voltage source. Source channel 1 was programmed to emulate a real-world rooftop solar PV power profile from the Pecan Street Dataset [118] using pulse-width modulation. Source channel 2 was set up to emulate a constant-power battery charger connected to the grid. Load 1 and Load 2 were assigned to be critical and non-critical respectively. Load 3 was not used in this experiment. The objective was to use solar when present and draw power from the grid-connected charger in other times, to charge the battery and supply loads. The non-critical load was to be curtailed during nighttime to minimize demand when solar was not available. The users were asked to meet these objectives by observing the sensor data on the data retrieval page, determining appropriate thresholds for each source/load channel, and sending them via the setpoint input page on the cloud dashboard.

10.3.1.3 Results

Results from one user are shown in Figure 10.5. We can observe that during "daytime" (until minute 10), the user turned off the charger while solar input was available. During "nighttime" (after minute 10), the user curtailed the non-critical load, reducing the total demand, and turned on the charger to charge the battery. The experiment highlights how the Picogrid platform, in conjunction with the proposed custom cloud dashboard, can be used as a virtual laboratory by off-campus students. Remote users can use more complex tools on their computer systems, such as machine learning for solar forecasting and optimization solvers for optimal actuation of loads, to generate better setpoints for

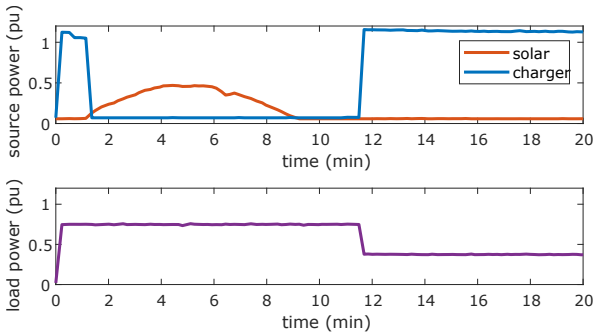

Figure 10.5: Demonstration of a smart solar home system, where 20 minutes are mapped to a full day. Remote users managed sources (top: solar or from charger input) and loads (bottom) according to solar PV availability.

further minimizing the electricity purchased from the grid.

10.3.2 Virtual Power Plant

The aim of this experiment is to illustrate tracking control for the operation of a virtual power plant (VPP). A VPP consists of an aggregator controlling a set of distributed energy resources (DERs) to match the bulk power system's needs [160]. The Picogrid platform includes a MATLAB Simulink and PLECS-based model of the Pico board, allowing for scaling by addition of software-based boards alongside the physical boards for a hardware-in-the-loop experiment. We present such an experiment below.

10.3.2.1 Learning Objectives

The target audience is graduate students and researchers. The learning objectives are: (1) Demonstrate the operation of a VPP using Pico boards (combination of physical boards and software models) to emulate households, (2) Implement a tracking control scheme to enable the Pico boards to track a target control signal, (3) Analyze the results to determine the tracking error and reflect on features necessary for developing models that accurately represent real-world systems.

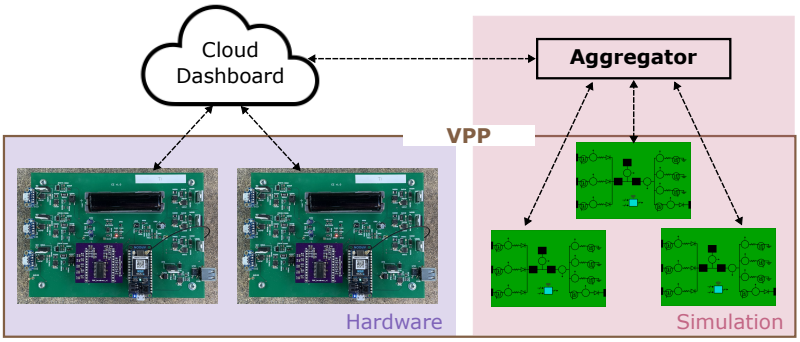

Figure 10.6: Sketch of VPP experimental setup illustrating hardware and simulated Pico boards, aggregator, cloud dashboard

10.3.2.2 Setup

As shown in Figure 10.6, the experiment had 5 Pico boards, 2 in real hardware and 3 modeled on a remote node using MATLAB Simulink and PLECS, each with three constant-power loads, rated at at 0.37 pu each. The aggregator was modeled in Simulink and computed thresholds to actuate loads in each real and modeled board for tracking a target control signal. The aggregator communicated these thresholds to the real boards via HTTP POST requests and to the modeled boards through a simultaneously running real-time simulation. For running real-time simulations in Simulink, there are broadly two options: Simulink Real-Time (SLRT) and Simulink Desktop Real-Time (SLDRT). SLRT supports high sampling frequencies (greater than 20 kHz) and needs dedicated real-time hardware, e.g., Speedgoat systems, which can be expensive. On the other hand, SLDRT is suitable for low sampling frequencies (less than 20 kHz) and can run on a desktop computer without additional dedicated expensive hardware. Since we assume that the VPP provides tertiary control services, the tracking signal is not expected to change faster than the order of minutes and the response time from the Pico boards can be of the order of seconds. Therefore, we chose to use SLDRT to conduct the real-time simulation.

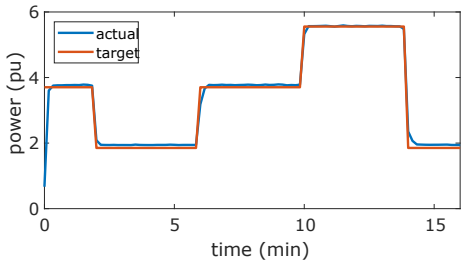

Figure 10.7: VPP operation: Power consumption of a combination of hardware and simulated Pico boards was coordinated to track a target signal

10.3.2.3 Results

Figure 10.7 shows the target control signal and actual aggregate power consumption of the Pico boards. The tracking signal has three levels, corresponding to one, two, and three loads being turned on on each board respectively. It is observed that the aggregate consumption tracks the target closely. The root mean squared percentage error (RMSPE) between the target and the actual aggregate power consumption is 9.6 %. Furthermore, the actual signal has a non-zero response time when there are changes in the tracking signal and has a positive offset. These artifacts, introduced due to hardware factors such as sensor calibration and communication delays, can be useful for encouraging students to reflect on features necessary for developing simulation models that model real-world phenomena more accurately.

Demonstration of more complex and scalable aggregate control schemes for tracking control in virtual power plants can be implemented using this setup in conjunction with SLRT and dedicated real-time hardware for high frequency sampling times. The custom cloud dashboard can enable researchers at different locations to concurrently conduct experiments on an aggregation of real and modeled Pico boards.

10.3.3 Demand Response

The aim of this experiment is to illustrate different demand response (DR) programs. We present a hardware-in-the-loop experiment conducted by two third-party users, with a Pico board each, in two different locations, in conjunction with a real-time simulation

running on a system at a third location. We demonstrate how the cloud dashboard enables students and researchers, who are not physically co-located, to participate in experiments with their custom-built Pico boards and simulation models.

10.3.3.1 Learning Objectives

The target audience is graduate students, senior undergraduate students, as also potential DR customers participating in energy awareness programs. The learning objectives are: (1) Explain the differences between price-based and incentive-based DR programs, (2) Design an optimal load schedule for participating households to minimize energy costs and user inconvenience, (3) Implement the load schedule using the Picogrid platform, (4) Reflect on the barriers for households to participate in such programs.

10.3.3.2 Setup

The 24-minute experiment emulated a 24-hour day. The setup of the experiment is illustrated in Figure 10.8.

i) DR programs: The utility, modeled in Simulink, was assumed to serve an energy community and offered two DR programs: price-based and incentive-based [161]. For a household on a price-based DR program, the price of electricity was 50 ¢/kWh between 4 p.m. to 9 p.m. (on-peak period) and 27 ¢/kWh at other times (off-peak period). For a household on an incentive-based DR program, the utility could execute direct load control for a maximum of 1 event lasting 4 hours daily. The price of electricity in this program was constant at 33 ¢/kWh and if the user chose to participate in this program, they would receive a bill credit of 60 ¢/day. The utility generated a 4-hour-ahead demand forecast for the energy community on an hourly basis, and called the DR event once the forecast exceeded a given threshold. In order to generate data for this forecast, we aggregated electricity usage data for 336 days for a household from the Pecan Street dataset [118].

ii) Pico boards: Two third-party users were given one hardware Pico board each, were located in two different buildings on campus with their assigned board, and actuated loads

on the board using the custom cloud dashboard. Pico board 1 was on the price-based DR program while Pico board 2 was on the incentive-based program. Two loads on the Pico boards were used: Load 1 represented a 3 kW HVAC system and Load 2 represented a 6 kW electric vehicle charger (EV). Additionally, there were 5 Pico boards, modeled using MATLAB Simulink and PLECS, that were assumed to be enrolled in the price-based DR program. These boards along with the utility were simulated using SLDRT on a system in a third location on campus.

iii) Home energy management: The objective of each user was to minimize the cost of electricity while meeting the following constraints: (1) The HVAC system was required to run for about 8 hours and the EV charger for about 4 hours (a soft constraint representing user comfort), (2) Both loads could be interrupted, i.e., they could be cycled on and off multiple times, (3) The user was assumed to take the EV to work between 7 a.m. and 2 p.m. Therefore, they could not turn a load on/off during this time. The 5 Pico boards modeled in software did not have dedicated energy managers and were used as a baseline case. They were modeled to have random start times for both loads while meeting the above constraints.

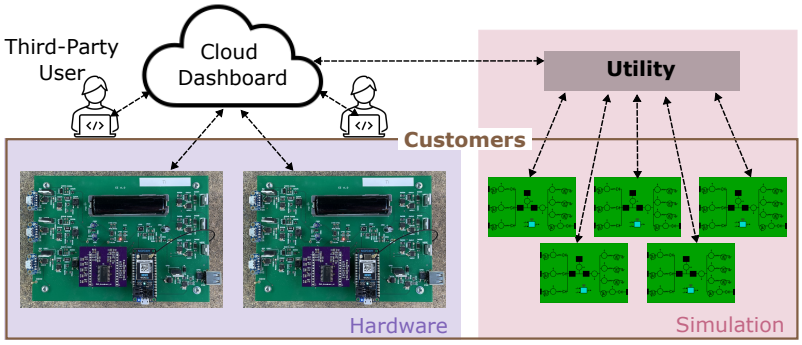

Figure 10.8: Sketch of DR experimental setup illustrating hardware and simulated Pico boards, third-party users, utility, cloud dashboard

10.3.3.3 Results

Figure 10.9 shows plots of the power consumed by loads on the two physical Pico boards. The time and power scaling factors between the experiment and the emulated system are

1 min : 1 hour and 1 pu : 6 kW respectively. Pico board 1 was enrolled in price-based DR. Therefore, the user chose to run the HVAC system for about 8 hours before 4 p.m. to pre-cool the house and use the EV charger for over 4 hours after 9 p.m. Pico board 2 was enrolled in the incentive-based DR program. Therefore, when the load forecast exceeded the assigned threshold (at 4 p.m.), the utility called a demand-response event and both its loads were turned off via direct load control. The user chose not to override the event and turned the loads back on after the 4-hour event was over, with the total run time of the HVAC and EV loads being just under 8 and 4 hours respectively. The electricity bill incurred by Pico boards 1 and 2 was \$13.44 and \$13.60 respectively, while the average cost incurred by boards modeled in software on the price-based DR program without any energy management was \$15.34. This illustrates the need for managing energy usage according to time-of-use pricing schedules.

Various DR programs and pricing schemes can be implemented using this setup, through a combination of hardware and software Pico boards participating in a hardware-in-the-loop experiment from different locations. Instructors can use this platform to facilitate conversations among students around barriers to participation in such programs. For example, households working long hours may not be at home to defer load usage when electricity prices are low and may not be able to afford home automation devices [162]. Researchers can use the platform to educate community members about DR and gather their inputs in informing equitable design of such programs, as discussed in the following section. In this way, the platform enables a holistic understanding of energy access problems and solutions.

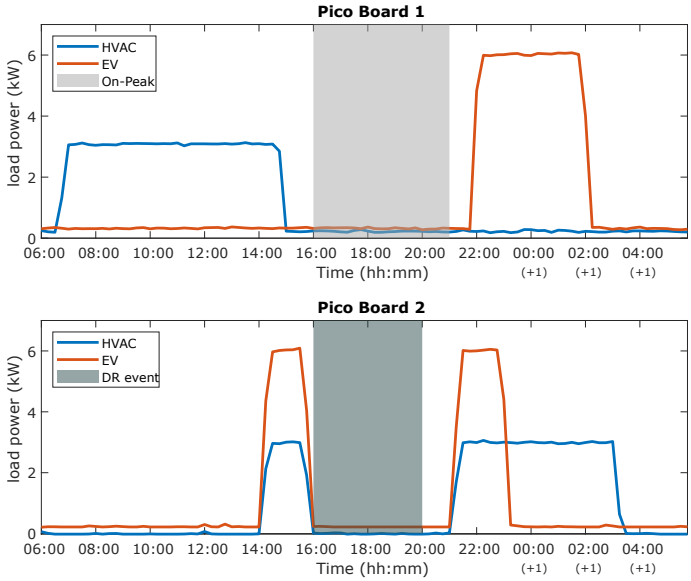

Figure 10.9: Top: User of Pico board on price-based DR reduced consumption during on-peak period between 16:00 and 21:00. Bottom: User of Pico board on incentive-based DR participated in direct load control during DR event from 16:00 to 20:00

10.4 Demonstration of Demand Response at a Community Workshop

This section briefly presents how the Picogrid platform was used for demonstrating demand response during a community workshop in Holyoke, MA. This demonstration was a part of a larger project by a team of researchers at the University of Massachusetts Amherst that aims to co-design equitable residential electrification solutions using community-engaged research [150]. The workshop had about 20 participants who have been a part of monthly meetings organized by the UMass project team. The goal of the team was to conduct three activities: (1) demonstrate a generation-demand mismatch leading to a blackout in order to present the need for demand response (DR), (2) demonstrate an incentive-based DR scheme, (3) demonstrate a price-based DR scheme. Through these activities, the team aimed to get inputs from the participants about their concerns and needs around participation in such DR schemes. The Picogrid platform was used as one of the educational tools to conduct the activities.

Figure 10.10 shows a photograph of a workshop facilitator showing a Pico board to

Figure 10.10: Photograph of a workshop facilitator showing a Pico board to participants

the participants. Pico boards were used to emulate households and were placed with the participants at their tables. The utility was emulated on a remote node (a laptop computer set up at the front of the room) operated by the author. The cloud dashboard was rendered on a display monitor to show total power consumption of loads on the Pico boards. As shown in Figure 10.11, the educational tools used at the participant tables included a Pico board, 3D printed models of three appliances (refrigerator, air conditioner, light bulb) represented by the three loads on the Pico board, and a device mat. The participants kept an appliance on the green part to indicate that they wanted to turn it on, i.e., not compromise on using it when necessary, while they kept it on the red part to indicate that they would be agreeable to turning it off. Participants seated at the same table had to make a unanimous decision about which appliances to turn on and which ones to turn off through their participation in incentive-based/price-based DR schemes.

The team observed that community members actively participated in the activities and engaged with the Picogrid platform. These hands-on activities facilitated interesting table discussions about potential challenges in keeping certain loads off, the amount of incentives needed to encourage participation, and potential savings on bills. This illustrates the potential of using the Picogrid platform in various community energy awareness programs

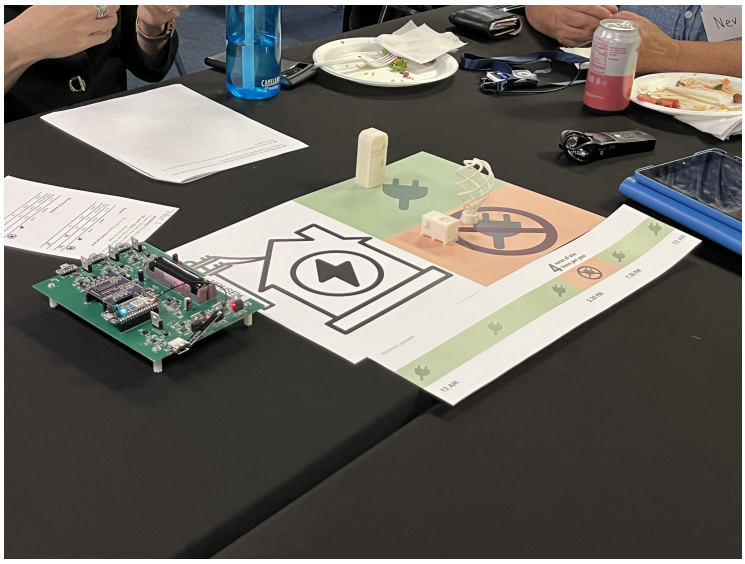

Figure 10.11: Photograph of the educational toolkit consisting of a Picoboard, 3D printed models of three appliances, and a device mat. Participants used the green area of the mat to indicate turning a device ON and the red area to indicate turning it OFF.

and workshops, in addition to academic research and coursework.

10.5 Conclusion

This study presents a custom cloud solution for remote access to a microgrid hardware platform. It enables the hardware to be made available for concurrent remote access by multiple users worldwide through a hardware-as-a-service model. It also enables educators to make hardware experimentation accessible to students who cannot be present on-campus, e.g., during times such as the COVID-19 pandemic, and for distance education programs. It allows for a more streamlined, secure, and cost efficient way to use the hardware platform as compared to using an out-of-the-box IoT solution. Future work includes enhancing data security through end-to-end encryption and further customization such as sending SMS/email alerts if variables exceed predefined bounds. In this study, the custom cloud solution was presented in conjunction with the Picogrid, a low-power experimental platform. The solution is hardware-agnostic and can be used with larger, high-power ac/dc setups, as well as non-electrical systems.

Chapter 11

Conclusions, Contributions, and Future Work

The work presented in this thesis develops energy access frameworks for resource-constrained environments. It proposes using a holistic approach, based on a combination of community-engagement and traditional power engineering research tools of analytical modeling, mathematical optimization, simulation, and hardware prototyping, for identifying and meeting the needs of energy poor and energy insecure households. Part I presents field experiences in three contexts: energy access in off-grid rural communities, energy resilience for individuals dependent on in-home medical devices, energy access for people experiencing homelessness. It outlines the constraints and heterogeneous requirements of the environments such as resilience to intermittent remote communication, compatibility with locally available heterogeneous hardware, affordability, and agreement with sociocultural elements of the community. Part II presents the threshold-based energy management framework as a candidate solution for reliable energy access in resource-constrained settings. It presents a proof of stability of entities operating using this framework and demonstrates the application of this framework to community-scale microgrids through numerical simulations and a hardware-in-the-loop experiment. Part III presents a tool to choose thresholds using mathematical optimization and demonstrates the application of the framework to effec-

tive energy rationing for prepaid electricity customers. The presented optimization models have minimal requirements for additional hardware, demand forecasts, and remote communication, making them suitable for low-income customers. Part IV presents a low-cost experimental platform for hardware validation of energy access frameworks. It lowers the barrier for energy researchers and educators to conduct hardware experiments. It presents a cloud dashboard for remote access to this platform that enables the platform to be made available through a hardware-as-a-service model for remote researchers, educators, and students.

The following sections of this chapter present the conclusions and contributions, and identify pathways for future work.

11.1 Conclusions and Contributions

11.1.1 Part I: Field Experiences

- Energy Access and Off-Grid Rural Communities: A framework for energy usage in an off-grid rural household based on the energy hub paradigm is developed. This can help to reduce indoor air pollution and the dependence on fossil fuels as primary energy sources.
- Energy Resilience and Home Healthcare: The largely unexplored intersection of energy resilience and home healthcare is identified. A load scheduler for in-home medical devices is developed with the goal of extending the time for which medically fragile families can comfortably shelter at home during a power outage. A proposal for a comprehensive study to understand the energy requirements of this community is presented.
- Energy Access and Homelessness: The need for energy access solutions for people experiencing homelessness is recognized. An electric Little Free Library (eLFL) was co-designed with the community and deployed at two locations, leading to legislative change in the zoning code of the City of Madison, legalizing the use of such struc-

tures in multiple districts. The project has generated documentation that can act as a roadmap for community engagement, engineering, and legislation which can be useful for other cities and communities. It has initiated multiple student-led projects focused on optimally locating eLFLs, involving middle school students and community partners in prototype development, and has attracted funding for deploying prototypes.

11.1.2 Part II: Threshold-Based Energy Management

- Stability Study: A proof for stability of prosumer entities using threshold-based energy management with time-invariant parameters is presented. Rules for operating entities and interconnecting them are presented and illustrated using numerical simulations.
- Application to Community-Scale Microgrids: A tertiary layer controller is overlaid on the threshold-based energy management framework in order to meet the multi-objective nature of the load scheduling problem in each participating entity. This is validated through numerical simulations and a hardware-in-the-loop experiment.

11.1.3 Part III: Optimized Threshold-Based Energy Management

- Energy Management for Prepaid Customers: The largely unexplored space of home energy management for low-income prepaid electricity customers is identified. A mixed-integer linear program-based model for optimizing thresholds is developed to aid in effective energy rationing for prepaid electricity customers. The numerical simulation case study demonstrates that the framework incorporating optimized thresholds outperforms both a baseline without energy management and a method with control thresholds fixed solely on load priority information. Specifically, the proposed method prioritizes higher priority loads and prevents unexpected disconnections by curtailing lower priority loads.
- Addressing Imperfect Forecasts and Implementation Constraints: A simpler linear

optimization-based model is used to generate optimized thresholds. It can be solved to optimality without an optimization solver and needs only daily average demand forecasts. The proposed model has comparable or improved performance compared with that of the MILP model benchmarks, while being computationally inexpensive. Consequently, it can be implemented on inexpensive local in-home hardware, as validated by implementing it on a low-cost 8-bit microcontroller, which is advantageous for privacy and cybersecurity.

11.1.4 Part IV: Picogrid

- Picogrid: An Experimental Platform for Prosumer Microgrids: The Picogrid platform is developed as a low-cost sandbox for hardware validation of energy access frameworks and for energy education. It lowers the barrier to entry for energy researchers into hardware validation.
- Custom Cloud-Based Solution for Remote Access to the Picogrid: A cloud-based solution which is a more streamlined, secure, and cost efficient way of accessing the Picogrid hardware as compared to a previously used out-of-the-box IoT solution is developed. It enables the hardware to be made available for concurrent remote access by multiple users worldwide through a hardware-as-a-service model. It also allows educators to provide hardware experimentation opportunities to students who are off-campus, such as during the COVID-19 pandemic or in distance education programs. A real-world use case of the Picogrid platform for community education is presented.

11.2 Future Work

11.2.1 Threshold-Based Energy Management

This part presented a proof of stability for entities with time-invariant parameters, i.e., constant thresholds and constant-power loads and sources. Since real-world systems can

have time-varying power draw by loads and power input by sources while thresholds can change depending on user demand and load priorities, stability studies for entities with time-varying parameters is required. Further, studying the stability of multiple interconnected entities (e.g., to form a microgrid) would be useful.

11.2.2 Optimized Threshold-Based Energy Management

The presented models assume a constant electricity rate. Incorporating time-varying rates in the models will increase their scope to include utility programs that offer time-of-use pricing. In order to extend optimized threshold-based energy management to solar home systems, it will be necessary to consider simultaneous power draw from loads and input from sources (solar PV, wall charger). Furthermore, it will be interesting to explore using threshold-based energy management for managing thermostatically controlled loads considering weather forecasts.

11.2.3 Picogrid

The platform can be extended to incorporate ac import/export between Pico boards in order to increase the scope of experiments it can support. Piloting the platform in classes on topics such as microgrids, energy markets, and DERs will help to identify necessary additional features and use cases. The platform can be developed into an energy literacy toolkit for workshops targeted towards various communities such as outage preparedness for medically fragile families, introducing stakeholders to different electricity tariff schemes, and power grid education for high school students.

11.2.4 Broader Questions

This section outlines studies that can be undertaken to investigate the broader questions that have come up through the course of this work.

Energy resilience and medically fragile families: To further study the intersection

of energy resilience and home healthcare, the proposed table-top exercise can be conducted. According to its findings, plug-n-play home energy backup systems with adequate capacity can be designed and lab prototypes can be developed. Working with end-users to incorporate their feedback and iterating through multiple versions would be essential. By partnering with engineering and medical-grade technology vendors, deployment-ready prototypes can be developed and tested through a pilot. In addition to providing energy backup during outages, these solutions can be designed to participate in demand response programs and help end-users save on their energy bills. Furthermore, this can be accompanied by energy literacy programming to increase awareness about day-to-day energy use and energy backup requirements. This research has the potential to have far-reaching impact ranging from better health outcomes for such individuals, to improving emergency response during outages and reducing emergency room admits.

Threshold-based energy management for multi-energy systems: Systems at the "grid edge", such as residential and commercial entities, can consist of multiple energy storage and carrier systems, like EVs, batteries, and micro-CHP plants. These systems can be modeled as multi-energy systems (MES). For low-income households without such expensive assets, it can be promising to explore MES modeling using proxies for energy storage, such as an energy budget (the amount of money they can spend on energy), a time budget (the amount of time they can spend on manually doing tasks which can be done using electric appliances; this is also a measure of the time that could have been spent on employment or education). An energy management framework enables households to make decisions such as scheduling loads, participating in demand-response, and choosing electricity rate plans, while ensuring effective utilization of their resources. Threshold-based energy management is a candidate framework for single-energy carrier systems, such as, battery storage and prepaid wallets. The framework ensures operational sufficiency at each household using simple local computation resources without remote communication. The framework is suitable for use with heterogeneous local hardware and is resilient to

intermittent remote communication. In order to extend this control framework to MES, the following questions can be explored: how to define thresholds when there are multiple energy carriers, how does computation of optimal setpoints scale with the number of households, what are the effects on system stability when households interconnect to form a network and exchange energy. Further, applications of this framework to multi-energy carrier transportation systems such as hybrid electric cars and aircraft can be explored.

Energy management for low-income households: The increasing investments in grid infrastructure to adapt to extreme weather and to meet increasing demands due to data center loads is expected to increase electricity prices. Furthermore, if low-income households are switching from gas-powered appliances like furnaces to cleaner alternatives like heat pumps, their electricity requirements will further increase. In order to help such households prioritize between using different loads and effectively manage a limited energy budget, it is necessary to build technology-driven solutions. By partnering with households on energy assistance programs, their energy usage data can be recorded and qualitative requirements can be understood through interviews and workshops. A variety of energy management solutions that range from highly intrusive and expensive smart switches for automatic device actuation to minimally intrusive and low-cost smart phone apps that notify users to switch devices on/off can be explored. A combination of off-the-shelf components and lab prototypes can be used to develop the candidate solutions, incorporating feedback from the end-users at each stage. The use of machine learning for generating forecasts and generative AI for energy education and awareness can be explored. Field deployments can help validate their use cases. This research can help to inform energy assistance programs, utility policies for disconnections, participation in virtual power plants, in addition to improving user experience and health outcomes for such households.

Summary

Reliable electricity access is crucial for fostering and promoting human development across emerging and developed economies. As we transition towards decarbonization, digitization, and decentralization of energy, it is essential that the transition is rooted in equitable access. Moreover, the developed energy access solutions must be context-aware, address the nuanced requirements of the end-user, and operate effectively in diverse, resource-constrained environments. This necessitates interdisciplinary translational research that extends beyond power engineering, incorporating community-engaged scholarship, energy policy, and other relevant disciplines.

This thesis aspires to be a roadmap for developing energy access solutions in resource-constrained environments through inter-disciplinary holistic approaches. It can serve as a guide for the power engineering community to engage with community partners, policymakers, and other stakeholders to distill technical questions from complex real-world problems and develop solutions that have the potential for tangible real-world impact. The work is a significant enabler for addressing the challenge of Sustainable Development Goal 7: "Ensure access to affordable, reliable, sustainable and modern energy for all".

Bibliography

[1] P. Nduhuura, M. Garschagen, and A. Zerga, "Impacts of electricity outages in urban households in developing countries: A case of accra, ghana," *Energies*, vol. 14, no. 12, p. 3676, 2021.

[2] U. Chakravorty, M. Pelli, and B. Ural Marchand, "Does the quality of electricity matter? evidence from rural india," *Journal of Economic Behavior & Organization*, vol. 107, pp. 228–247, 2014.

[3] A. X. Andresen, L. C. Kurtz, D. M. Hondula, S. Meerow, and M. Gall, "Understanding the social impacts of power outages in north america: a systematic review," *Environmental Research Letters*, vol. 18, no. 5, p. 053004, 2023.

[4] United Nations General Assembly, "Transforming our world: the 2030 agenda for sustainable development." sdgs.un.org/2030agenda, 2015. Accessed: November 2024.

[5] "Tracking SDG 7: The Energy Progress Report," tech. rep., IEA, IRENA, UNSD, World Bank, WHO, 2024.

[6] H. Ritchie and M. Roser, "Access to energy." Available at `ourworldindata.org/energy-access#access-to-electricity`. Accessed: 2022-09-23.

[7] J. Ayaburi, M. Bazilian, J. Kincer, and T. Moss, "Measuring "reasonably reliable" access to electricity services," *The Electricity Journal*, vol. 33, no. 7, p. 106828, 2020.

[8] "U.S. Energy Information Administration, Form EIA-861, Annual Electric Power Industry Report," tech. rep., 2023.

[9] I. Ferrall, D. Callaway, and D. M. Kammen, "Measuring the reliability of sdg 7: the reasons, timing, and fairness of outage distribution for household electricity access solutions," *Environmental Research Communications*, vol. 4, no. 5, p. 055001, 2022.

[10] J. Peters, M. Sievert, and M. A. Toman, "Rural electrification through mini-grids: Challenges ahead," *Energy Policy*, vol. 132, pp. 27–31, 2019.

[11] A. Scott-George, C. Li, Y. K. Tang, S. Saha, M. T. B. Ali, A. Marma, and S. Pal, "A review on the sustainability of solar home system for rural electrification," in *E3S Web of Conferences*, vol. 294, p. 02003, EDP Sciences, 2021.

[12] M. Brown, C. Fassett, P. Whittle, J. McConnaughey, and J. Lo, "Storms batter aging power grid as climate disasters spread." apnews.com/article/wildfires-storms-science-business-health-7a0fb8c998c1d56759989dda62292379, April 2022. Accessed: October 2024.

[13] G. Ryan, "Power crisis: Despite transparency failures, utility information reveals major home shutoff problem, more than 1 million household power disconnects reported across 17 states," tech. rep., Center for Biological Diversity, 2021.

[14] U.S. Energy Information Administration, "Residential Energy Consumption Survey (RECS)," 2020. `eia.gov/consumption/residential/data/2020/` Accessed October 2024.

[15] S. C. Ganz, C. Duan, and C. Ji, "Socioeconomic vulnerability and differential impact of severe weather-induced power outages," *PNAS nexus*, vol. 2, no. 10, p. pgad295, 2023.

[16] J. C. Burns, D. Y. Cooke, and C. Schweidler, "A short guide to community based participatory action," tech. rep., 2011.

[17] R. A. Virzi, "What can you learn from a low-fidelity prototype?," in *Proceedings of the Human Factors Society Annual Meeting*, vol. 33, pp. 224–228, SAGE Publications Sage CA: Los Angeles, CA, 1989.

[18] A. Manur, *Communication, Computing, and Control Solutions for Smart Microgrids*. PhD thesis, University of Wisconsin-Madison, 2019.

[19] A. Manur, M. Marathe, A. Manur, A. Ramachandra, S. Subbarao, and G. Venkataramanan, "Smart Solar Home System with Solar Forecasting," in *2020 IEEE International Conference on Power Electronics, Smart Grid and Renewable Energy (PESGRE2020)*, pp. 1–6, IEEE, 2020.

[20] N. L. Lam, K. R. Smith, A. Gauthier, and M. N. Bates, "Kerosene: A Review of Household Uses and their Hazards in Low- and Middle-Income Countries," *Journal of Toxicology and Environmental Health, Part B*, vol. 15, no. 6, pp. 396–432, 2012. PMID: 22934567.

[21] X. Hou and J. Urpelainen, "Lock-in for lighting: The puzzle of continued kerosene use among electrified households in six Indian states," *Energy Research & Social Science*, vol. 69, p. 101592, 2020.

[22] "Gaps and barriers preventing effective implementation of microgrids in India: A summary of technical, financial, social, operational and political factors," tech. rep., SELCO Foundation.

[23] R. Tongia, "Microgrids in India," tech. rep., Brookings India. `brookings.edu/wp-content/uploads/2018/02/impact_series_microgrid-folder_feb10-2.pdf`, Accessed: September 2022.

[24] M. Geidl and G. Andersson, "Optimal power flow of multiple energy carriers," *IEEE Transactions on power systems*, vol. 22, no. 1, pp. 145–155, 2007.

[25] M. Rastegar, M. Fotuhi-Firuzabad, and M. Lehtonen, "Home load management in a residential energy hub," *Electric Power Systems Research*, vol. 119, pp. 322–328, 2015.

[26] F. Brahman, M. Honarmand, and S. Jadid, "Optimal electrical and thermal energy management of a residential energy hub, integrating demand response and energy storage system," *Energy and Buildings*, vol. 90, pp. 65–75, 2015.

[27] T. Ma, J. Wu, and L. Hao, "Energy flow modeling and optimal operation analysis of the micro energy grid based on energy hub," *Energy conversion and management*, vol. 133, pp. 292–306, 2017.

[28] A. Hussain, S. M. Arif, M. Aslam, and S. D. A. Shah, "Optimal siting and sizing of tri-generation equipment for developing an autonomous community microgrid considering uncertainties," *Sustainable cities and society*, vol. 32, pp. 318–330, 2017.

[29] J. Apple, R. Vicente, A. Yarberry, N. Lohse, E. Mills, A. Jacobson, and D. Poppendieck, "Characterization of particulate matter size distributions and indoor concentrations from kerosene and diesel lamps," *Indoor air*, vol. 20, no. 5, pp. 399–411, 2010.

[30] "Kerosene." iocl.com/kerosene. Accessed: October 2024.

[31] S. Mahapatra, H. Chanakya, and S. Dasappa, "Evaluation of various energy devices for domestic lighting in india: Technology, economics and co2 emissions," *Energy for Sustainable Development*, vol. 13, no. 4, pp. 271–279, 2009.

[32] N. Ravindranath and J. Ramakrishna, "Energy options for cooking in india," *Energy policy*, vol. 25, no. 1, pp. 63–75, 1997.

[33] "A report on "housing condition" based on data collected in state sample of 58th round of national sample survey," tech. rep., Government of Maharashtra, 2002. Available at `mahades.maharashtra.gov.in/files/report/nss_58_1.2_vol_1_&_2.pdf`, accessed 2022-09-21.

[34] "No ceiling for ceiling heights," *The Hindu*, 2011. Available at `thehindu.com/features/homes-and-gardens/No-ceiling-for-ceiling-heights/article14675568.ece`, accessed 2022-09-21.

[35] R. M. Weltman, R. D. Edwards, L. T. Fleming, A. Yadav, C. L. Weyant, B. Rooney, J. H. Seinfeld, N. K. Arora, T. C. Bond, S. A. Nizkorodov, *et al.*, "Emissions measurements from household solid fuel use in haryana, india: implications for climate and health co-benefits," *Environmental Science & Technology*, vol. 55, no. 5, pp. 3201–3209, 2021.

[36] G. Shen, C. K. Gaddam, S. M. Ebersviller, R. L. Vander Wal, C. Williams, J. W. Faircloth, J. J. Jetter, and M. D. Hays, "A laboratory comparison of emission factors, number size distributions, and morphology of ultrafine particles from 11 different household cookstove-fuel systems," *Environmental science & technology*, vol. 51, no. 11, pp. 6522–6532, 2017.

[37] I. Dunning, J. Huchette, and M. Lubin, "Jump: A modeling language for mathematical optimization," *SIAM Review*, vol. 59, no. 2, pp. 295–320, 2017.

[38] "WHO air quality guidelines for particulate matter, ozone, nitrogen dioxide and sulfur dioxide," *World Health Organization*, 2005.

[39] "HHS emPOWER Map: Medicare electricity-dependent populations by geography." empowerprogram.hhs.gov/empowermap. Accessed: October 2024.

[40] A. Shapiro and M. Mango, "Home Health Care in the Dark: Why Climate, Wildfires and Other Risks Call for New Resilient Energy Storage Solutions to Protect Medically Vulnerable Households From Power Outages," tech. rep., Clean Energy Group, Meridian Institute, Apr. 2019.

[41] A. Manur, G. Venkataramanan, and D. Sehloff, "Simple electric utility platform: A hardware/software solution for operating emergent microgrids," *Applied energy*, vol. 210, pp. 748–763, 2018.

[42] A. Manur, D. Sehloff, and G. Venkataramanan, "Energyan: A portable platform for microgrid education, research, and development," in *2018 IEEE International Conference on Power Electronics, Drives and Energy Systems (PEDES)*, pp. 1–6, IEEE, 2018.

[43] A. Manur, M. Marathe, and G. Venkataramanan, "A distributed approach for secondary and tertiary layer control in dc microgrids," in *IEEE Energy Conversion Congress and Exposition*, pp. 1284–1291, 2020.

[44] O. Reynolds, S. Wheeldon, J. Galan, J. Thomas, L. Blyth, S. Conibear, E. Lai, R. Macdonald, M. Drent, T. van Bieman, A. Kot, and C. Asma, "Global Off-Grid Solar Market Report Semi-Annual Sales and Impact Data," tech. rep., GOGLA and Lighting Global, ESMAP, World Bank and Efficiency for Access Coalition, Energy Saving Trust and Efficiency for Access Coalition, CLASP and Efficiency for Access Coalition, CLASP, 2021. Accessed: May 2022.

[45] "NSF's innovation corps (I-Corps)." new.nsf.gov/funding/initiatives/i-corps. Accessed: October 2024.

[46] A. Osterwalder, *The business model ontology a proposition in a design science approach*. PhD thesis, Université de Lausanne, Faculté des hautes études commerciales, 2004.

[47] Strategyzer, "Business model canvas – download the official template." strategyzer.com/canvas/business-model-canvas. Accessed: October 2024.

[48] S. Blank and B. Dorf, *The startup owner's manual: The step-by-step guide for building a great company*. John Wiley & Sons, 2020.

[49] M. Marathe and A. Manur, "Energy resilience for home healthcare." smplabs.wisc.edu/nsf-icorps, 2020.

[50] E. G. Vendrell and S. A. Watson, "Chapter 28 - emergency planning," in *The Professional Protection Officer* (IFPO, ed.), pp. 331 – 347, Boston: Butterworth-Heinemann, 2010.

[51] A. Chandra, M. V. Williams, C. Lopez, J. Tang, D. Eisenman, and A. Magana, "Developing a tabletop exercise to test community resilience: Lessons from the los angeles county community disaster resilience project," *Disaster medicine and public health preparedness*, vol. 9, no. 5, pp. 484–488, 2015.

[52] D. J. Dausey, J. W. Buehler, and N. Lurie, "Designing and conducting tabletop exercises to assess public health preparedness for manmade and naturally occurring biological threats," *BMC public health*, vol. 7, no. 1, p. 92, 2007.

[53] E. H. High, K. A. Lovelace, B. M. Gansneder, R. W. Strack, B. Callahan, and P. Benson, "Promoting community preparedness: Lessons learned from the implementation of a chemical disaster tabletop exercise," *Health promotion practice*, vol. 11, no. 3, pp. 310–319, 2010.

[54] "General Algebraic Modeling System." www.gams.com Accessed: October 2024.

[55] "Power outage potentially deadly for those on home life-support." `cleveland.com/health/2009/01/power_outage_potentially_deadl.html`. Accessed May 2022.

[56] T. Nakayama, S. Tanaka, M. Uematsu, A. Kikuchi, N. Hino-Fukuyo, T. Morimoto, O. Sakamoto, S. Tsuchiya, and S. Kure, "Effect of a blackout in pediatric patients with home medical devices during the 2011 eastern Japan earthquake," *Brain and Development*, vol. 36, pp. 143–147, Feb. 2014.

[57] P. W. Greenwald, A. F. Rutherford, R. A. Green, and J. Giglio, "Emergency Department Visits for Home Medical Device Failure during the 2003 North America Blackout," *Academic Emergency Medicine*, vol. 11, pp. 786–789, July 2004.

[58] P. Kourtza, M. Marathe, A. Shetty, and D. Kiedanski, "Identification of medical devices using machine learning on distribution feeder data for informing power outage response." arxiv.org/abs/2211.08310, 2022.

[59] K. Cowan, R. Sussman, S. Rotmann, and R. Cox, "Designing a behaviour change programme for hospital facilities staff," in *International Energy Agency, Demand Side Management*, 2017.

[60] The Council of Economic Advisers, "The state of homelessness in america." nhipdata.org/local/upload/file/The-State-of-Homelessness-in-America.pdf, 2019. Accessed: September 2022.

[61] W. Thurman, M. Semwal, L. Moczygemba, and M. Hilbelink, "Smartphone technology to empower people experiencing homelessness: Secondary analysis," *J Med Internet Res*, 2021.

[62] M. C. Raven, L. M. Kaplan, M. Rosenberg, L. Tieu, D. Guzman, and M. Kushel, "Mobile phone, computer, and internet use among older homeless adults: Results from the hope home cohort study," *JMIR Mhealth and Uhealth*, 2018.

[63] M. Kim, "Designs on mobility: Perceptions of mobile phones among the homeless." cogsci.ucsd.edu/_files/undergraduates/past-honors-theses/2013-2014/2014_thesis_melody_kim_designsonmobility.pdf, 2014. Accessed: September 2022.

[64] "Great lakes community conservation corps." greatlakesccc.org. Accessed: November 2024.

[65] "Little free library." littlefreelibrary.org. Accessed: November 2024.

[66] B. Bondi, S. Bradshaw, M. Marathe, and W. Keenan, "Electric little free library: Solar kiosks for energy access." smplabs.wisc.edu/electric-little-free-library/#documents, 2022.

[67] "City of madison legislative information center." madison.legistar.com/LegislationDetail.aspx?ID=5807727&GUID=4BF2B996-38A1-4ED2-95F5-E059F86A86F4. Accessed: November 2024.

[68] "State of wisconsin clean energy plan progress report," tech. rep., Wisconsin Office of Sustainability and Clean Energy, May 2023.

[69] K. Wenzel and I. Bohachek, "Lifelines: Optimal locations in madison for community access to solar energy for cell phone charging," May 2024.

[70] "Youth climate action fund disperses eight $5,000 grants to local young people driving climate solutions." cityofmadison.com/news/2024-08-08/youth-climate-action-fund-disperses-eight-5000-grants-to-local-young-people-driving Accessed: October 2024.

[71] "CDC/ATSDR Social Vulnerability Index (CDC/ATSDR SVI): Overview." atsdr.cdc.gov/placeandhealth/svi/index.html. Accessed: November 2024.

[72] A. S. Duran and F. G. Sahinyazan, "An analysis of renewable mini-grid projects for rural electrification," *Socio-Economic Planning Sciences*, vol. 77, p. 100999, 2021.

[73] S. Fobi, J. Mugyenyi, N. J. Williams, V. Modi, and J. Taneja, "Predicting levels of household electricity consumption in low-access settings," in *Proceedings of the IEEE/CVF Winter Conference on Applications of Computer Vision*, pp. 3902–3911, 2022.

[74] F. Antonanzas-Torres, J. Antonanzas, and J. Blanco-Fernandez, "State-of-the-art of mini grids for rural electrification in west africa," *Energies*, vol. 14, no. 4, p. 990, 2021.

[75] A. Newcombe and E. K. Ackom, "Sustainable solar home systems model: Applying lessons from bangladesh to myanmar's rural poor," *Energy for Sustainable Development*, vol. 38, pp. 21–33, 2017.

[76] D. E. Olivares, A. Mehrizi-Sani, A. H. Etemadi, C. A. Cañizares, R. Iravani, M. Kazerani, A. H. Hajimiragha, O. Gomis-Bellmunt, M. Saeedifard, R. Palma-Behnke, *et al.*, "Trends in microgrid control," *IEEE Transactions on smart grid*, vol. 5, no. 4, pp. 1905–1919, 2014.

[77] C. H. Hauser, D. E. Bakken, and A. Bose, "A failure to communicate: next generation communication requirements, technologies, and architecture for the electric power grid," *IEEE Power and Energy Magazine*, vol. 3, no. 2, pp. 47–55, 2005.

[78] V. Nasirian, S. Moayedi, A. Davoudi, and F. L. Lewis, "Distributed cooperative control of dc microgrids," *IEEE Transactions on Power Electronics*, vol. 30, no. 4, pp. 2288–2303, 2014.

[79] L. Meng, T. Dragicevic, J. M. Guerrero, and J. C. Vasquez, "Dynamic consensus algorithm based distributed global efficiency optimization of a droop controlled dc microgrid," in *2014 IEEE international energy conference (ENERGYCON)*, pp. 1276–1283, IEEE, 2014.

[80] S. Moayedi and A. Davoudi, "Distributed tertiary control of dc microgrid clusters," *IEEE Transactions on Power Electronics*, vol. 31, no. 2, pp. 1717–1733, 2015.

[81] S. Liptak, M. Miranbeigi, S. Kulkarni, R. Jinsiwale, and D. Divan, "Self-organizing nanogrid (song)," in *2019 IEEE Decentralized Energy Access Solutions Workshop (DEAS)*, pp. 206–212, IEEE, 2019.

[82] D. Li and C. N. M. Ho, "A module-based plug-n-play dc microgrid with fully decentralized control for ieee empower a billion lives competition," *IEEE Transactions on Power Electronics*, vol. 36, no. 2, pp. 1764–1776, 2020.

[83] L. Richard, D. Frey, A. Derbey, M.-C. Alvarez-Herault, and B. Raison, "Experimental design of solar dc microgrid for the rural electrification of africa," in *PCIM Europe 2022; International Exhibition and Conference for Power Electronics, Intelligent Motion, Renewable Energy and Energy Management*, pp. 1–10, VDE, 2022.

[84] M. Marathe and G. Venkataramanan, "Distributed optimal scheduling in community-scale microgrids," in *IEEE Energy Conversion Congress and Exposition*, pp. 833–840, 2021.

[85] D. Sehloff, M. Marathe, A. Manur, and G. Venkataramanan, "Self-sufficient participation in cloud-based demand response," *IEEE Transactions on Cloud Computing*, vol. 10, no. 1, pp. 4–16, 2021.

[86] J.-J. E. Slotine, W. Li, *et al.*, *Applied nonlinear control*, vol. 199. Prentice hall Englewood Cliffs, NJ, 1991.

[87] J. Li, Y. Liu, and L. Wu, "Optimal operation for community-based multi-party microgrid in grid-connected and islanded modes," *IEEE Transactions on Smart Grid*, vol. 9, no. 2, pp. 756–765, 2016.

[88] S. Emili, F. Ceschin, and D. Harrison, "Product–service system applied to distributed renewable energy: A classification system, 15 archetypal models and a strategic design tool," *Energy for Sustainable Development*, vol. 32, pp. 71–98, 2016.

[89] J. Löfberg, "Yalmip : A toolbox for modeling and optimization in matlab," in *In Proceedings of the CACSD Conference*, (Taipei, Taiwan), 2004.

[90] J. Currie and D. I. Wilson, "OPTI: Lowering the Barrier Between Open Source Optimizers and the Industrial MATLAB User," in *Foundations of Computer-Aided Process Operations* (N. Sahinidis and J. Pinto, eds.), (Savannah, Georgia, USA), 8–11 January 2012.

[91] M. Berkelaar, K. Eikland, P. Notebaert, *et al.*, "lpsolve: Open source (mixed-integer) linear programming system," 2004. `lpsolve.sourceforge.net/5.5/` Accessed October 2024.

[92] M. Marathe and L. A. Roald, "Optimal energy rationing for prepaid electricity customers," in *2023 IEEE Belgrade PowerTech*, pp. 01–06, 2023.

[93] J. Bhattacharya, T. DeLeire, S. Haider, and J. Currie, "Heat or eat? cold-weather shocks and nutrition in poor american families," *American Journal of Public Health*, vol. 93, no. 7, pp. 1149–1154, 2003.

[94] S. Cong, D. Nock, Y. L. Qiu, and B. Xing, "Unveiling hidden energy poverty using the energy equity gap," *Nature communications*, vol. 13, no. 1, p. 2456, 2022.

[95] "Almost half a million could be forced onto pricey pay-as-you-go meters by the end of the year, warns citizens advice." `citizensadvice.org.uk/about-us/about-us1/media/press-releases/almost-half-a-million-could-be-forced-onto-pricey-pay-as-you-go-meters-by-the-end-of-the-year-warns-citizens-advice/` Accessed October 2024.

[96] LIHEAP Clearinghouse, "Prepaid utility service, low-income customers and LIHEAP," tech. rep., LIHEAP Clearinghouse, 2014.

[97] "Hostage to heat: Prepaid utility plans leave some customers in the dark with little warning." `stories.usatodaynetwork.com/hostagetoheat/prepaid-utility-plans-leave-some-customers-without-electricity/` Accessed October 2024.

[98] "Smart Prepaid Utilities in the United States: Forecasts & Analysis," tech. rep., Quindi Research, 2017.

[99] N. Thomas, "Uk energy suppliers force vulnerable on to prepayment meters." `ft.com/content/b2be6681-42a7-42d5-a6e5-ab5b8cf1e682` Accessed January 2023.

[100] Y. Qiu, B. Xing, and Y. D. Wang, "Prepaid electricity plan and electricity consumption behavior," *Contemporary Economic Policy*, vol. 35, no. 1, pp. 125–142, 2017.

[101] M. Ozog, "The effect of prepayment on energy use," tech. rep., Integral Analytics, Inc, 2013. Report for the Distributed Energy Financial Group (DEFG) Prepay Energy Working Group.

[102] D. Eryilmaz and S. Gafford, "Can a daily electricity bill unlock energy efficiency? evidence from texas," *The Electricity Journal*, vol. 31, no. 3, pp. 7–11, 2018.

[103] G. R. Telles Esteves, F. L. Cyrino Oliveira, C. H. Antunes, and R. C. Souza, "An overview of electricity prepayment experiences and the brazilian new regulatory framework," *Renewable and Sustainable Energy Reviews*, vol. 54, pp. 704–722, 2016.

[104] M. Beaudin and H. Zareipour, "Home energy management systems: A review of modelling and complexity," *Renewable and sustainable energy reviews*, vol. 45, pp. 318–335, 2015.

[105] D. S. Callaway and I. A. Hiskens, "Achieving controllability of electric loads," *Proceedings of the IEEE*, vol. 99, no. 1, pp. 184–199, 2010.

[106] B. K. Sovacool and D. D. F. Del Rio, "Smart home technologies in europe: A critical review of concepts, benefits, risks and policies," *Renewable and sustainable energy reviews*, vol. 120, p. 109663, 2020.

[107] "Paying upfront: A review of salt river project's m-power prepaid program," tech. rep., Electric Power Research Institute, 2010.

[108] H. Shareef, M. S. Ahmed, A. Mohamed, and E. Al Hassan, "Review on home energy management system considering demand responses, smart technologies, and intelligent controllers," *Ieee Access*, vol. 6, pp. 24498–24509, 2018.

[109] T. Narmada, M. Lakshmaiah, and N. Nagamma, "Design and development of raspberry pi based system for prepaid electricity meter," in *IEEE Int. Conf. on Power, Control, Signals and Instrumentation Engineering*, pp. 2343–2347, IEEE, 2017.

[110] N. Gaur, A. Gupta, A. K. Sharma, and R. Malviya, "HDL implementation of prepaid electricity billing machine on FPGA," in *5th Int. Conf. on The Next Generation Information Technology Summit (Confluence)*, pp. 972–975, IEEE, 2014.

[111] M. S. Parvin and S. L. Kabir, "A framework of a smart system for prepaid electric metering scheme," in *IEEE Int. Conf. on Informatics, Electronics & Vision*, pp. 1–5, IEEE, 2015.

[112] R. Anderson and S. Fuloria, "Who controls the off switch?," in *IEEE Int. Conf. on Smart Grid Communications*, pp. 96–101, IEEE, 2010.

[113] M. S. Parvin and S. L. Kabir, "Standard and interoperable database for pre-paid electricity metering systems in bangladesh," in *Int. Conf. on Informatics, Electronics & Vision*, pp. 356–361, IEEE, 2012.

[114] W. Souza, F. Garcia, A. Moreira, F. Marafao, and L. Silva, "Automatic consumption management for prepaid electricity meter with nilm," *IEEE Latin America Transactions*, vol. 18, no. 06, pp. 1102–1110, 2020.

[115] N. Ismail, Z. Yahia, M. Gheith, and A. B. Eltawil, "A mixed integer programming formulation for optimal scheduling of household appliances with budget constraint," in *IEEE Int. Conf. on Industrial Engineering and Applications (ICIEA)*, pp. 20–24, IEEE, 2021.

[116] C. G. Monyei, A. O. Adewumi, D. Akinyele, O. M. Babatunde, M. O. Obolo, and J. C. Onunwor, "A biased load manager home energy management system for low-cost residential building low-income occupants," *Energy*, vol. 150, pp. 822–838, 2018.

[117] K. E. Ouedraogo, P. O. Ekim, and E. Demirok, "Feasibility of low-cost energy management system using embedded optimization for pv and battery storage assisted residential buildings," *Energy*, vol. 271, p. 126922, 2023.

[118] "Pecan street dataset." `pecanstreet.org/dataport/` Accessed: October 2023.

[119] "SRP M-Power prepaid price plan | SRP." `srpnet.com/price-plans/residential-electric/m-power` Accessed October 2024.

[120] J. Bezanson, A. Edelman, S. Karpinski, and V. B. Shah, "Julia: A fresh approach to numerical computing," *SIAM review*, vol. 59, no. 1, pp. 65–98, 2017.

[121] I. Dunning, J. Huchette, and M. Lubin, "Jump: A modeling language for mathematical optimization," *SIAM review*, vol. 59, no. 2, pp. 295–320, 2017.

[122] Gurobi Optimization, LLC, "Gurobi Optimizer Reference Manual." `www.gurobi.com` Accessed October 2024.

[123] M. Marathe and L. A. Roald, "Energy management for prepaid customers: A linear optimization approach," in *2024 IEEE International Conference on Communications, Control, and Computing Technologies for Smart Grids (SmartGridComm)*, pp. 492–498, IEEE, 2024.

[124] L. Li, C. J. Meinrenken, V. Modi, and P. J. Culligan, "Short-term apartment-level load forecasting using a modified neural network with selected auto-regressive features," *Applied Energy*, vol. 287, p. 116509, 2021.

[125] M. Blonsky, K. McKenna, J. Maguire, and T. Vincent, "Home energy management under realistic and uncertain conditions: A comparison of heuristic, deterministic, and stochastic control methods," *Applied Energy*, vol. 325, p. 119770, 2022.

[126] "PrepaidEnergyManagement," May 2024. `github.com/WISPO-POP/PrepaidEnergyManagement`.

[127] G. B. Dantzig, "Discrete-variable extremum problems," *Operations research*, vol. 5, no. 2, pp. 266–288, 1957.

[128] M. Marathe and G. Venkataramanan, "Picogrid: An experimental platform for prosumer microgrids," in *2023 IEEE Energy Conversion Congress and Exposition (ECCE)*, pp. 718–725, IEEE, 2023.

[129] R. Wallsgrove, J. Woo, J.-H. Lee, and L. Akiba, "The emerging potential of microgrids in the transition to 100% renewable energy systems," *Energies*, vol. 14, no. 6, p. 1687, 2021.

[130] M. F. Zia, M. Benbouzid, E. Elbouchikhi, S. Muyeen, K. Techato, and J. M. Guerrero, "Microgrid transactive energy: Review, architectures, distributed ledger technologies, and market analysis," *Ieee Access*, vol. 8, pp. 19410–19432, 2020.

[131] A. Kantamneni, L. E. Brown, G. Parker, and W. W. Weaver, "Survey of multi-agent systems for microgrid control," *Engineering applications of artificial intelligence*, vol. 45, pp. 192–203, 2015.

[132] "The genius of microgrids in higher education," tech. rep., Microgrid Knowledge, 2020.

[133] V. Jately, B. Azzopardi, S. Bhattacharya, and R. Sadula, "Living Laboratory Microgrid: A Learning and Research Platform - IEEE Smart Grid," 2022.

[134] B. Blackstone, C. Hicks, O. Gonzalez, and Y. Baghzouz, "Development of an outdoor diesel generator–pv microgrid for education and research," in *2018 IEEE Power & Energy Society General Meeting (PESGM)*, pp. 1–5, IEEE, 2018.

[135] A. N. Akpolat, Y. Yang, F. Blaabjerg, E. Dursun, and A. E. Kuzucuoğlu, "Design implementation and operation of an education laboratory-scale microgrid," *IEEE Access*, vol. 9, pp. 57949–57966, 2021.

[136] J. A. Momoh and S. S. Reddy, "Value of hardware-in-loop for experimenting microgrid performance system studies," in *2016 IEEE PES PowerAfrica*, pp. 199–203, IEEE, 2016.

[137] C. Patrascu, N. Muntean, O. Cornea, and A. Hedes, "Microgrid laboratory for educational and research purposes," in *2016 IEEE 16th international conference on environment and electrical engineering (EEEIC)*, pp. 1–6, IEEE, 2016.

[138] J. F. Patarroyo-Montenegro, J. E. Salazar-Duque, S. I. Alzate-Drada, J. D. Vasquez-Plaza, and F. Andrade, "An ac microgrid testbed for power electronics courses in the university of puerto rico at mayagüez," in *2018 IEEE ANDESCON*, pp. 1–6, IEEE, 2018.

[139] Q. Hu, F. Li, and C.-f. Chen, "A smart home test bed for undergraduate education to bridge the curriculum gap from traditional power systems to modernized smart grids," *IEEE Transactions on Education*, vol. 58, no. 1, pp. 32–38, 2014.

[140] L. Guo and J. Kors Jr, "Design of a laboratory scale solar microgrid cyber-physical system for education," *Electronics*, vol. 10, no. 13, p. 1562, 2021.

[141] H. Chai, M. Priestley, X. Tang, and J. Ravishankar, "Implementation of microgrid virtual laboratory in a design course in electrical engineering," in *2020 IEEE International Conference on Teaching, Assessment, and Learning for Engineering (TALE)*, pp. 509–515, IEEE, 2020.

[142] H. Y. Lai, W. Mai, and C. Chung, "Educational simulation platform for microgrid," in *2014 IEEE PES Asia-Pacific Power and Energy Engineering Conference (APPEEC)*, pp. 1–7, IEEE, 2014.

[143] L. Guo, M. Vengalil, N. M. M. Abdul, and K. Wang, "Design and implementation of virtual laboratory for a microgrid with renewable energy sources," *Computer Applications in Engineering Education*, vol. 30, no. 2, pp. 349–361, 2022.

[144] N. Lidula and A. Rajapakse, "Microgrids research: A review of experimental microgrids and test systems," *Renewable and Sustainable Energy Reviews*, vol. 15, no. 1, pp. 186–202, 2011.

[145] E. Hossain, E. Kabalci, R. Bayindir, and R. Perez, "Microgrid testbeds around the world: State of art," *Energy conversion and management*, vol. 86, pp. 132–153, 2014.

[146] "Picogrid," May 2024. `github.com/smplabs/picogrid`.

[147] "Particle Docs." `docs.particle.io` Accessed: October 2024.

[148] "ThingSpeak." `thingspeak.com` Accessed: October 2024.

[149] V. Balan, M. Marathe, and G. Venkataramanan, "A cloud-based solution for remote access to a microgrid experimental platform," in *11th IEEE International Conference on Power Electronics Drives and Energy Systems PEDES 2024*, IEEE (accepted), 2024.

[150] K. Harper, N. Caverly, R. Arku, C. Barchers, J. Krupczynski, E. D. Baker, M. Ash, J. C. Cardenas, P. Shenoy, B. Weil, and E. Markowitz, "Community-engaged co-design of residential electrification for a just and sustainable energy transition." `cfpub.epa.gov/ncer_abstracts/index.cfm/fuseaction/display.abstractDetail/abstract_id/11398/report`, 2023. Accessed: October 2024.

[151] J.-H. Jeon, J.-Y. Kim, H.-M. Kim, S.-K. Kim, C. Cho, J.-M. Kim, J.-B. Ahn, and K.-Y. Nam, "Development of hardware in-the-loop simulation system for testing operation and control functions of microgrid," *IEEE Transactions on Power Electronics*, vol. 25, no. 12, pp. 2919–2929, 2010.

[152] W. Domski, "Remote laboratory offered as hardware-as-a-service infrastructure," *Electronics*, vol. 11, no. 10, p. 1568, 2022.

[153] S. Zhang, A. Pandey, X. Luo, M. Powell, R. Banerji, L. Fan, A. Parchure, and E. Luzcando, "Practical adoption of cloud computing in power systems—drivers, challenges, guidance, and real-world use cases," *IEEE Transactions on Smart Grid*, vol. 13, no. 3, pp. 2390–2411, 2022.

[154] K. A. A. Sumarmad, N. Sulaiman, N. I. A. Wahab, and H. Hizam, "Microgrid energy management system based on fuzzy logic and monitoring platform for data analysis," *Energies*, vol. 15, no. 11, p. 4125, 2022.

[155] C. N. Oton and M. T. Iqbal, "Low-cost open source iot-based scada system for a bts site using esp32 and arduino iot cloud," in *2021 IEEE 12th Annual Ubiquitous Computing, Electronics & Mobile Communication Conference (UEMCON)*, pp. 0681–0685, IEEE, 2021.

[156] C. Alexakos, A. Komninos, C. Anagnostopoulos, G. Kalogeras, A. Savvopoulos, and A. Kalogeras, "Building an industrial iot infrastructure with open source software for smart energy," in *2019 First International Conference on Societal Automation (SA)*, pp. 1–8, IEEE, 2019.

[157] N. Mills, P. Rathnayaka, H. Moraliyage, D. De Silva, and A. Jennings, "Cloud edge architecture leveraging artificial intelligence and analytics for microgrid energy optimisation and net zero carbon emissions," in *2022 15th International Conference on Human System Interaction (HSI)*, pp. 1–7, IEEE, 2022.

[158] C. A. Marino, F. Chinelato, and M. Marufuzzaman, "Aws iot analytics platform for microgrid operation management," *Computers & Industrial Engineering*, vol. 170, p. 108331, 2022.

[159] J. Vagdoda, D. Makwana, A. Adhikaree, T. Faika, and T. Kim, "A cloud-based multiagent system platform for residential microgrids towards smart grid community," in *2018 IEEE Power & Energy Society General Meeting (PESGM)*, pp. 1–5, IEEE, 2018.

[160] H. M. Rouzbahani, H. Karimipour, and L. Lei, "A review on virtual power plant for energy management," *Sustainable Energy Technologies and Assessments*, vol. 47, p. 101370, 2021.

[161] J. L. Mathieu, "Demand response: Coordination of flexible electric loads," in *Encyclopedia of Systems and Control*, pp. 530–534, Springer, 2021.

[162] B. Parrish, P. Heptonstall, R. Gross, and B. K. Sovacool, "A systematic review of motivations, enablers and barriers for consumer engagement with residential demand response," *Energy Policy*, vol. 138, p. 111221, 2020.